JAMS

JOURNAL OF ASSOCIATED MEDICAL SCIENCES

Volume 51 Number 1 January-Aprill 2018 E-ISSN : 2539-6056

Journal of Associated Medical Sciences

Aims and scope

The Journal of Associated Medical Sciences belongs to Faculty of Associated Medical Sciences (AMS), Chiang Mai University, Thailand. The journal specifically aims to provide the platform for medical technologists, physical therapists, occupational therapists, radiologic technologists, speech-language pathologists and other related professionals to distribute, share, discuss their research findings, inventions, and innovations in the areas of:

1. Medical Technology
2. Physical Therapy
3. Occupational Therapy
4. Radiologic Technology
5. Communication Disorders
6. Other related fields

Submitted manuscripts within the scope of the journal will be processed strictly following the double-blinded peer review process of the journal. Therefore, the final decision can be completed in 1-3 months average, depending on the number of rounds of revision.

Objectives

The Journal of Associated Medical Sciences aims to publish integrating research papers in areas of Medical Technology, Physical Therapy, Occupational Therapy, Radiologic Technology, and related under peer-reviewed via double-blinded process by at least two internal and external reviewers.

Types of manuscript

Manuscripts may be submitted in the form of review articles, original articles, short communications, as an approximate guide to length:

- **Review articles** must not exceed 20 journal pages (not more than 5,000 words), including 6 tables/figures, and references (maximum 75, recent and relevant).
- **Original articles** must not exceed 15 journal pages (not more than 3,500 words), including 6 tables/figures, and 40 reference (maximum 40, recent and relevant).
- **Short communications** including technical reports, notes, and letters to the editor must not exceed 5 journal pages (not more than 1,500 words), including 2 tables/figures, and references (maximum 10, recent and relevant).

Peer review process

By submitting a manuscripts to Journal of Associated Medical Sciences, the authors agree to subject it to the confidential double-blinded peer-review process. Editors and reviewers are informed that the manuscripts must be considered confidential. After a manuscripts is received, it is assigned by a specific Associate Editor. The Associate Editor prepares a list of expert reviewers, which may include some suggested by the Editor-in-Chief. Authors can indicate specific individuals whom they would like to have excluded as reviewers. Generally, requests to exclude certain potential reviewers will be honored except in fields with a limited number of experts. All potential reviewers are contacted individually to determine availability. Manuscripts files are sent to at least two expert reviewers. Reviewers are asked to complete the review of the manuscripts within 2 weeks and to return a short review form. Based on the reviewers' comments, the Associate Editor recommends a course of action and communicates the reviews and recommendations to the Editor-in-Chief for a final decision.

The Associate Editor considers the comments made by the reviewers and the recommendation of the Editor-in-Chief, selects those comments to be shared with the authors, makes a final decision concerning the manuscripts, and prepares the decision letter for signature by the Editor-in-Chief. If revisions of the manuscripts are suggested, the Associate Editor also recommends who should review the revised paper when resubmitted. Authors are informed of the decision by e-mail; appropriate comments from reviewers and editors are appended.

Publication frequency

Journal of Associated Medical Sciences publishes 3 issues a year

Issue 1: January-April
Issue 2: May-August
Issue 3: September-December

Journal Impact Factor
The journal's 2017 Impact Factor is 0.237

Journal website
Homepage https://www.tci-thaijo.org/index.php/bulletinAMS/index

Journal E-ISSN:
2539-6056

Editorial Office
Faculty of Associated Medical Sciences, Chiang Mai University
110 Inthawaroros Road, Suthep, Muang, Chiang Mai, 50200
Phone 053 935072 Facsimile 053 936042

Journal of Associated Medical Sciences

Vol. 51 No. 1 : January 2018

Content

Journal of Associated Medical Sciences 2018; 51(1): 1-5

JAMS
Journal of Associated Medical Sciences

Thai-Journal Citation Index Centre (TCI) & ASEAN Citation Index (ACI)

Journal of Associated Medical Sciences

Journal homepage: https://www.tci-thaijo.org/index.php/bulletinAMS/index

Change in gait speed using the timed 10 meter walk test in individuals with neck pain

Nipaporn Wannaprom Somporn Sungkarat Sureeporn Uthaikhup*

Department of Physical Therapy, Faculty of Associated Medical Sciences, Chiang Mai University, Thailand

ARTICLE INFO

Article history:
Received 29 October 2017
Accepted as revised 6 December 2017
Available online 1 January 2018

Keywords:
Cervical pain, gait speed, neck pain, timed 10 meter walk test, walking speed

ABSTRACT

Background: Gait speed is an informative marker of individual's functional capacity and health status. Neck pain is suggested to be associated with impaired gait speed. However, there is limited evidence for a clinical assessment of gait speed in patients with neck pain.

Objectives: To investigate maximum gait speed using the timed 10 meter walk test in individuals with and without neck pain. Relationships between gait speed and characteristics of neck pain were also determined.

Materials and methods: Twenty six men and women aged between 18 and 59 years with chronic neck pain and 26 healthy controls of similar age and gender were recruited into the study. Participants were instructed to walk barefoot at their maximum speed along a 10 meter walk way. Time was recorded for the intermediate 6 meters. Test was performed twice and mean maximum gait speed was calculated for analysis.

Results: Participants with neck pain demonstrated a slower gait speed during walking at maximum speed compared to the control group (p<0.001). Maximum gait speed was moderately correlated with neck pain intensity (p<0.001) and disability (p<0.01).

Conclusion: Individuals with neck pain walked slower than those without neck pain at maximum speed, indicating that gait is compromised in individuals with neck pain. Gait assessment should be considered in patients with neck pain and the timed 10 meter walk test can be used as a clinical test.

Introduction

Control of balance and gait is complex and depends on sensory inputs from visual, vestibular and somatosensory systems including cervical proprioception.[1,2] It is well documented that abnormal cervical afferent input contributes to postural instability.[2,3] Several studies demonstrated that patients with neck pain had decreased stability during both static and dynamic standing balance.[4-6] There is also a growing body of research suggesting that patients with neck pain had altered gait characteristics.[7-9] Poole *et al.* investigating gait parameters during walking with and without head turns using a stride analyzer found that elders with neck pain had a decrease in self-selected gait speed and cadence when walking with head turns.[8] Likewise, Uthaikhup *et al.* using GAITRite instrumentation demonstrated that patients with chronic neck pain had slower gait speed, shorter step length, and narrower step width during walking with head movements and at maximum speed compared to healthy controls.[9] These findings indicate that patients with neck pain have gait disturbances. However, implementing such research results in clinical practice is still limited as only sophisticated equipment like GAITRite and stride analyzer was used.[8,9]

A timed 10 meter walk test is a frequently used measurement for gait speed. It has been recommended as an important indicator of physical performance and associated

* **Corresponding author.**
Author's Address: *Department of Physical Therapy, Faculty of Associated Medical Sciences, Chiang Mai University, Thailand*
** **E-mail address:** sureeporn.uthaikhup@cmu.ac.th
doi: 10.14456/jams.2018.1
E-ISSN: 2539-6056

with risk for falls.[10-12] It is a simple, quick, and inexpensive gait evaluation.[13] It was also shown to have good validity and reliability.[14] Timed 10 meter walk test has been widely used to measure gait speed in various populations such as elderly,[15] and patients with neuromuscular,[16] neurological,[17] and orthopedic conditions.[18] It can be performed at preferred walking speed or fastest speed possible. However, evidence suggests that the fastest gait speed provide a better assessment when compared to self-selected speed as it measures the ability to adapt gait speed to environmental demands.[19]

As there is a limited evidence for a clinical assessment of gait speed in persons with neck pain, this study aimed to investigate gait speed in individuals with neck pain compared to healthy controls using timed 10 meter walk test. Gait disturbances associated with neck pain are frequently observed during challenging gait tasks.[7,20] Thus, maximum gait speed was chosen to be measured in this study. The relationships between maximum gait speed and characteristics of neck pain (intensity, duration and disability) were also determined as a previous study found a significant relationship between postural sway and pain intensity in patients with non-specific neck pain.[21] The findings of this study would support the contribution of cervical afferent input to postural control system and have a direct application to patients with neck pain.

Materials and methods

Participants

Twenty six participants (age range 18-59 years) with idiopathic neck pain and 26 healthy controls of a similar age and gender participated in the study. All participants were recruited from local hospitals, physical therapy clinics, universities and communities. To be included in the neck pain group, participants had to have neck pain for morer than 3 months with a score of at least 10 out of 100 on Thai version of the Neck Disability Index (NDI-TH).[22] They might have either dizziness or headache associated with neck pain. The control group had no history of neck pain, headache or dizziness in the past 6 months. Participants were excluded if they had a previous history of neck injury, known or suspected vestibular pathology, neurological and musculoskeletal conditions that could affect postural control, and taking more than four medications.[23] All eligible participants were asked to refrain from consuming alcohol and taking analgesic/muscle relaxant medications for at least 24 hours prior to testing.

Ethical approval for the study was obtained from the ethical review committee for research in humans, Faculty of Associated Medical Sciences, Chiang Mai University (Ref. no AMSEC-60EX-023). All participants signed a written informed consent before the commencement of the study.

Questionnaires

All participants completed a general questionnaire designed to collect demographic data, characteristics of neck pain, dizziness symptoms and treatment, if relevant. Participants with neck pain also completed a 10 cm Visual Analogue Scale (VAS) and the NDI-TH. VAS was used to measure intensity of neck pain[24] while NDI-TH was used to determine how neck pain affects an individual's daily life.[25] NDI-TH consists of 10 items including pain intensity, personal care, lifting, reading, headaches, concentration, work, driving, sleeping, and recreation.[25] Total possible score ranges from 0 to 50 and can be expressed as percentage. A higher score indicates greater disability.[25] NDI-TH was shown to be a reliable measure of functional limitation and disability in Thai persons with neck pain.[22]

Gait speed measure

The timed 10 meter walk test (TMW) was used to measure gait speed. Color tape was placed on the floor to mark the beginning and end of a 10 meter distance, with additional marking line at 2 and 8 meters. Participants were asked to walk barefoot with their maximum speed. Specific verbal instructions were given prior to the test: "I will say: ready, set, go. When I say 'Go', walk as fast as you safely can until I say stop".[26] Time for the intermediate 6 meters was measured to allow for acceleration and deceleration by a digital stopwatch.[27] Each participant performed the test twice.[28] Maximum gait speed (m/s) was calculated by dividing distance walked (6 m) by time (s) required to complete the trial. Maximum gait speed was computed for each trial and mean value was used for analysis.

Statistical Analysis

Sample size calculation was based on our pilot study (5 participants with neck pain and 5 controls). The means of maximum gait speed were 1.93±0.59 m/s for the neck pain group and 2.53±0.81 m/s for the control group. The sample size required for each group was 26 (effect size =0.80, power =0.80 and significant level =0.05).

All data were presented by descriptive statistics. Kolmogorov-Smirnov test was used to test a normal distribution of gait speed data. Independent t-tests were used to analyze differences in demographics and maximum gait speed between the neck pain and control groups. Pearson's correlation coefficients were used to determine the relationships between maximum gait speed and pain intensity (VAS score), disability (NDI-TH score) and pain duration. Significance was set at 0.05. All statistical analyses were conducted using SPSS statistical package.

Results

Demographic characteristics of the participants are presented in Table 1. There were no significant differences between the groups with respect to age, gender, weight, height, and body mass index (all $p>0.05$). Thirteen (50.00%) participants with neck pain received treatment (i.e. medicine, modalities, massage and acupuncture) to relieve their pain.

Mean and standard deviation (SD) values of maximum gait speed for the neck pain and control groups were 1.49±0.17 m/s and 1.79±0.17 m/s, respectively. Independent t-test revealed that the neck pain group had significantly slower gait speed than controls ($p<0.001$).

Results of Pearson's correlation coefficients revealed that maximum gait speed was moderately negatively

correlated with VAS and NDI-TH scores (p<0.001 and p<0.01, respectively) (Table 2). There was no correlation between maximum gait speed and pain duration (p>0.05).

Table 1 Demographic data for the neck pain and control groups.

	Neck pain (n=26)	Controls (n=26)
Age (years)	31.80±11.10	29.54±10.26
Gender (% female)	57.69	57.69
Weight (kg)	63.77±14.83	59.23±12.35
Height (cm)	163.31±8.10	162.42±9.13
Body mass index (kg/m^2)	23.87±5.28	22.42±4.12
Neck pain and disability (% NDI)	22.00±13.30	-
Neck pain intensity (0-10 VAS)	4.90±1.97	-
Neck pain duration (months)	26.46±26.36	-
Pain on the testing day (%)	84.62	-
Dizziness (%)	26.92	0

Note: *Data are presented as mean±SD unless otherwise indicated. VAS: Visual analogue scale. NDI: Neck disability index.*

Table 2 Correlations between neck pain characteristics and gait speed .

	Gait speed
Pain intensity (VAS score)	- 0.67**
Neck pain and disability (NDI score)	- 0.59*
Pain duration	- 0.22

*Note: *p<0.01, **p<0.001, VAS: Visual analogue scale, NDI: Neck disability index.*

Discussion

The study demonstrated that participants with neck pain had slower gait speed during walking at their maximum speed compared to healthy controls. There were also relationships between higher levels of pain intensity and disability and slower gait speed. Our results support the notion that patients with neck pain have altered gait characteristics which may be resulted from abnormal cervical affferent inputs.[2]

A slower gait speed in individuals with neck pain in this study is consistent with previous findings which gait speed was measured with sophicated equipments.[8,9] This may imply that timed 10 meter walk test as a clinical assessment is useful for assessing gait speed in individuals with neck pain. The mean of maximum gait speed in our neck pain participants was relatively similar to that reported in patients with neck pain in Uthaikhup et al' s study[9] (1.49±0.17 m/s in this study and 1.55±0.18 m/s in Uthaikhup et al's study). However, our participants with neck pain tend to walk slower at maximum speed compared to caucasian people with a similar age (2.34±0.34 m/s).[28] Evidence suggests that slower gait is associated with increased risk of falls.[29,30] Although the prevalence of falls in people with neck pain is unknown, decreased maximum gait speed may be associated with falls in this population, especially in more challenging enviroment.

Altered cervical afferent input may contribute to decrease in maximum gait speed in our participants with neck pain.[1,2] It is well known that afferent information from vestibular, visual, and proprioceptive systems is important for control of postural stability and locomotion.[1,31] If one source of information is disrupted, it can cause declines in the maintainance of postural stability and locomotion.[1,2] Cervical spine has a high percentage of muscle spindles providing proprioceptive information.[32,33] Previous studies suggested that pain originating in the neck could alter muscle spindle sensitivity and cervical afferent input.[2,34] Thus, decreased maximum gait speed may be due to a mismatch between aberrant cervical proprioception and other normal sensory afferent inputs, or changes in sensorimotor integration.[1,2] Alternatively, maintaining dynamic balance is suggested to be an important component of walking function.[31] A previous study demonstrated that patients with neck pain had an impaired dynamic balance when compared with healthy controls.[6] While maximum gait speed is progressively more challenged and requires greater dynamic stability,[9] a slower gait speed may be a compensation related to postural instability during walking in participants with neck pain. However, it was noted that about 27% of our individuals with neck pain reported dizziness associated with neck pain. Dizziness symptom may influence slower gait speed in our participants with neck pain. Further research in this area is warranted.

In this study, decreased gait speed was moderately

correlated to pain intensity and disability. Participants with highers level of neck pain and disability tended to walk slower than controls at their maximum speed. This result is in accordance with a previous study which demonstrated a moderate correlation between maximum gait speed and pain intensity and disability using GAITRite instrumentation.[9] No correlation between maximum gait speed and neck pain duration was found in this study. Likewise, decrease in postural stability was found to be related to a higher level of pain intensity but not pain duration in patients with neck pain.[21]

There are some limitations of this study. A few participants had dizziness associated with their neck pain. However, previous studies found impaired postural stability in neck pain patients either with or without dizziness but to a different extent.[4,35] Additionally, individuals may adjust their gait speed based on their strength. Lower extremity muscle strength was not measured in this study but our participants were relatively young and active and had no other musculoskeletal problems. Further investigation is required to clarify influence of dizziness on gait speed in patients with neck pain. A relationship between gait speed and falls in patients with neck pain should also be addressed in future research.

Conclusions

This study suggests that timed 10 meter walk test is a clinically useful measurement for assessing gait speed in individuals with neck pain. Individuals with neck pain had decreased gait speed during walking at maximum speed. Additionally, decrease in maximum gait speed was moderately correlated with higher levels of neck pain intensity and disability. Maximum gait speed should be considered in clinical assessment and mangement of neck pain.

Acknowledments

This study was funded by the Faculty of Associated Medical Sciences, Chiang Mai University, Chiang Mai, Thailand.

References

[1] Kristjansson E, Treleaven J. Sensorimotor function and dizziness in neck pain: implications for assessment and management. J Orthop Sports Phys Ther 2009; 39: 364-77. doi: 10.2519/jospt.2009.2834.

[2] Treleaven J. Sensorimotor disturbances in neck disorders affecting postural stability, head and eye movement control. Man Ther 2008; 13: 2-11. doi: 10.1016/j.math.2007.06.003.

[3] Bove M, Courtine G, Schieppati M. Neck muscle vibration and spatial orientation during stepping in place in humans. J Neurophysiol 2002; 88: 2232-41. doi: 10.1152/jn.00198.2002.

[4] Field S, Treleaven J, Jull G. Standing balance: a comparison between idiopathic and whiplash-induced neck pain. Man Ther 2008; 13: 183-91. doi: 10.1016/j.math.2006.12.005.

[5] Silva AG, Cruz AL. Standing balance in patients with whiplash-associated neck pain and idiopathic neck pain when compared with asymptomatic participants: A systematic review. Physiother Theory Pract 2013; 29: 1-18. doi:10.3109/09593985.2012.677111.

[6] Stokell R, Yu A, Williams K, Treleaven J. Dynamic and functional balance tasks in subjects with persistent whiplash: A pilot trial. Man Ther 2011; 16: 394-8. doi: 10.1016/j.math.2011.01.012.

[7] Sjostrom H, Allum JH, Carpenter MG, Adkin AL, Honegger F, Ettlin T. Trunk sway measures of postural stability during clinical balance tests in patients with chronic whiplash injury symptoms. Spine J 2003; 28: 1725-34. doi: 10.1097/01.brs.0000083170.34304.a3.

[8] Poole E, Treleaven J, Jull G. The influence of neck pain on balance and gait parameters in community -dwelling elders. Man Ther 2008; 13: 317-24. doi: 10.1016/j.math.2007.02.002.

[9] Uthaikhup S, Sunkarat S, Khamsaen K, Meeyan K, Treleaven J. The effects of head movement and walking speed on gait parameters in patients with chronic neck pain. Man Ther 2014; 19: 137-41. doi: 10.1016/j.math.2013.09.004.

[10] Cesari M, Kritchevsky SB, Penninx BW, Nicklas BJ, Simonsick EM, Newman AB, et al. Prognostic value of usual gait speed in well-functioning older people--results from the health, aging and body composition study. J Am Geriatr Soc 2005; 53: 1675-80. doi: 10.1111/j.1532-5415.2005.53501.x.

[11] Abellan van Kan G, Rolland Y, Andrieu S, Bauer J, Beauchet O, Bonnefoy M, et al. Gait speed at usual pace as a predictor of adverse outcomes in community-dwelling older people an International Academy on Nutrition and Aging (IANA) Task Force. J Nutr Health Aging 2009; 13: 881-9.

[12] Quach L, Galica AM, Jones RN, Procter-Gray E, Manor B, Hannan MT, et al. The non-linear relationship between gait speed and falls: The mobilize boston study. J Am Geriatr Soc 2011; 59: 1069-73. doi: 10.1111/j.1532-5415.2011.03408.x.

[13] Graham JE, Ostir GV, Fisher SR, Ottenbacher KJ. Assessing walking speed in clinical research: a systematic review. J Eval Clin Pract 2008; 14: 552-62. doi: 10.1111/j.1365-2753.2007.00917.x.

[14] Peters DM, Fritz SL, Krotish DE. Assessing the reliability and validity of a shorter walk test compared with the 10-Meter Walk Test for measurements of gait speed in healthy, older adults. J Geriatr Phys Ther 2013; 36: 24-30. doi: 10.1519/JPT.0b013e318248e20d.

[15] Kim H-j, Park I, Lee Hj, Lee O. The reliability and validity of gait speed with different walking pace and distances against general health, physical function, and chronic disease in aged adults. J Exerc Nutrition Biochem 2016; 20: 46-50. doi: 10.20463/jenb.2016.09.20.3.7.

[16] Pirpiris M, Wilkinson AJ, Rodda J, Nguyen TC, Baker RJ, Nattrass GR, et al. Walking speed in children and young adults with neuromuscular disease: comparison between two assessment methods. J Pediatr Orthop 2003; 23: 302-7.

[17] Nagano K, Hori H, Muramatsu K. A comparison of at-home walking and 10-meter walking test parameters of individuals with post-stroke hemiparesis. J Phys Ther Sci 2015; 27: 357-9. doi: 10.1589/jpts.27.357.

[18] Unver B, Baris RH, Yuksel E, Cekmece S, Kalkan S, Karatosun V. Reliability of 4-meter and 10-meter walk tests after lower extremity surgery. Disabil Rehabil 2017; 39: 2572-6. doi:10.1080/09638288 .2016.1236153.

[19] Beaman CB, Peterson CL, Neptune RR, Kautz SA. Differences in self-selected and fastest comfortable walking in post-stroke hemiparetic persons. Gait Posture 2010; 31: 311-6. doi:10.1016/j. gaitpost.2009.11.011.

[20] Findling O, Schuster C, Sellner J, Ettlin T, Allum JH. Trunk sway in patients with and without, mild traumatic brain injury after whiplash injury. Gait Posture 2011; 34: 473-8. doi: 10.1016/j. gaitpost.2011.06.021.

[21] Ruhe A, Fejer R, Walker B. Altered postural sway in patients suffering from non-specific neck pain and whiplash associated disorder - A systematic review of the literature. Chiropr Man Ther 2011; 19: 13. doi: 10.1186/2045-709X-19-13.

[22] Uthaikhup S, Paungmali A, Pirunsan U. Validation of Thai versions of the Neck Disability Index and Neck Pain and Disability Scale in patients with neck pain. Spine (Phila Pa 1976) 2011; 36: 1415-21. doi: 10.1097/BRS.0b013e31820e68ac.

[23] Huang ES, Karter AJ, Danielson KK, Warton EM, Ahmed AT. The association between the number of prescription medications and incident falls in a multi-ethnic population of adult type-2 diabetes patients: the diabetes and aging study. J Gen Intern Med 2010; 25: 141-6. doi: 10.1007/s11606-009-1179-2.

[24] Ara T, Iizuka H, Sorimachi Y, Iizuka Y, Nakajima T, Nishinome M, et al. Evaluation of neck pain by using a visual analog scale before and after laminoplasty in patients with cervical myelopathy: relationship with clinical results. J Neurosurg Spine 2010; 12: 635-40. doi: 10.3171/2009.12. spine09181.

[25] Vernon H, Mior S. The Neck Disability Index: a study of reliability and validity. J Manipulative Physiol Ther 1991; 14: 409-15.

[26] Marques A, Cruz J, Quina S, Regencio M, Jacome C. Reliability, agreement and minimal detectable change of the Timed Up & Go and the 10-Meter Walk Tests in older patients with COPD. J Chronic Obstr Pulm Dis 2016; 13: 279-87. doi: 10.3109/ 15412555.2015.1079816.

[27] Lindemann U, Najafi B, Zijlstra W, Hauer K, Muche R, Becker C, et al. Distance to achieve steady state walking speed in frail elderly persons. Gait Posture 2008; 27: 91-6. doi: 10.1016/j. gaitpost.2007.02.005.

[28] Bohannon RW. Comfortable and maximum walking speed of adults aged 20-79 years: reference values and determinants. Age Ageing 1997; 26: 15-9.

[29] Luukinen H, Koski K, Laippala P, Kivela SL. Predictors for recurrent falls among the home-dwelling elderly. Scand J Prim Health Care 1995; 13: 294-9.

[30] Campbell AJ, Borrie MJ, Spears GF. Risk factors for falls in a community-based prospective study of people 70 years and older. J Gerontol 1989; 44: 112-7.

[31] Shumway-Cook A, Woollacott M. Motor control: translating research into clinical practice. Philadelphia: Lippincott Williams & Wilkins; 2012.

[32] Boyd-Clark LC, Briggs CA, Galea MP. Muscle spindle distribution, morphology, and density in longus colli and multifidus muscles of the cervical spine. Spine J 2002; 27: 694-701.

[33] Kulkarni V, Chandy MJ, Babu KS. Quantitative study of muscle spindles in suboccipital muscles of human foetuses. Neurol India 2001; 49: 355-9.

[34] Flor H. Cortical reorganisation and chronic pain: implications for rehabilitation. J Rehabil Med 2003; 41: 66-72.

[35] Treleaven J, Jull G, Lowchoy N. Standing balance in persistent whiplash: a comparison between subjects with and without dizziness. J Rehabil Med 2005; 37: 224-9. doi: 10.1080/16501970510027989.

Journal of Associated Medical Sciences 2018; 51(1): 6-10

JAMS
Journal of Associated Medical Sciences

Thai-Journal Citation Index Centre (TCI) & ASEAN Citation Index (ACI)

Journal of Associated Medical Sciences

Journal homepage: https://www.tci-thaijo.org/index.php/bulletinAMS/index

Common statistical errors in logarithmic data of viral load

Suthon Vongsheree*

Department of Medical Sciences, Ministry of Public Health, Nonthaburi Province, Thailand.

ARTICLE INFO

Article history:
Received 30 June 2017
Accepted as revised 20 November 2017
Available online 3 January 2018

Keywords:
Geometric mean, logarithm, measurement uncertainty, viral load

ABSTRACT

Background: The mathematical operation of logarithm data follows the rules of logarithm as the numbers relate to specific meanings. The numbers prior to the decimal are the mantissa or the transformed power of 10 and the numbers after the decimal are the significant numbers of a given numeric data. Such operations result in errors in statistical calculations and lead to erroneous conclusions and eventual miss-interpretation of data.

Objectives: The principal aims of this study were to demonstrate and discuss several commonly made mistakes in calculation of logarithm data of viral load assays, and the subsequent errors in calculation of precision that affects the estimation of measurement uncertainty of the test.

Materials and methods: The study reviewed scholarly articles in 2017, using' viral load' as a keyword. Several sets of log data from inter-laboratory comparison of human immunodeficiency virus (HIV) load and multi-center evaluation of cytomegalovirus (CMV) load assays were used for this study to demonstrate the errors in calculation when the statistical calculations were performed using logarithm data.

Results: It was observed that presentation of average viral load data as arithmetic mean and calculation of other statistical measures directly from log viral load data was quite common, in spite of that fact that such average was log geometric mean of the viral load. Standard deviations (SD) calculated directly from log viral loads gave a new-undefined values that were irrelevant to the deviation of viral load from its mean. Such errors in SD calculation lead to extraordinarily low coefficient of variance and very low measurement uncertainty.

Conclusion: The SD, calculated from the log, and those SD calculated from the viral load per milliliter are different. Mathematically, such statistics should be calculated from the number of viruses per milliliter and could then be converted to a log scale for downstream use. Traditionally, the SD were calculated from the log which was very low. This study recommends that for all statistical measures, the absolute value is important, should use the viral load per milliliter in the calculations and then convert it into a log scale for correct usage.

* **Corresponding author.**
Author's Address: *Department of Medical Sciences, Ministry of Public Health, Nonthaburi Province, Thailand.*
** **E-mail address:** suthon.v@dmsc.mail.go.th
doi: 10.14456/jams.2018.2
E-ISSN: 2539-6056

Introduction

It is mathematically obsolete to calculate statistical measures directly from logarithmic data, given the fact that such log data have very specific meaning, *i.e.*, all numbers prior to the decimal point are only the level or the mantissa and all numbers after the decimal points are characteristics or the significant figures.[1, 2]

The value of the numbers after the decimal point are limited in the range of 1 to 10, not 0 to 1 as the normal values whereas the numbers before the decimal points range from 10 to +infinity, and not 1 to + infinity. Mathematical operations typically comply with logarithmic rules, especially when the absolute values have certain meaning or are relevant to the subsequent interventions such as human immune deficiency virus (HIV) viral load which is one of the important surrogate markers for monitoring acquired immune deficiency syndrome (AIDS) progression, which in turn determines the therapeutic failure or success for a patient. A systematic review of the accuracy and precision of HIV viral load determination methods reveal that for treatment monitoring the average intra and inter assay precision of 3-5 % for the two US-FDA approved assays, Amplicore Monitor v 1.5 and Abbott Realtime HIV-1.[3] Such extremely low precision might relate to the direct calculation of the mean and standard deviations (SD) directly from the log values and thus, reflect a very low coefficient of variance (CV). Another study described the SD of cytomegalovirus (CMV) load assays from three laboratories and reported an overall SD of 0.18 $\log_{10}$ or 0.15 copies/mL which was too low for any real assay.[4] This study, therefore presented the common errors in calculation and presentation of statistics from logarithm (log) data. Thus, one needs to avoid these errors when using HIV load as a study model for further therapeutic interventions. Results reported from this study on CMV load assays were also included in the analysis, for the completeness of the raw data and for its relevance to the statistical treatment of the data. We found that the two calculated SD were different, *i.e*. the first method used SD of logarithmic data of HIV load and the second method used logarithm of SD that were calculated from absolute data of HIV load. These conditions easily lead to confusion in data interpretation prior to any further applications.

Materials and methods

In this study, we reviewed published scholarly articles from 2017 by searching key terms such as "levels of HIV-1" using Google Scholar as a literature database to observe the presentation of the average levels of HIV loads; e.g. arithmetic and/or geometric mean. The tables of the CMV load [5] were checked for the errors in statistical calculations, using Microsoft Excel ((Microsoft Corporation, Redmond, WA). Robust statistical measures was applied for inter-laboratory comparisons of HIV loads reported from 11 medical laboratories, using AMC Robstat as a Microsoft Excel add-in program.[6]

Results

Errors in calculation and presentation of statistics from log data

From a Google Scholar search conducted on June 12, 2017, there were 2,190 research articles displaying mean or average HIV load, and 1,470 articles providing geometric mean HIV loads, whereas only 222 articles displaying arithmetic mean HIV loads. The arithmetic and geometric means were not comparable. Indeed, the arithmetic mean of log HIV load was just the log geometric mean of HIV load, if this mean was calculated directly from the summation of log HIV load divided by number of observation, as simply proved by the following calculation.

Let x_i was HIV copies/mL, and n as number of observations and geometric mean $=(x1+x2+...+xn)^{1/n}$ Then, $\log_{10}$ geometric mean of log HIV equaled $1/n(\Sigma \log x_i)$ or was equivalent to what most publications stated as mean or arithmetic mean of log HIV load.

It is obsolete to calculate and present HIV load as arithmetic mean if the study directly calculated the arithmetic mean HIV load from log HIV load, given that such an arithmetic mean is just the log geometric mean and both values are not always comparable. Such errors are demonstrated in Table 1.

Table 1 A hypothetical HIV load from an inter-laboratory comparison consensus HIV load, log copies/mL=5.85.

Laboratory	A. log HIV	B. copies/mL	C. convert B. to log	Robust Z from log	Robust Z from copies/mL
1	5.99	9.77E+05	5.99	0.256	0.573
2	5.85	7.08E+05	5.85	0.000	0.000
3	5.04	1.10E+05	5.04	-1.481	-1.273
4	5.03	1.07E+05	5.03	-1.499	-1.278
5	5.97	9.33E+05	5.97	0.219	0.479
6	5.96	9.12E+05	5.96	0.201	0.434
7	5.01	1.02E+05	5.01	-1.536	-1.288
8	5.99	9.77E+05	5.99	0.256	0.573
9	5.04	1.10E+05	5.04	-1.481	-1.273
10	5.00	1.00E+05	5.00	-1.554	-1.293
11	5.91	8.13E+05	5.91	0.110	0.233

Table 1 A hypothetical HIV load from an inter-laboratory comparison consensus HIV load, log copies/mL= 5.85. (continues)

Statistics	A. from log	B. from copies/mL	C. convert B. to log
Mean	5.526	5.318E+05	5.726
Geometric mean	5.507	3.360E+05	5.526
Median	5.850	7.079E+05	5.850
SD	0.483	4.148E+05	5.618
CV.%	8.73	78.00	78.00

Difference of arithmetic mean and geometric mean of HIV load

The information collected from the literature showed that if the data were quite closed or clustered in a narrow range, the arithmetic and geometric mean were same. This characteristic was also observed for blood pH by Boutilier and Shelton 1979.[7] Rare HIV load data sets might behave like those of blood pH variation; e.g. the HIV load from inter-laboratory comparison based on the same specimens, using the same analytical system and performed by personnel with comparable skills and competencies. The arithmetic and the geometric means were not much different when the study dealt with the variation of the last 3 digits of log data. This trend was similar to blood pH which was strictly controlled at the physiological range which is very narrow. It is clear that such conditions are not applicable to viral load data where the analytical values are far more variable.

A previous study reported on the failure in statistical calculations from log values[8] using data from a multi-centered evaluation of CMV load. This study reported that the study calculated arithmetic means from log CMV load data from 23 participants and obtained the mean CMV loads in $\log_{10}$ as 2.96, 3.81, 4.77 and 5.66 copies/mL. In contrast, the mean CMV load calculated from copies/mL and converted into $\log_{10}$ were 3.33, 4.21, 5.14 and 6.19 copies/mL for the samples of known CMV load of 2.7, 3.7, 4.7 and 5.7 copies/mL respectively. These errors are described in details in Table 2.

Table 2 Mean CMV load in log scales from 23 laboratories participating the multi-center evaluation of CMV load assays.

	Known CMV Viral DNA Panel			
Laboratory	**2.70 copies/mL**	**3.70 copies/mL**	**4.70 copies/mL**	**5.70 copies/mL**
1	4.12	4.37	5.08	5.97
2	*	*	4	4.78
3	3.27	4.04	5.18	5.74
4	2.92	3.89	5.01	5.75
5	2.54	3.17	4.47	5.02
6	3.02	3.64	4.79	5.94
7	3.53	4.72	5.77	6.58
8	3.06	3.98	4.97	6.02
9	2.79	3.59	4.76	5.7
10	3.36	4.31	5.27	6.25
11	2.77	3.84	4.92	5.93
12	2.98	3.76	4.63	5.68
13	2.59	3.8	4.71	5.66
14	4.08	5.2	6.1	7.25
15	2.04	3.2	4.26	5.56
16	2.71	3.68	4.73	5.67
17	*	3.45	4.14	4.75
18	2.51	3.5	4.62	5.63
19	*	3.29	4.3	4.97
20	2.6	3.68	4.72	5.68
21	2.53	3.54	4.46	5.47
22	2.3	2.95	3.74	4.83

*(*CMV loads were less than 50 copies/mL, statistics are calculated directly from log CMV load values with the values calculated from copies/mL in parenthesis after each statistics)*

Table 2 Mean CMV load in log scales from 23 laboratories participating the multi-center evaluation of CMV load assays. (continues)

	Known CMV Viral DNA Panel			
Laboratory	**2.70 copies/mL**	**3.70 copies/mL**	**4.70 copies/mL**	**5.70 copies/mL**
23	3.41	4.3	5.04	5.45
Mean*	2.96 (3.33)	3.81 (4.21)	4.77 (5.14)	5.66 (6.19)
SD*	0.54 (3.57)	0.53 (4.53)	0.53 (5.43)	0.58 (6.56)
%CV*	18.40 (171)	13.86 (209)	11.17 (196)	10.20 (256)

*(*CMV loads were less than 50 copies/mL, statistics are calculated directly from log CMV load values with the values calculated from copies/mL in parenthesis after each statistics)*

Most seriously affected statistics were calculated directly from log values of SD

The SD reported in the articles were a new terminology since mathematical operations do not conform to logarithmic rules. The SD from log viral load were irrelevant to the SD of viral load, and thus, could not be converted back to the SD since it was SD of the log values. The common characteristics of these special SD were extraordinarily low SD, typically as low as 0.5 or lower. From the same study on CMV load, very low SD of four samples as log CMV as 0.54, 0.53, 0.53 and 0.58 copies/mL were reported, which when converted to copies/mL were 3.5, 3.4, 3.4, and 3.8 copies/mL, respectively. When SD is computed from copies/mL, the SD after conversion into log scales are 3.57, 4.53, 5.43, and 6.56 which when converted into copies/mL were 3.7×10^3, 3.4×10^4, 2.7×10^5, 3.6×10^6 copies/mL, or 10^3 to 10^6 folds to those calculated from the log viral load data, respectively. Such irrelevant SD showed lower deviation and claimed higher precision of the assay as very low SD.

One suggestion for handling these log SD viral load was that simple addition and subtraction of anti log SD should not be performed, but multiplication and division are acceptable. This approach does not have a sound basis for this specific special treatment of SD, given that SD is a measure of deviation from mean. For example, mean CMV load and SD in log scale were 2.7 and 0.5, respectively, where mean+SD should have been 2.7+0.5 or anti log 3.2 which corresponds to only 1,585 copies/mL. However, the general operation resulted in antilog 2.7 + antilog 0.5 equal to 504 copies/mL. Both are irrelevant to the SD of the test assay of 3.57 log CMV load which corresponded to 4,217 copies/mL.

The use of plasma HIV RNA levels as surrogate markers[9] for monitoring the progression of AIDS and efficacy of therapy, as a threefold change or 0.5 log scale change was derived from another study cohort. This three-fold change was one of the strongest predictor, but the three-fold change was not derived from the precision or corresponding SD of any laboratories, except that the same laboratory produced this data.

Erroneous calculation of mean and SD resulted in the estimation of measurement of uncertainty of the test method

At least two types of uncertainties add up to represent the measurement of uncertainty of a quantitative evaluation system. Type A uncertainties are those of quality control material used in routine works and type B uncertainties relate to the calibrators provided from the manufacturers. From the CMV data mentioned earlier, if mean and SD were both calculated directly from log CMV as 2.7 and 0.54, the relative type A uncertainty would be 3.5/501 or 0.007 copies/mL and the standard uncertainty of type B was calculated to be 3 %. According to the policy and requirement on estimation of uncertainty measurement and traceability N0715007 of Thailand Accreditation Body,[10] the combined relative uncertainty is defined as the square root of summation of (relative uncertainty) 2 which equals to 0.031 and the expanded uncertainty is only 0.062 copies/mL. However, the corrected mean and SD of 3.33 and 3.57 expanded the uncertainty to 3.48 copies/mL or 56 times more than those calculated from logarithm values. For log CMV of 2.8, a physician might get wrong uncertainty and would predict the result as 631±39 copies/mL for the measurement of uncertainty using direct calculation from the logarithm value while the corrected one would be 631±2194 or 0-2825 copies/mL.

Algorithm A for robust z-score analysis of the proficiency testing result.

There was no indication that such log values could be directly analyzed by this robust z-score statistics. Fortunately, robust statistics used median as the average and the final grading of participant laboratory results of log viral load was still the comparable to using copies/mL. However, the value of each z-score has a specific meaning, not just satisfied or not, but also how the values were far from the consensus ones, thus, helping the participant laboratories to improve their testing quality. Some robust statistics are illustrated in Table 1.

Discussion

Direct calculation of arithmetic mean from log viral load data yields a false arithmetic mean as it is just a log geometric mean of the HIV load. Direct calculation of standard deviation provides a new undefined statistical measure which tends to over express extremely low SD and hence provide extraordinarily high precision as well as very low measurement uncertainty. The robust z-scores for scoring the laboratory-specific performance of the participants in proficiency testing programs using log data certainly provide imprecise and unreliable results. These errors may affect the clinical usage of the viral load when such precision

is low and might alter the treatment by misleading lower precision of the assay. This study has reviewed such errors and has suggested calculation of statistics directly from the viral copies/mL and then performing a log-transformation for further applications. The measurement of uncertainty may also apply the mean and SD from the copies/mL of internal quality control (QC) as type A uncertainty and acquire type B uncertainty from the manufacturer that is derived from the copies/mL. However, this study only showed that SD calculated by both methods, one using log of SD and the other was SD of log, were not the same at all, and are neither comparable nor convertible. More exhaustive mathematical studies shall verify this claim in future studies. However, the QC of laboratory report will be confusing for actual SD transformed to log scale which is different from standard methods using SD of log HIV load values. This study therefore reminds investigators dealing with log data if its absolute value would be interpreted to some comparison such as the viral load assays. The paper does not lower the value of logarithm for other purposes that apply relative log values in risks modeling or logistic regression. More exhaustive approaches may be needed to gather insights on suitable application of these data.

Acknowledments

The author would like to thank Dr. Biswapriya B. Misra, Texas Biomedical Research Institute, for kindly and timely revising and editing the manuscript and thank Ms. Prasan Julwong for her assistance in preparation of this manuscript.

References

[1] PurpleMATH. Basic log rules & Expanding log expression. Illinois, USA [cited 2018 Jul 4]. Available from: http://www.purplemath.com/modules/logrules.htm

[2] Sollis KA, Smit PW, Fiscus S, Ford N, Vitoria M, Essajee S, Barnett D, et al. Systematic review of the performance of HIV viral load Technologies on plasma samples. PLoS One 2014; 9(2): e85869.

[3] Grys TE, Duquette D, White B, Irish C, Hata DJ, Pritt BS. Precision across the analytical measuring range of a quantitative real-time PCR assay for cytomegalovirus detection among three clinical laboratories. JCM 2011; 49(8): 3044-6.

[4] Wolff DJ, Heaney DL, Neuwald PD, Stellrecht KAS, Press RD. Multi-site PCR-based CMV viral load assessment-assays demonstrate linearity and precision, but lack numeric standardization. J Mol Diag 2009; 11(2): 87-92.

[5] Royal Society of Chemistry. MS Excel Add-in for Robust Statistics. Cambridge, UK [cited 2017 Jul 4] Available from: http://www.rsc.org/errorpage.asp?404;http://www.rsc.org:80/membership/networking/interestgroups/analytical/amc/software/RobustStatistics.asp

[6] Boutilier RG, Randall DJ, Shelton G and Toews DP. Acid-Base relationships in the blood of the toad, Bufo marinus. J Exp Biol 1979; 82: 357-65.

[7] Vongsheree S, Keardrit K, Muenphon S, Homchan M, Dissara P . Failure in calculating the statistics from logarithm values: Case Study. Bull. DMSC 2015; 57(2): 197-203.

[8] U.S. Department of Health and human services. Guidelines for the use of antiretroviral agent in HIV-1 infected adults and adolescents. [cited 2017 Aug 25]. Available from: https://aidsinfo.nih.gov/guidelines/html/1/adult-and-adolescent-arv-guidelines/458/plasma-hiv-1-rna--viral-load--and-cd4-count-monitoring

[9] The Bureau of Laboratory Quality Standards, BLQS DMSC. Policy and requirement on estimation of uncertainty measurement and traceability. N0715007. [cited 2018 Jul4]. Available from: http://dmsc2.dmsc.moph.go.th/webroot/qa/webblqs/userfiles/N%2007%2015%20007%20Rev.03.pdf

Journal of Associated Medical Sciences 2018; 51(1): 11-18

JAMS
Journal of Associated Medical Sciences

Thai-Journal Citation Index Centre (TCI) & ASEAN Citation Index (ACI)

Journal of Associated Medical Sciences

Journal homepage: https://www.tci-thaijo.org/index.php/bulletinAMS/index

Investigation of sulfated glycosaminoglycans and their agarose gel electrophoresis patterns from plant extracts

Kanyamas Choocheep* **Chidchanok Saenkham** **Supawita Borwornchaiyarit** **Kanlayanee Chaiisaraseree** **Jariya Chimchai** **Thunyaluk Moonpa**

Division of Clinical Chemistry, Department of Medical Technology, Faculty of Associated Medical Sciences, Chiang Mai University, Chiang Mai , Thailand

ARTICLE INFO

Article history:
Received 20 November 2017
Accepted as revised 18 December 2017
Available online 15 January 2018

Keywords:
DMMB, uronic acids, glycosaminoglycans, agarose gel electrophoresis, spectrophotometry

ABSTRACT

Background: Many kinds of sulfated glycosaminoglycans (GAGs) play an essential role in both physiological and pathological conditions. Most of them are obtained from animal sources, and used as nutraceuticals or therapeutic applications.

Objectives: In this study, we aimed to screen for the presence of sulfated GAGs from 8 locally available plants, including ginger (*Zingiber officinale*), turmeric (*Curcuma longa*), star fruit (*Averrhoa carambola*), Namwa banana (*Musa ABB* 'Kluai Namwa'), bitter gourd (*Momordica charantia*), purple-fruited pea eggplant (*Solanum trilobatum*), noni (*Morinda citrifolia*), and finger root (*Boesenbergia rotunda*).

Materials and methods: All plants were extracted, and sulfated GAGs from the extracts were investigated by dimethylmethylene blue (DMMB) dye-binding assay, uronic acid assay, UV-Vis spectrophotometry, and agarose gel electrophoresis.

Results: DMMB dye-binding and uronic acids assays revealed the presence of sulfated GAGs in all extracts with various degrees of sulfated GAGs levels. These results correlated to UV-Vis spectrophotometry that showed the maximum absorbance peaks from all extracts at 190-210 nm, which was similar to sulfated GAGs standard absorption. Interestingly, agarose gel electrophoresis suggested that sulfated GAGs in all extracts exhibited diverse patterns in alcian blue, toluidine blue and safranin O staining.

Conclusion: Our results indicate that all plant extracts contain sulfated GAGs at certain levels, which could be a new approach for future study in bioprospecting.

Introduction

Glycosaminoglycans (GAGs), also called heteropolysaccharides or mucopolysaccharides, are classified as carbohydrates. Their structures consist of long linear polymer of repeated disaccharide units, comprising uronic acids with either N-acetylglucosamine (GlcNAc) or N-acetylgalactosamine (GalNAc).[1] There are two types of GAGs depending on their sulfation: non-sufated GAGs, such as hyaluronic acid (HA); and sulfated GAGs, such as chondroitin sulfate (CS), dermatan sulfate (DS), heparin (HP), heparan sulfate (HS), and keratan sulfate (KS).[2-4] These GAGs are naturally found in animals, and most of them are incorporated with core proteins to form proteoglycans (PGs) in the extracellular matrix (ECM), or plasma membrane in various cell types. The GAGs backbone of PGs (also PGs themselves) play an important role in both physiological and pathological conditions, including inflammation, wound healing, coagulation cascade, cell behavior, tissue development, tumorigenesis and metastasis.[5-17] Owing to their functions, some medical aspects of GAGs as nutraceuticals or therapeutic applications are widely studied, and most of them are

* **Corresponding author.**
Author's Address: *Division of Clinical Chemistry, Department of Medical Technology, Faculty of Associated Medical Sciences, Chiang Mai University, Chiang Mai , Thailand*
** **E-mail address:** kanyamas.c@cmu.ac.th
doi: 10.14456/jams.2018.3
E-ISSN: 2539-6056

derived mainly from animal sources.[18,19] For example, CS derived from bovine and shark cartilage is used as pharmacological agent or dietary supplement for osteoarthritis treatment.[20-23] Pharmaceutical heparin, usually obtained from bovine lung or porcine intestinal mucosa, is also used as anti-thrombotic agent.[24,25] In contrast to GAGs isolated from animal sources, little is known about GAGs isolated from plants. However, some studies have implied the presence of GAGs, and their biological effects from some plant species. For instance, there have been found GAGs which show heparin-like activity in the higher plants, including *Filipendula ulmaria*, *Paeonia anomala,* and *Paeonia suffruticosa*.[26-28] The presence of GAGs-like glycans have been observed in marine plants; *Ruppia maritima, Halodule wrightii, Halophila decipiens, Avicennia schaueriana, Rhizophora mangle*; and freshwater plants; *Eichhornia crassipes, Hydrocotyle bonariensis, Nymphaea ampla*.[29-31] Interestingly, the study of *Orthosiphon stamineus*, a medicinal plant which is widely distributed in Malaysia, and also Africa, revealed the presence of GAGs structure with uronic acids by FTIR and NMR analysis.[32] In addition, previous studied have exhibited the pressence of GAGs in crude garlic and mushroom extracts, which were detected by dimethylmethylene blue (DMMB) dye-binding assay and UV-Vis spectrophotometry.[33,34] As a consequence to these findings, we thought that screening for GAGs from terrestrial plants should be an interesting approach. Hence, the aim of this study was to screen for the presence of sulfated GAGs from 8 terrestrial plant extracts, including ginger, turmeric, star fruit, Pisang Awak banana, purple-fruited pea eggplant, bitter gourd, noni, and finger root.

Materials and methods

1. Preparation of plant extracts

One hundred grams of each sample, comprising ginger (*Zingiber officinale*), turmeric (*Curcuma longa*), star fruit (*Averrhoa carambola*), Namwa banana (*Musa ABB* 'Kluai Namwa'), bitter gourd (*Momordica charantia*), purple-fruited pea eggplant (*Solanum trilobatum*), noni (*Morinda citrifolia*), and finger root (*Boesenbergia rotunda*) were extracted as previously described with some modifications.[35] Briefly, each sample was extracted in deionized water pH 4.5 at 37 ° C in water bath for 18 hours. Then, the extracts were boiled for 10 minutes, filtered through a muslin cloth and Whatman filter papers, and centrifuged. After that, supernatant of the extracts was collected, and the same extracts were pooled together. These crude plant extracts were then lyophilized, and stored at -20° C until they were used for the experiments. About 5 mg of each plant extract powder was dissolved in 1 mL of deionized water, and subjected to analyses unless otherwise noted.

2. Measurement of glycosaminoglycan levels

The levels of sulfated GAGs in the extracts were determined by 1,9-dimethylmethylene blue (DMMB) dye-binding (Sigma-Aldrich, USA) assay using chondroitin sulfate (CS) (Sigma-Aldrich, USA) as standard.[36] Briefly, 50 µL of either the extracts or standards were added into 96-well plates. Next, 200 µL of DMMB solution was added, and the mixtures were mixed. Then, the absorbance was read at 630 nm. The levels of GAGs were estimated by the calibration curve of chondroitin sulfate standards against their known concentrations.

3. Measurement of uronic acid levels

The levels of uronic acids in the extracts were measured by carbazole reaction using D-glucuronic acid lactone (Sigma-Aldrich, USA) as standard.[37] Briefly, 60 µL of either the extracts or standards were incubated with 300 µL of carbazole reagent A at 100° C for 15 minutes. Then, they were cooled down in ice slurry. After that, the mixtures were added with 12 µL of carbazole reagent B, incubated at 100° C for 15 minutes, and cooled down. The absorbance was read at 562 nm. The levels of uronic acids were estimated by the calibration curve of D-glucuronic acid lactone standards against their known concentrations.

4. UV-Vis spectrophotometry analysis

The extracts were examined by spectrum mode on UV-Vis spectrometer (UV2401, Shimadsu, Japan), using chondroitin sulfate as GAGs standard. Then, standard and the extracts at 50 µg/mL in deionized water were scanned from 190 to 700 nm, and analyzed.

5. Agarose gel electrophoresis

GAGs from the extracts were analyzed by agarose gel electrophoresis with some modifications.[38] Briefly, loading buffer was mixed with standards and the extracts. Then, 5 mg of GAGs chondroitin sulfate standard (Sigma, USA), or 50 mg of each extract except finger root and ginger which was used at 70 mg, were applied to a 1% agarose gel having a thickness of about 5 mm, and run for 30 minutes at 70 V in TBE buffer. Next, GAGs were fixed in the gel with 0.1% N-cetyl-N,N,N-trimethylammonium bromide (CTAB) solution for overnight at room temperature. After that, air-dried the gels for 2 hours, they were then stained with 0.5% (w/v) alcian blue (Himedia laboratories, India) in 2% acetic acid for 2.5 hours, 0.1% (w/v) toluidine blue (Sigma, USA) in acetic acid/ethanol/water (1:50:49, v/v) for 2 hours, and 0.1% safranin O (Merck, USA) for 3 hours, respectively. Then, the gels were destained, and photographed by G:BOX F3 gel documentation system (GeneSys, USA).

6. Statistical analysis

Data were presented as mean with standard deviation. Student's t-test was used to analyze the association of GAGs levels in DMMB dye-binding, and uronic acids assays. The significant difference was considered at $p<0.05$.

Results

Glycosaminoglycans screening of the plant extracts

The levels of glycosaminoglycans (GAGs) in the extracts were shown in Figure 1. All extracts contained GAGs in various degrees. The highest level was observed in tumeric, followed by star fruit, ginger, banana, noni, bitter gourd, finger root, and purple-fruited pea eggplant, respectively. In addition, when compared GAGs levels of other plant extracts to ginger, the significant difference of GAGs levels

was observed in all the extracts except banana, and noni. These results suggested that the variation of GAGs levels highly depends on the kinds of plants.

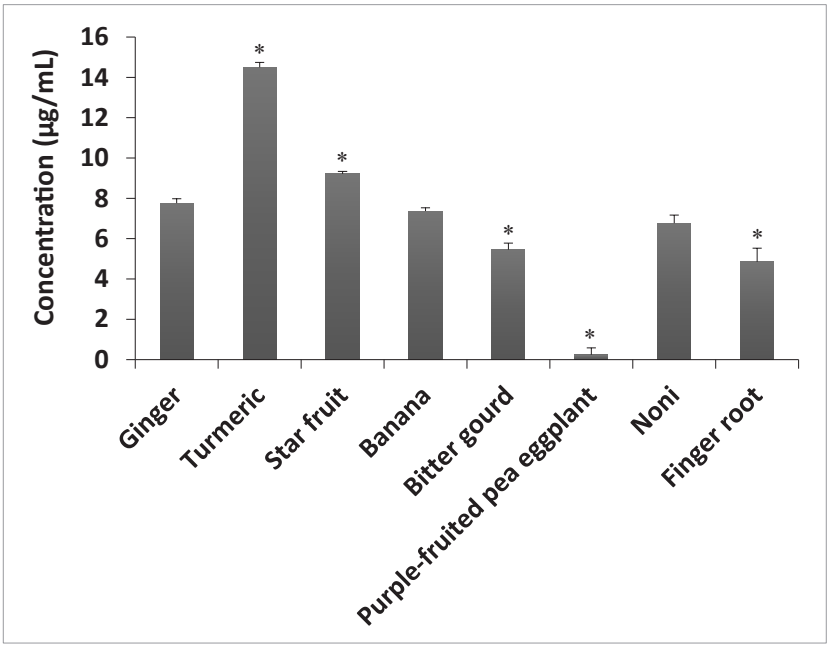

Figure 1. *Dimethylmethylene blue (DMMB) dye-binding assay of glycosaminoglycans from 8 plant extracts. Note: The levels of sulfated GAGs in the 8 plant extracts presented as mean±S.D. Asterisks (*) indicate significant difference from ginger (t- test, *p<0.05).*

Uronic acids content of the plant extracts

The levels of uronic acids in the extracts were shown in Figure 2. The highest level of uronic acids was observed in noni, followed by banana, star fruit, purple-fruited pea eggplant, bitter gourd, ginger, turmeric, and finger root, respectively. These results supported the presence of GAGs in all extracts because uronic acids were incorporated as a subunit of GAGs chains. However, when compared uronic acids levels of other plant extracts to ginger, the significant difference of uronic acids was observed only in star fruit, banana, and noni. Therefore, it seemed likely that uronic acids content was slightly different among the plants used in this study.

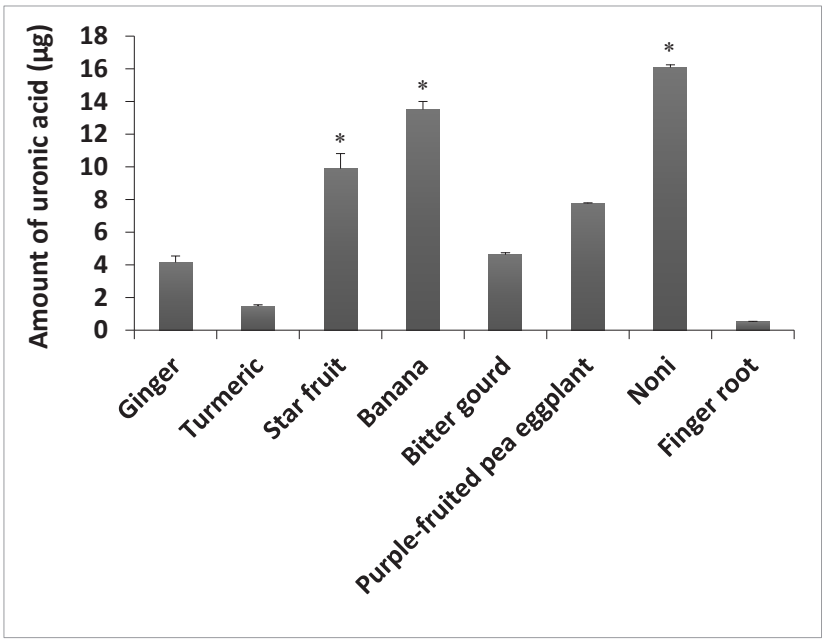

Figure 2. *Uronic acids assay of glycosaminoglycans from 8 plant extracts. Note: The levels of uronic acids in the 8 plant extracts presented as mean±S.D. Asterisks (*) indicate significant difference from ginger (t- test, *p<0.05).*

UV-Vis spectrophotometry analysis

Scanning UV-Vis spectra of the extracts was observed in Figure 3. The results demonstrated that CS standard had the maximum absorption at 190 nm (peak shown without any arrow). In addition, we also found that most extracts, including ginger, turmeric, star fruit, bitter gourd, purple-fruited pea eggplant, and noni had the same absorption patterns around 190-210 nm that resembled to CS standard, as indicated by the arrows in Figure 3, A-C and E-G, respectively. Though, the absorption patterns from banana and finger root extracts (Figure 3, D and H) showed a lesser extent of absorbance near 190-210 nm, their absorption patterns were also similar to most extracts and standard. These results suggested the presence of GAGs because the carboxylate chromophore of iduronic acid, glucuronic acid, and N-acetyl chromophores presented in the GAGs chains were found at peak 190-210 nm.[2,3,38]

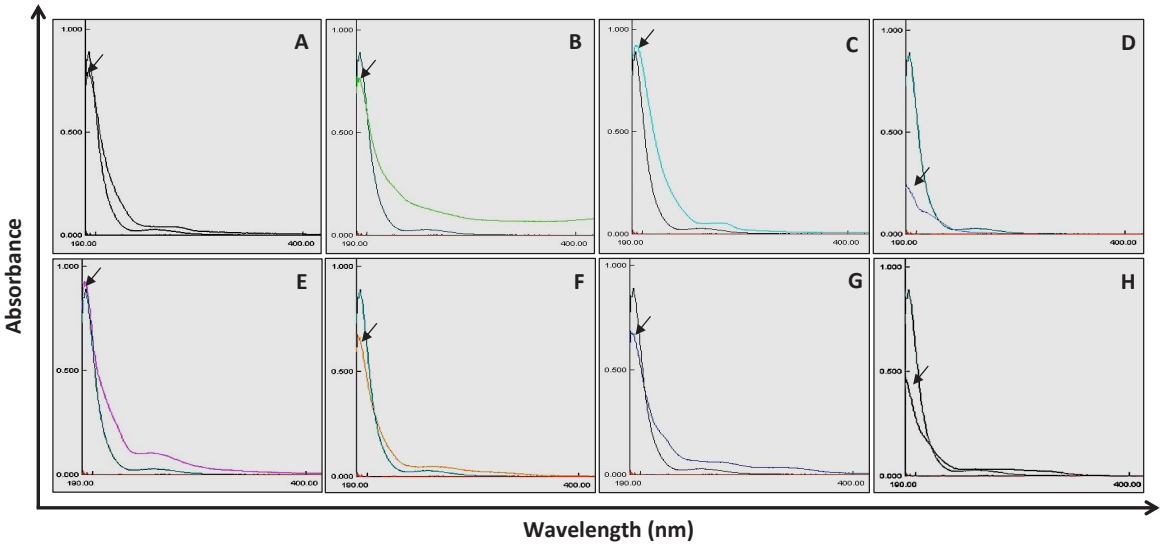

Figure 3. *UV-Vis spectrophotometry patterns of glycosaminoglycans from 8 plant extracts. Peaks of plant extracts are indicated by the arrows. A, ginger; B, turmeric; C, star fruit; D, banana; E, purple-fruited pea eggplant; F, bitter gourd; G, noni; and H, finger root.*

Agarose gel electrophoresis patterns

A qualitative analysis of the GAGs from the extracts was carried out by agarose gel electrophoresis in Figure 4. The staining pattern of CS standard (MW≈60kDa) was seen in lane 1 (Figure 4, A-C). For alcian blue staining, there was considerably faint band of GAGs from ginger extract above standard, and there were 2 bands of GAGs from turmeric extract; one band was above, and the other band was below standard (Figure 4A, lane 2 and 3). In contrast, for toluidine blue and safranin O stainining, there were bands of GAGs from ginger and turmeric extracts presenting near the site of standard (Figure 4B and 4C, lane 2 and 3). The staining patterns of the extracts, comprising star fruit, banana, purple-fruited pea eggplant, bitter gourd, and noni similarly exhibited large bands of GAGs above and overlap standard (Figure 4B and 4C, lane 4-8) except the small faint bands of GAGs from finger root extracts that appeared near the site of standard (Figure 4B and 4C, lane 9), which could be observed in all kinds of the staining dyes. These results indicated the presence of GAGs at different sizes from the extracts.

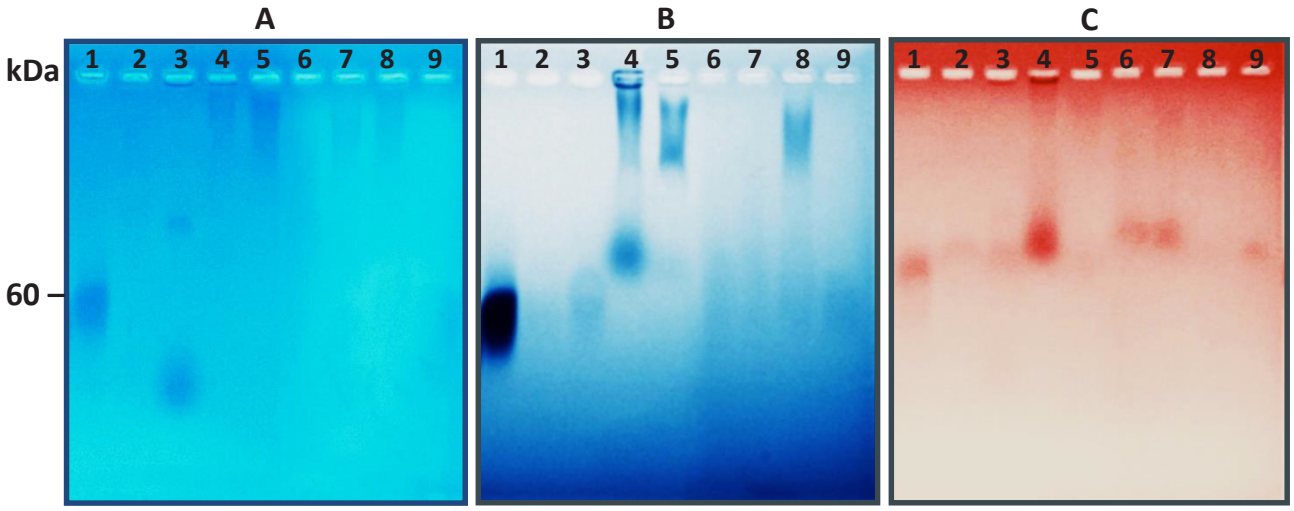

Figure 4. *Agarose gel electrophoresis of 8 plant extracts. A, alcian blue staining; B, toluidine blue staining; and C, safranin O staining. Lane 1, standard chondroitin sulfate (~60 kDa); Lane 2-9, ginger, turmeric, star fruit, banana, purple-fruited pea eggplant, bitter gourd, noni, and finger root, respectively.*

Discussion

In this study, we screened for the presence of GAGs from plant extracts by DMMB dye-binding and uronic acid assays. DMMB dye-binding assay is the most common cationic dye used to quantify sulfated GAGs in tissue samples, culture media, and bodily fluids.[36,39,40] The ability of DMMB method to detect GAGs is based on the binding to sulfated GAGs, and results in DMMB dye shift.[41] However, the limitation of this method is the interference from other polyanionic substances that can cause false negative results.[42] Since the levels of uronic acids from purple-fruited pea eggplant extract was rather high, the very low levels of GAGs from purple-fruited pea eggplant extract detected by DMMB dye-binding method could be due to some interferences. The simple subunit of GAGs is composed of long chains of repeated disaccharide units, comprising uronic acids with either GlcNAc or GalNAc.[1] Thus, the measurement of uronic acids is another method that can be used for GAGs screening.[37] However, there have been reported that detection of GAGs by the measurement of uronic acids through carbazole reaction is less sensitive than DMMB dye-binding method, and may be interfered by some sugars or salts.[42-44] These may lead to the explanation why the levels of uronic acids in each extract are not relatively shown as the similar trend levels of GAGs measured by DMMB dye-binding assay. For spectrophotometric analysis, it is thought to be the consequence of the carboxylate chromophore of iduronic acid, glucuronic acid, or N-acetyl chromophores at peaks 190-210 nm which suggested the presence of GAGs in all extracts. This evidence supports the presence of GAGs detected by DMMB dye-binding, and uronic acids assays. Nevertheless, previous studies found that the peaks of these chromophores are only slightly shifted among different GAGs types.[45, 46] Hence, it seems unlikely that this method could specifically distinguish the types of GAGs.[2, 3, 38] Though each method, including DMMB dye-binding method, uronic acids assay, and spectrophotometry has some limitations, a detection of GAGs is still reliable when thoroughly interpreted the correlation among these methods. Thus, further investigation of GAGs should be considered to implement other reliable analytical techniques, such as high-performance liquid chromatography (HPLC), magnetic resonance spectroscopy (NMR), mass spectrometry (MS), and disaccharide analyses.[40]

Agarose gel electrophoresis is one of the most qualitative and quantitative techniques used to evaluate GAGs in the mixtures.[47] It is also applied for various purposes, such as separation of GAGs from tissues, organs, or biological fluids, determination of GAGS content and purity for pharmaceutical application, utilization in the medical field for screening monitoring, and diagnosis for mucopolysaccharidoses (MPS).[40, 47-49] In this study, the presence of sulfated GAGS were confirmed by an agarose gel electrophoresis. After their separation, the visualization of sulfated GAGs are based on their negative charged carboxyl and sulfate groups binding to cationic dyes, such as alcian blue, toluidine blue, and safranin O. Our results showed that the staining patterns of most extracts, including star fruit, banana, purple-fruited pea eggplant, bitter gourd, noni, and finger root were similarly observed in all 3 staining dyes. In contrast, alcian blue staining patterns of sulfated GAGs from ginger and turmeric extracts were different from the patterns seen in the other dyes. These are perhaps cause by some substances in the extracts, which are still intriguing for further study. Though, all 3 cationic dyes can stain sulfated GAGs and show the similar patterns of staining GAGs, we observed various degrees of more intense staining of GAGs from toluidine blue, alcian blue, and safranin O, respectively. This is probably due to the fact that toluidine blue has a higher affinity for the sulfur compared to safranin O.[50] Also, toluidine blue and alcian blue have different limit of detection for sulfated GAGs staining because it depends on the procedures used.[47] Thus, staining by toluidine blue is particularly suited for our study. As we did not have standards of several GAGs types with various molecular mass, we used CS-C standard for the estimation of GAGs size. It seems likely that the size of GAGs found in most extracts were supposed to be ≥60 kDa because the results exhibited large bands of GAGs above and overlap the area of standard. However, it could not surely estimated the size of GAGs, for these crude extracts are not well treated or purified. To specifically identify the size of actual GAGs present by electrophoresis separation, it is needed to purify the extracts, treat with GAGS degrading enzymes, i.e. chondroitinase ABC, heparin lyase, or heparinase, and it is then subjected to electrophoresis with different molecular mass of standards.

GAGs are mainly found in animals, particularly in vertebrates. They are widely studied in both physiological and pathological circumstances, and also used as nutraceuticals or therapeutic applications in some certain conditions or diseases.[5-19] Due to these extensively studies, they are well known for their structures which consist of repeating disaccharides units of uronic acids with either GlcNAc or NGalNAc with distinct sulfation pattern.[1-4] In contrast, little is known about the structure of GAGs and their biological functions from plants; however, some studied have reveled the presence of GAGs or GAGs-like glycans from some plant species. For example, the presence of GAGs-like glycans have been observed in marine plants.[9, 10] In addition, monosaccharides found in GAGs-like glycans from the root of freshwater plants, especially *Eichhornia crassipes*, contain galactose, glucose and arabinose.[29] A terrestrial medicinal plant, *Orthosiphon stamineus*, also contains uronic acids as a subunit of GAGs structure.[32] Besides these plants, it is interesting that there is another rich non-animal source of sulfated glycans obtained from seaweeds. In seaweeds, the structure of sulfated glycans depends on the type of them. For instance, the most well known brown seaweed contains sulfated fucans that mostly composed of α-L-fucose polymers.[51] Green and red seaweeds contain sulfated galactans which mosly contain β-D-galactose polymers.[51] It is noticed that most sulfated glycans found in brown, green, and red seaweeds are composed of repeating disaccharides units with several patterns of sulfation. They also exhibit various biomedical functions in inflammation, coagulation, angiogenesis, cell adhesion, and involve many pathophysiological systems.[51] Taken together, the structures of GAGs or sulfated glycans from plants, and another non-animal source, such as seaweed

usually contain long chains of simple sugars polymers, which rather different from GAGs polymers of animals. However, they are all similar in term of sulfation. In this study, we measured GAGs by DMMB dye-binding method, using animal GAGs as standard. As mentioned above, the structures of GAGs from plants are rather different from animals GAGs polymers, but all of them still have degree of sulfation. Since the ability of dye-binding method to detect GAGs is based on the binding to sulfated GAGs, we think that any sulfated glycans from non-animal sources could be quantified by this method. In addition, de Araújo et al. also performed DMMB dye-binding method to monitored sulfated polysaccharides obtained from red seaweed.[52] On the other hand, we also realize that it would be more reliable if we use non-animal standard to estimate the concentration of GAGs from plants for future study.

As we could observe from our current study, we think that the tentative potential benefits of GAGs obtained from the plant extracts may be further used as a source of non-animal nutraceuticals, especially they may be useful for vegetarian diet. However, we could not surely conclude whether it can be used instead of animal GAGs because some studies about the purity, structure, and clinical trials of them are still left to be elucidated.

Conclusion

Our results have shed new light on the investigation of sulfated GAGs that contain in the plant extracts. This evidence supports the view that plants heteropolysaccharides as bioprospecting should not be disregarded.

Conflict of interests

The authors declare that they have no conflict of interests regarding the publication of this paper.

Acknowledgements

We would like to express our sincere thanks to division of microbiology for the gel documentation system support. We also would like to thank Dr. Preeyanat Vongchan, division of transfusion science, for standard glycosaminoglycans supply, and Thailand excellence center for tissue engineering and stem cells, department of biochemistry, faculty of medicine, for technical assistance and consultation.

References

[1] Scott JE. Supramolecular organization of extracellular matrix glycosaminoglycans, in vitro and in the tissues. FASEB J 1992; 6(9): 2639–45.

[2] Kjellén L, Lindahl U. Proteoglycans: structures and interactions. Annu Rev Biochem 1991; 60: 443–75.

[3] Varki A, Cummings RD, Esko JD, Stanley P, Hart G, Aebi M, et al., editors. Essentials of Glycobiology [internet]. Cold Spring Harbor Laboratory Press; 2009 [cited 2017 May 30]. Available from: http://www.ncbi.nlm.nih.gov/books/NBK1900/2009.

[4] Prydz K, Dalen KT. Synthesis and sorting of proteoglycans. J Cell Sci 2000; 113 (Pt 2): 193–205.

[5] Souza-Fernandes AB, Pelosi P, Rocco PRM. Bench-to-bedside review: the role of glycosaminoglycans in respiratory disease. Crit Care 2006; 10(6): 237. doi: 10.1186/cc5069.

[6] Pomin VH. Sulfated glycans in inflammation. Eur J Med Chem 2015; 92: 353–69.

[7] Wight TN, Kang I, Merrilees MJ. Versican and the control of inflammation. Matrix Biol 2014; 35: 152–61.

[8] Kosir MA, Quinn CC, Wang W, Tromp G. Matrix glycosaminoglycans in the growth phase of fibroblasts: more of the story in wound healing. J Surg Res 2000; 92(1): 45–52.

[9] Ghatak S, Maytin EV, Mack JA, Hascall VC, Atanelishvili I, Moreno Rodriguez R, et al. Roles of Proteoglycans and Glycosaminoglycans in Wound Healing and Fibrosis. Int J Cell Biol 2015; 2015: 834893. doi: 10.1155/2015/834893

[10] Bourin MC, Lindahl U. Glycosaminoglycans and the regulation of blood coagulation. Biochem J. 1993; 289(2): 313–30.

[11] Yamada S, Sugahara K. Potential therapeutic application of chondroitin sulfate/dermatan sulfate. Curr Drug Discov Technol 2008; 5(4): 289–301.

[12] Smith RAA, Meade K, Pickford CE, Holley RJ, Merry CLR. Glycosaminoglycans as regulators of stem cell differentiation. Biochem Soc Trans 2011; 39(1): 383–7.

[13] Tanino Y, Coombe DR, Gill SE, Kett WC, Kajikawa O, Proudfoot AEI, et al. Kinetics of chemokine-glycosaminoglycan interactions control neutrophil migration into the airspaces of the lungs. J Immunol 2010; 184(5): 2677–85.

[14] Suwan K, Choocheep K, Hatano S, Kongtawelert P, Kimata K, Watanabe H. Versican/PG-M Assembles Hyaluronan into Extracellular Matrix and Inhibits CD44-mediated Signaling toward Premature Senescence in Embryonic Fibroblasts. J Biol Chem 2009; 284(13): 8596–604.

[15] Choocheep K, Hatano S, Takagi H, Watanabe H, Kimata K, Kongtawelert P, et al. Versican facilitates chondrocyte differentiation and regulates joint morphogenesis. J Biol Chem 2010; 285(27): 21114–25.

[16] Afratis N, Gialeli C, Nikitovic D, Tsegenidis T, Karousou E, Theocharis AD, et al. Glycosaminoglycans: key players in cancer cell biology and treatment. FEBS J 2012; 279(7): 1177–97.

[17] Liu D, Shriver Z, Qi Y, Venkataraman G, Sasisekharan R. Dynamic regulation of tumor growth and metastasis by heparan sulfate glycosaminoglycans. Semin Thromb Hemost 2002; 28(1): 67–78.

[18] Volpi N. Therapeutic applications of glycosaminoglycans. Curr Med Chem 2006; 13(15): 1799–810.

[19] Choi B-D, Choi YJ. Nutraceutical functionalities of polysaccharides from marine invertebrates. Adv Food Nutr Res 2012; 65: 11–30.

[20] Ronca G, Conte A. Metabolic fate of partially depolymerized shark chondroitin sulfate in man. Int J Clin Pharmacol Res 1993; 13 (Suppl): S27–34.

[21] Uebelhart D. Clinical review of chondroitin sulfate in osteoarthritis. Osteoarthr Cartil 2008; 16 (Suppl 3): S19-21.

[22] Volpi N. Oral bioavailability of chondroitin sulfate (Condrosulf) and its constituents in healthy male volunteers. Osteoarthr Cartil 2002; 10(10): 768–77.

[23] Kubo M, Ando K, Mimura T, Matsusue Y, Mori K. Chondroitin sulfate for the treatment of hip and knee osteoarthritis: current status and future trends. Life Sci 2009; 85(13–14): 477–83.

[24] Linhardt RJ, Gunay NS. Production and chemical processing of low molecular weight heparins. Semin Thromb Hemost 1999; 25 (Suppl 3): S5–16.

[25] Gandhi NS, Mancera RL. The structure of glycosaminoglycans and their interactions with proteins. Chem Biol Drug Des 2008; 72(6): 455–82.

[26] Liapina LA, Koval'chuk GA. A comparative study of the action on the hemostatic system of extracts from the flowers and seeds of the meadowsweet (Filipendula ulmaria (L.) Maxim.). Izv Akad Nauk Ser Biol 1993; 4: 625–8.

[27] Liapina LA, Novikov VS, Pastorova VE, Uspenskaia MS, Smolina TI, Liapin GI. An anticoagulant from extracts of peony roots: its isolation and properties. Izv Akad Nauk Ser Biol 1995; 2: 249–51.

[28] Liapina LA, Kondashevskaia MV, Ziadetdinova GA, Uspenskaia MS. Comparative study of anticoagulants obtained from various extracts of Paeonia anomala. Izv Akad Nauk Ser Biol 2000; 3: 345–9.

[29] Dantas-Santos N, Gomes DL, Costa LS, Cordeiro SL, Costa MSSP, Trindade ES, et al. Freshwater plants synthesize sulfated polysaccharides: heterogalactans from Water Hyacinth (Eicchornia crassipes). Int J Mol Sci 2012; 13(1): 961–76.

[30] Aquino RS, Landeira-Fernandez AM, Valente AP, Andrade LR, Mourão PAS. Occurrence of sulfated galactans in marine angiosperms: evolutionary implications. Glycobiology 2005; 15(1): 11–20.

[31] Aquino RS, Grativol C, Mourão PAS. Rising from the sea: correlations between sulfated polysaccharides and salinity in plants. PLoS ONE 2011; 6(4): e18862. doi: 10.1371 /journal.pone.0018862.

[32] Zahari, C.N.M.B.C. & Azmi, N.S.B. Halal source of medication: Glycosaminoglycan derived medicinal plant. International Journal of Applied Chemistry 2016; 12(4): 803–10.

[33] Nathip N. Screening for glycosaminoglycans phytochemicals and antioxidant activity from local mushrooms [Term paper]. Faculty of Associated Medical Sciences: Chiang Mai University; 2014 [in Thai]

[34] Chunjarean M. Screening for phytochemicals and chondroprotective effect of garlic extracts [Term paper]. Faculty of Associated Medical Sciences: Chiang Mai University; 2015 [inThai]

[35] Nakano T, Igawa N, Ozimek L. An economical method to extract chondroitin sulphate-peptide from bovine nasal cartilage. Canadian Biosystems Engineering 2000; 42(4): 205–08.

[36] Farndale RW, Sayers CA, Barrett AJ. A direct spectrophotometric microassay for sulfated glycosaminoglycans in cartilage cultures. Connect Tissue Res 1982; 9(4): 247–8.

[37] Dietz JH, Rouse AH. A rapid method for estimating pectic substances in citrus juices. Food Res 1983; 18: 169–77.

[38] Lima MA, Rudd TR, de Farias EHC, Ebner LF, Gesteira TF, de Souza LM, et al. A new approach for heparin standardization: combination of scanning UV spectroscopy, nuclear magnetic resonance and principal component analysis. PLoS ONE 2011 Jan; 6(1): e15970. doi: 10.1371 /journal.pone.0015970.

[39] Zheng CH, Levenston ME. Fact versus artifact: avoiding erroneous estimates of sulfated glycosaminoglycan content using the dimethylmethylene blue colorimetric assay for tissue-engineered constructs. Eur Cell Mater 2015; 29: 224–36.

[40] Kubaski F, Osago H, Mason RW, Yamaguchi S, Kobayashi H, Tsuchiya M, et al. Glycosaminoglycans detection methods: Applications of mass spectrometry. Mol Genet Metab 2017 ; 120(1–2): 67–77.

[41] Stone JE. Urine analysis in the diagnosis of mucopolysaccharide disorders. Ann Clin Biochem 1998 ; 35 (Pt 2): 207–25.

[42] Stone JE, Akhtar N, Botchway S, Pennock CA. Interaction of 1,9-dimethylmethylene blue with glycosaminoglycans. Ann Clin Biochem 1994 Mar; 31 (Pt 2): 147–52.

[43] Frazier SB, Roodhouse KA, Hourcade DE, Zhang L. The Quantification of Glycosaminoglycans: A Comparison of HPLC, Carbazole, and Alcian Blue Methods. Open Glycosci 2008; 1: 31–9.

[44] Mort JS, Roughley PJ. Measurement of glycosaminoglycan release from cartilage explants. Methods Mol Med 2007; 135: 201–9.

[45] Saenkham C. Detection of phytochemicals and optimization of glycosaminoglycans by agarose gel electrophoresis in eggplant, bitter gourd, finger root and noni [Term paper]. Faculty of Associated Medical Sciences: Chiang Mai University; 2017 [in Thai]

[46] Borwornchaiyarit S. Detection of phytochemicals and optimization of glycosaminoglycans by agarose gel electrophoresis in in ginger, turmeric, star fruit and banana [Term paper]. Faculty of Associated Medical Sciences: Chiang Mai University; 2017 [in Thai]

[47] Volpi N, Maccari F. Electrophoretic approaches to the analysis of complex polysaccharides. J Chromatogr B Analyt Technol Biomed Life Sci 2006; 834(1–2): 1–13.

[48] Nader HB, Takahashi HK, Guimarães JA, Dietrich CP, Bianchini P, Ozima B. Heterogeneity of heparin: characterization of one hundred components with different anticoagulant activities by a combination of electrophoretic and affinity chromatography methods. International Journal of Biological Macromolecules 1981; 3(6): 356–60.

[49] Tomatsu S, Shimada T, Mason RW, Montaño AM, Kelly J, LaMarr WA, et al. Establishment of glycosaminoglycan assays for mucopolysaccharidoses. Metabolites 2014; 4(3): 655–79.

[50] Camplejohn KL, Allard SA. Limitations of safranin "O" staining in proteoglycan-depleted cartilage demonstrated with monoclonal antibodies. Histochemistry 1988; 89(2): 185–8.

[51] Vasconcelos AA, Pomin VH. The Sea as a Rich Source of Structurally Unique Glycosaminoglycans and Mimetics. Microorganisms 2017; 5(3). e51. doi: 10.3390/microorganisms5030051

[52] de Araújo IWF, Vanderlei ESO, Rodrigues JAG, Coura CO, Quinderé ALG, Fontes BP, et al. Effects of a sulfated polysaccharide isolated from the red seaweed Solieria filiformis on models of nociception and inflammation. Carbohydr Polym 2011; 86(3): 1207–15. doi: 10.1016/j.carbpol. 2011 .06.016.

Journal of Associated Medical Sciences 2018; 51(1): 19-25

JAMS
Journal of Associated Medical Sciences

Thai-Journal Citation Index Centre (TCI) & ASEAN Citation Index (ACI)

Journal of Associated Medical Sciences

Journal homepage: https://www.tci-thaijo.org/index.php/bulletinAMS/index

Lower frequency of certain nonconformities against ISO/IEC 17025 after many year accreditation

Suthon Vongsheree* **Soavanee Aromsuk** **Piyawan Chainarongkuekul** **Awiruth Kejonnit**

Department of Medical Sciences, Ministry of Public Health, Nonthaburi Province, Thailand.

ARTICLE INFO

Article history:
Received 30 June 2017
Accepted as revised 15 January 2018
Available online 15 January 2018

Keywords:
Nonconformities, ISO/IEC 17025, accreditation cycles, difference in nonconformities

ABSTRACT

Background: It is predictable that the laboratories with many years of accreditation should get lower amount of nonconformities than those of the new ones. The objectives of the study are to find the differences in characteristics and nonconformities among ISO/IEC 17025 accredited laboratories undergoing on-site assessment in 2015 and verify the above prediction.

Materials and methods: A cross-sectional study of the characteristics and the nonconformities from 2015 assessment of 134 laboratories were compared between the laboratories with 6 or more years or at least 3 cycles of accreditation and the ones with shorter accreditation year. Statistical analyses were done by using Stata-intercooled version 6.

Results: There were 1,459 total nonconformities, 572 (39%) were those against management requirements and 887 (61%) were those from technical ones. Longer and new accredited laboratories shared similar basic characteristics. Longer accredited laboratories got lower total nonconformities (mean±SD; 9.1±4.8 vs 12.7±9.0: t-test=2.89, p=0.003), and lower technical nonconformities (mean±SD; 5.0±3.1 vs 8.3±6.9: t-test=3.57, p<0.001). The proportion of longer accredited laboratories was lower on nonconformities against clause 5.6 Measurement traceability (14/87 vs 28/67, Chi square=5.060, p=0.024) and the ones against clause 5.9 Assuring quality of test results (27/67 vs 44/67, Chi-square=6.450, p=0.011) than those of the new accredited laboratories.

Conclusion: This study demonstrated that many year accreditations may enable the accredited laboratories to comply with the requirements more effectively. Lower proportions of the longer accredited laboratories had lower certain nonconformities on clause 5.6 Measurement traceability and 5.9 Assuring quality of test results.

Introduction

The Bureau of Laboratory Quality Standards, BLQS, is an accreditation body for accreditation of medical and public health laboratories complying with the requirements of the International Organization for Standardization, ISO 15189 and ISO/IEC 17025 after getting Mutual Recognition Arrangement from Asian Pacific Laboratory Accreditation Co-operation, APLAC MRA and from International Laboratory Accreditation Co-operation, ILAC MRA, for testing since 2002 and 2003, respectively.[1] In 2015, BLQS has accredited 134 laboratories, with ISO/IEC 17025:2005,[2] 14 are initial accreditations and 120 are reassessment ones. Total numbers of nonconformities and specific clause deviations are so diverse and questionable on how different among these accredited laboratories. A report on trends of nonconformities from BLQS has showed irregular patterns of the distribution of such nonconformities during 2008-2011, with highest frequencies of nonconformities against clause 5.4, Test and calibration methods and method validation.[3] A similar report from Hong Kong Accreditation Service in 2012 has illustrated the frequencies of nonconformities against the requirement of ISO 15189. Interestingly, 27 medical

* **Corresponding author.**
Author's Address: *Department of Medical Sciences, Ministry of Public Health, Nonthaburi Province, Thailand.*
** **E-mail address:** suthon.v@dmsc.mail.go.th
doi: 10.14456/jams.2018.4
E-ISSN: 2539-6056

laboratories have showed statistically reduction of nonconformities from 13.5 nonconformities per laboratory at the initial assessment to 6.6 nonconformities per laboratory at the reassessment.[4] A previous report in 2015 also has demonstrated the factors affecting correction time among ISO/IEC 17025 accredited laboratories in the public health sectors. By using multiple logistic regression, the report reveals that a longer correction time statistically related to the type of laboratory services in microbiology with chemistry, the presence of nonconformities against clause 4.2 the management system and the presence of nonconformities against technical requirement especially clause 5.4 Test and calibration methods and method validation, with adjusted odd ratio of 3.35-7.58.[5] The objectives of the study are to find the differences in characteristics and nonconformities among ISO/IEC 17025 accredited laboratories undergoing on-site assessment in 2015 and verify whether there are some differences in characteristics and certain nonconformities among accredited laboratories with longer accreditation of 6 years or at, least 3 cycles of accreditation, comparing to those of the shorter accreditation.

Materials and methods

A cross-sectional study of basic characteristics and the nonconformities against the requirements of ISO/IEC 17025:2005 from the latest assessment of 134 laboratories in 2015 were summarized. The mean accreditation of 6 years or three cycles of accreditation was applied to equally classify the laboratories as 67 older ones with accreditation of 6 years or more and 67 newer ones with accreditation of less than 6 years. Out of 134 assessed laboratories, 14 were initial accreditations while the remaining laboratories were reassessed or extension assessed. Stata- intercooled version 6 was used for calculation of normality, mean, Standard deviation (SD), Kruskal Wallis test where all sets of the data cannot be normal distribution,[6] t-test for mean difference and *p*-values.

Results

1. Characteristic properties of 134 ISO/IEC 17025 accredited laboratories. Majorities were the private laboratories. Four of five facilities located in provincial areas outside Bangkok, the capital of Thailand. More than half (61%) served food testing, using chemistry and microbiology. They offered testing scope of 38 tests, with wide range of the scope from only 1 test to 631 tests. They got accreditation for 0- 16 years; with mean of 6 years or 3 cycles of 2 years accreditation. The average 6 year accreditation was applied to classify the laboratories into 2 equal groups of 67 laboratories. Out of 67 new ones, 14 (21%) are those of initial accredited laboratories in 2015. Details of characteristics were illustrated in Table 1. Comparison of characteristics and numbers of nonconformities between the longer accreditation laboratories with those of the shorter ones were illustrated in table 2.

Table 1 Characteristics of 134 accredited laboratories.

Characteristics	Number	Percentage
Sector		
- Governmental	40	29.85
- Private	94	70.15
Location		
- Bangkok	30	22.39
- Other places	104	77.61
Laboratory services		
- Foods	82	61.19
- Others	52	38.81
Assessment		
- Initial	14	10.45
- Reassessment, and others	120	89.55
Scope (test menu)		
- ≥38	102	76.12
- <38	32	23.88
Years of accreditation		
- ≥6	67	50.00
- <6	67	50.00
Service objective		
- Self quality check	78	58.21
- Public service	56	41.79

2. Total 1462 nonconformities were against 575 management requirements (39%) and 887 technical ones (61%). The distribution of these nonconformities, numbered as the specific clauses of ISO/IEC 17025:2005 [2] were illustrated in table 3. The top 3 nonconformities related to management were 4.3 Document control (150,10%), 4.1 The organization (94,6%) and 4.13 Control of records (59,4%). For those of 887 technical nonconformities, the top 3 frequently cited were 5.4 Validation of the methods (315,22%), 5.5 Equipment (153,11%) and 5.9 Assuring quality of results (106,7%). Table 4 showed that the longer accreditation laboratories had lower mean of total nonconformities (mean±SD; 9.1±4.8 vs 12.7±9.0: t-test=2.89, p=0.003) and technical nonconformities (mean±SD; 5.0±3.1 vs 8.3±6.9: t-test=3.57, p<0.001) than those of the new laboratories.

Table 2 Comparison of characteristics and numbers of nonconformities between the longer accreditation laboratories with those of the shorter accreditation, new laboratories, 67 laboratories each. The proportional differences were tested by Kruskal Wallis to avoid non-normal distribution of certain data set and presented the test results as Chi-square, *denotes significant difference when p<0.05

Characteristics (number)	Longer accreditation	New	Chi-square	*p* value
Sector				
Governmental (40)	21	19		
- Private (94)	46	48	0.106	0.745
Location				
- Bangkok (30)	51	53		
- Other place (104)	16	14	0.128	0.721
Testing services				
- Foods (82)	39	43		
- Others (52)	28	24	0.374	0.541
Assessment				
- Initial (14)	14	0		
- Others (120)	53	67	11.638	<0.001*
Scope (test menu)				
- ≥ 38 (102)	63	39		
- < 38 (32)	4	28	17.04	<0.001*
Service objective				
- Self quality check (78)	44	34		
- Public service (56)	23	33	2.284	0.131
Characteristics (mean±SD)	**Longer accreditation**	**New**	**t-test**	**(*p* value)**
1. Years of accreditation (6±3.7)	9.2±2.2	3.1±2.1	16.42	<0.001 *
2. Scope (38.0±79.2)	64.0±104.4	12.1±19.3	4.00	<0.001*
3. Correction days (112.1±71.5)	106.5±72.8	117.6±70.3	0.90	0.371
4. Nonconformities (10.9±7.4)	9.1±4.8	12.7±9.0	2.89	0.005*
5. NC management (4.3±3.5)	4.1±3.0	4.5±3.9	0.58	0.561
6. NC technical (6.6±5.6)	5.0±3.1	8.3±6.9	3.57	<0.001*

3. Factors that might associate to years of accreditation were illustrated in table 4 for qualitative data, table 5 for continuous data and table 4 for various nonconformities, NC, against the specific clauses of the requirements of ISO/IEC 17025:2005. Significantly lower proportions of the longer accreditation laboratories were observed among these factors; total nonconformities, technical nonconformities, as showed above. NC against clause 5.6 Measurement traceability (14 vs 28, Chi square=5.060, p=0.024) and NC against clause 5.9 Assuring quality of test results (27 vs 44, Chi-square=6.450, p=0.011)

Table 3 Distribution of nonconformities against specific requirements of ISO/IEC 17025:2005, present in number and percentage of each relevant clause.

Clause 4	Brief description	Number	%
4.1	Organization	94	6.4
4.2	Management system	36	2.5
4.3	Document control	150	10.3
4.4	Review of contracts	18	1.2
4.5	Subcontracting	5	0.3
4.6	Purchasing services	56	3.8
4.7	Customer services	20	1.4
4.8	Complaints	8	0.5
4.9	Control of NC works	26	1.8
4.10	Improvement	13	0.9
4.11	Corrective action	18	1.2
4.12	Preventive action	15	1.0
4.13	Control of records	59	4.0
4.14	Internal audits	28	1.9
4.15	Management reviews	29	2.0
Total	Management	575	39.3
Mean		38.8	
Clause 5	**Brief description**	**Number**	**%**
5.1	General	3	0.2
5.2	Personnel	76	5.2
5.3	Accommodation/environment	60	4.1
5.4	Calibration/validation	315	21.5
5.5	Equipment	153	10.5
5.6	Measurement traceability	56	3.8
5.7	Sampling	5	0.3
5.8	Handling test and calibrators	56	3.8
5.9	Assuring quality of results	106	7.3
5.10	Reporting of results	57	3.9
Total	Technical	887	60.7
Mean		88.7	
Grand total	Management & technical	1462	100.0

Table 4 Proportions of accredited laboratories by nonconformities against reference clause of ISO/IEC 17025, comparing between the longer accreditation laboratories and the new laboratories, 67 laboratories each. The proportional differences were tested by Kuskal Wallis to avoid non-normal distribution of certain data set and presented the test results as Chi-square, *denotes significant difference when $p<0.05$

Reference clause	Longer accreditation	New	Chi-square	*p* value
4.1 Organization				
- Absent, 72	33	39		
- Present, 61	34	27	0.965	0.326
4.2 Management system				
- Absent, 106	51	55		
- Present, 28	16	12	0.538	0.463
4.3 Document control				
- Absent, 41	22	19		
- Present, 93	45	48	0.235	0.628
4.4 Review of requests				
- Absent, 116	59	57		
- Present, 18	8	10	0.191	0.662
4.5 Subcontracting				
- Absent, 129	66	63		
- Present, 5	1	4	1.392	0.238
4.6 External services and supplies				
- Absent, 85	40	45		
- Present, 49	27	22	0.599	0.439
4.7 Service to customer				
- Absent, 115	57	58		
- Present, 19	10	9	0.046	0.831
4.8 Complaints				
- Absent, 126	62	64		
- Present, 8	5	3	0.396	0.529
4.9 Control of NC testing				
- Absent, 112	52	60		
- Present, 22	15	7	2.591	0.108
4.10 Improvement				
- Absent, 121	60	61		
- Present, 13	7	6	0.063	0.801
4.11 Corrective action				
- Absent, 116	57	59		
- Present, 18	10	8	0.191	0.662
4.12 Preventive action				
- Absent, 119	59	60		
- Present, 15	8	7	0.056	0.813
4.13 Control of records				
- Absent, 86	47	39		
- Present, 48	20	28	1.547	0.214
4.14 Internal audits				
- Absent, 107	53	54		
- Present, 27	14	13	0.035	0.853

Table 4 Proportions of accredited laboratories by nonconformities against reference clause of ISO/IEC 17025, comparing between the longer accreditation laboratories and the new laboratories, 67 laboratories each. The proportional differences were tested by Kuskal Wallis to avoid non-normal distribution of certain data set and presented the test results as Chi-square, *denotes significant difference when $p<0.05$. (continues)

Reference clause	Longer accreditation	New	Chi-square	*p* value
4.15 Management reviews				
- Absent, 108	55	53		
- Present, 26	12	14	0.142	0.706
5.1 General				
- Absent, 131	66	65		
- Present, 3	1	2	0.254	0.614
5.2 Personnel				
- Absent, 78	43	35		
- Present, 56	24	32	1.462	0.227
5.3 Accommodation and environments				
- Absent, 93	49	44		
- Present, 41	18	23	0.654	0.419
5.4 Test methods and validation				
- Absent, 23	16	7		
- Present, 111	51	60	3.165	0.075
5.5 Equipment				
- Absent, 57	31	26		
- Present, 77	36	41	0.568	0.451
5.6 Measurement traceability				
- Absent, 92	53	39		
- Present, 42	14	28	5.060	0.024
5.7 Sampling				
- Absent, 129	63	66		
- Present, 5	4	1	1.392	0.238
5.8 Handling test and calibration items				
- Absent, 78	90	44		
- Present, 56	20	24	0.403	0.526
5.9 Assuring quality of the test				
- Absent, 63	40	23		
- Present, 71	27	44	6.445	0.011
5.10 Reporting the results				
- Absent, 84	41	43		
- Present, 50	26	24	0.095	0.758

Discussion

Accreditation years are one among indicators for experiences in quality improvement of the laboratories. According to ISO/IEC 17011:2004 clause 7.11.2, the accreditation body shall establish procedures and plans for on-sites assessments at sufficient close intervals to monitor the continued fulfillment by the accredited laboratories to comply the requirements.[7] BLQS has the policy on reassessment for every 2 years after successful initial accreditation, in order to monitor the continued fulfillment by the accredited laboratories. All basic characteristics of the experienced ones and the new ones are not different statistically, except for the number of service scope which just confirms that the longer accreditation are more competence. In this report, the mean accreditation time of 6 years or 3 cycles of 2 year accreditation can classify the

laboratories into 2 equal groups of 67 laboratories; some comparisons are feasible for a cross-sectional study. A report from Hong Kong[4] used different year of ISO 15189 accredited medical laboratories and got a strong evidence that lower nonconformities were observed after a number of reassessments. However, a laboratory always faces with changes and new challenges that are certainly affect to the quality management system in each year, thus, such comparison on different years are less valid. Another report[5] uses the correction times as the output variable and finds that some factors related to a longer correction time are nonconformities against clause 4.2 management system and nonconformities against the technical requirements. A previous report[6] reveals that certain nonconformities: the design for safety, safety procedures, personnel responsibilities and safe work practices relate to higher total number of nonconformities in the safety assessment of medical laboratories using ISO 15190 as audit criteria. This report demonstrates how many year accreditation help quality improvement as evidently decreasing nonconformities are observed among those of the longer accredited laboratories.

Conclusions

This study demonstrated that the new laboratories with less than 6 year accreditation had higher chance to get more total nonconformities, especially on the technical requirements clause 5.6 traceability and 5.9 Assuring quality of test results. Such nonconformities need experiences to resolve and improve. Many years of accreditation will help laboratories to comply with each requirement of the standards after many visits from the assessors.

Acknowledgements

The authors would like to thank staffs of the sector Public Health Laboratory Accreditation, The Bureau of Laboratory Quality Standards for their kindly providing and check the validity of the data.

References

[1] International Laboratory Accreditation Cooperation. (2016). ILAC MRA and signatories. Retrieved from: http://ilac.org/signatory-search/?q=b/.

[2] International Organization for Standardization. ISO/IEC 17025:2005.General requirements for the competence of testing and calibration laboratories. Geneva, Switzerland 2005.

[3] Aromsuk S, Sinthusarn C, Tanankat A and Jarunuch S. Trend analysis of condition on accredited assessment for public health laboratory of government and public laboratories service in accordance with ISO/IEC 17025:2005 from the fiscal year 2008 to 2011. Rajabhat Chiang Mai Research Journal.2013: 14(2). English abstract.

[4] Bella Ho and Eric Ho.The most common nonconformities encountered during the assessment of medical laboratories in Hong Kong using ISO 15189 as accreditation criteria. Biochem Med (Zagreb) 2012: 22(2): 247-57.

[5] Aromsuk S, Chainarongkuekul P, Khejonnit A and Vongsheree S. Factors affecting the duration of the correction time for public health laboratory and veterinary laboratory in accordance with ISO/IEC 17025:2005.Journal of Applied Animal Science. 2016:9(1): 9-24. English abstract.

[6] Buthmann A. Dealing with Non-normal Data: Strategies and Tools.Available at https://www.isixsigma.com/tools-templates/normality/dealing-non-normal-data-strategies-and-tools/

[7] Muenphon S, Wiroonboonpat P, Kumsai S, et al. Factors affecting the numbers of nonconformities from the assessment of safety in medical laboratory according to ISO 15190:2003.Bull Chaing Mai Assoc Med Sci 2016: 49(2): 255-62. English abstract.

[8] International Organization for Standardization.ISO/IEC 17011:2004.Conformity assessment-General requirements for accreditation bodies accrediting conformity assessment bodies. Geneva, Switzerland 2004.

Journal of Associated Medical Sciences 2018; 51(1): 26-31

JAMS
Journal of Associated Medical Sciences

Thai-Journal Citation Index Centre (TCI) & ASEAN Citation Index (ACI)

Journal of Associated Medical Sciences

Journal homepage: https://www.tci-thaijo.org/index.php/bulletinAMS/index

Luminescence characteristics of gadolinium-calcium-silicoborate glass scintillators

Siriprapa Kaewjaeng[1*] Suchart Kothan[1] HongJoo Kim[2] Jakrapong Kaewkhao[3]

[1]Department of Radiologic Technology, Faculty of Associated Medical Sciences, Chiang Mai University, Chiang Mai Province, Thailand
[2]Department of Physics, Faculty of Natural Science, Kyungpook National University, Daegu, South of Korea
[3]Center of Excellence in Glass Technology and Materials Science (CEGM), Nakhon Pathom Rajabhat University, Nakhon Pathom Province, Thailand

ARTICLE INFO

Article history:
Received 25 March 2017
Accepted as revised 9 January 2018
Available online 19 January 2018

Keywords:
Glass, luminescence, scintillator; BGO, dopant

ABSTRACT

Backgroud: The research aimed to study the investigate properties of glass having increasing compositions of (55-x) B_2O_3: 25Gd_2O_3: 10SiO_2: 10CaO: xA_2O_3 where A_2O_3 are Sm_2O_3, Eu_2O_3 and Dy_2O_3 and x=0.05 to 0.50 mol%. X-ray luminescence properties of these glass samples using a BGO crystal were then compared.

Materials and methods: Glasses were prepared by conventional melt quenching technique. Density, optical properties and x-ray scintillation properties were studied and compared.

Results: The was found that density of glass increased with increasing dopant concentration. Eleven absorption bands of Sm_2O_3 were observed from the $^6H_{15/2}$ ground state to 360 ($^4D_{3/2}$), 373 ($^6P_{7/2}$), 403 ($^6P_{3/2}$), 475 ($4I_{11/2}$), 944 ($^6F_{11/2}$), 1077 ($^6F_{9/2}$), 1225 ($^6F_{7/2}$), 1368 ($^6F_{5/2}$), 1468 ($^6F_{3/2}$), 1520 ($^6H_{15/2}$) and 1586 ($^6F_{1/2}$) nm. Two absorption bands of Eu_2O_3 were observed from the $^7F_0$ ground state to 2100 ($^7F_1$) and 2203 ($^7F_6$) nm. Nine absorption bands of Dy_2O_3 were observed to transitions from the $^6H_{15/2}$ ground state to 387 ($^4I_{13/2}$+$^4F_{7/2}$+$^4M_{21/2}$+$^4K_{17/2}$), 426 ($^4G_{11/2}$), 455 ($^4I_{15/2}$), 751 ($^6F_{3/2}$), 805 ($^6F_{5/2}$), 898 ($^6F_{7/2}$), 1085 ($^6H_{7/2}$ + $^6F_{9/2}$), 1261 ($^6F_{11/2}$ + $^6H_{9/2}$) and 1672 ($^6H_{11/2}$) nm. The comparisons done on x-ray luminescence properties between glass samples with BGO scintillator crystal determined that glass doped with 0.35 mol% Sm_2O_3 have four relatively strong emission peaks. Glass doped with 0.35 mol% of Eu_2O_3 have six relatively strong emission peaks. Glass doped with 0.45 mol% of Dy_2O_3 have four relatively strong emission peaks.

Conclusion: The comparisons done on x-ray luminescence properties between glass samples with the BGO scintillator crystal determined that the scintillation efficiency of glass samples doped with Sm_2O_3, Eu_2O_3 and Dy_2O_3 was 25% that of commercial BGO scintillator crystals.

Introduction

Scintillators or Scintillation materials emit ultraviolet light (UV) or visible light after radiation interaction of ionizing radiation with a material. Scintillators are used in industry, agriculture, and medical technology. In medical professional technology, it is used in film-screens, digital radiography, image receptors, computed tomography (CT), scintillation gamma cameras, and positron emission tomography (PET).[1-3]

When ionizing radiation interacts with scintillation materials, electrons from ground state are raised to an excited state. Instability electrons fall back to ground state with the emission of ultraviolet or visible light having characteristic decay constants are called luminescence. The luminescence is emission of light after excitation. Scintillation materials having a prompt emission of light is called fluorescence and delayed emission of light is afterglow or phosphorescence.[4-8]

The desired properties of scintillation materials are high

* **Corresponding author.**
Author's Address: Department of Radiologic Technology, Faculty of Associated Medical Sciences, Chiang Mai University, Chiang Mai Province, Thailand
** **E-mail address:** bulli99@windowslive.com
doi: 10.14456/jams.2018.6
E-ISSN: 2539-6056

conversion efficiency, short decay time, high transparency, a frequency spectrum matching with light receptor, high detection efficiencies, high density, a large attenuation coefficient, radiation hardness, high light yield, fast decay time, they are inexpensive, and show high proficiency and stability. Additionally, most scintillation materials require high luminescence efficiencies and dopant or activators from preferred sites in inorganic scintillation for the activator excited electrons before returning to the ground state. Rare-earth ions (RE^{3+}) doped in scintillation materials has been used as photonic materials in recent years, as they have a broad emission wavelength at the visible light to the infrared region because of its 4f-5d and 4f-4f transition and fast decay time. The 4f–4f transition gives a sharp fluorescence because of the shielding effects of the outer 5s and 5p orbitals on the 4f electrons.[1-8]

The rare earth oxide, intensive Gadolinium Oxide (Gd_2O_3) is the most popular substance due to the efficiencies in energy transfer from Gd^{3+} ions to the luminescence activators and increased light yield emission.[2, 9-12] Most of the popular rare earth doped in scintillation materials have high emission efficiencies based on literature reviews such as Samarium Oxide (Sm_2O_3),[10-18] Europium Oxide (Eu_2O_3),[5, 6, 18, 19] and Dysprosium Oxide (Dy_2O_3).[17, 18, 20-23]

This article focuses on rare earth doped in glass scintillator because these glasses have a wide variety of applications, have good forming ability, high optical properties, are inexpensive, are non-hygroscopic, are chemically resistant, can be produced in large volumes, and are easy to synthesize. This type of glass can also easily be fabricated into glass scintillators with doping chemical concentrations by using the melt-quenching technique.[2-28] Among the various glasses that have been used for quite some time, borate glasses play a significant role in various applications such as solid state lasers, optical and electrical applications, fiber optics, optical waveguides, and luminescence materials. Borate glasses are an especially appropriate optical material because of its high chemical resistance, high thermal stability, and high optical properties.[10, 13, 20] Earlier, silicate glasses were used due to good mechanical and optical properties. Also, borosilicate glasses have been formally used due to their high thermal resistance and low melting point. The effects of doping concentrations can result from oxide ions in calcium oxide, as it can increase luminescence emission and are also non-hygroscopic.[10, 20]

The purpose of this article is to demonstrate how the formula CaO: Gd_2O_3: SiO_2: B_2O_3 obtained by melt-quenching technique can be doped with Samarium Oxide (Sm_2O_3), Europium Oxide (Eu_2O_3) and Dysprosium Oxide (Dy_2O_3) for the desired effects. The dopant concentrations are studied regarding their physical, optical, and luminescence properties by comparing them with a standard crystal scintillator composed of Bismuth Germinate (BGO). The findings will be used for developing these glasses as candidates for glass scintillators in the future.

Materials and methods

Glass preparations

Glasses compositions of 10CaO: $25Gd_2O_3$: $10SiO_2$: (55-x) B_2O_3: xA_2O_3 (where x=0.05, 0.10, 0.15, 0.20, 0.25, 0.30, 0.35, 0.45 and 0.50 %mol) and xA_2O_3=Sm_2O_3, Eu_2O_3, Dy_2O_3 were prepared by melt-quenching technique. The high purity chemical concentrations of CaO, Gd_2O_3, SiO_2, H_3BO_3, Sm_2O_3, Eu_2O_3, and Dy_2O_3 were mixed thoroughly in an aluminium crucible. About 30 gm of the each compositions were thoroughly and mixed into an aggregate and the homogeneous mixture was placed into an aluminium crucible and melted in an electrical furnace at 1400 °C for 3 hours. These melted glass samples were quenched at room temperature. The glass samples were annealed at 550 °C for 3 hrs to reduce the thermal stress and then were cut and polished into squares having dimensions of 1x1.5x0.3 cm^3.

Characterization process

Physical Properties

The density measurements were obtained by applying Archimedes' principle, the weights of the prepared glass samples were measured in air and in xylene using a 4-digit sensitive microbalance (AND, HR 200). Afterward, the density (ρ) was determined from the following equation.[30, 31]

$$\rho = \frac{w_a}{w_a - w_b} \times \rho_b$$

Where ρ is density (g/cm^3) W_a is weight in air (g), W_b is weight in Xylene (g), and ρ_b is Xylene density (0.863 g/cm^3)

Optical properties

Absorption spectra were measured with a UV-Vis-NIR spectrophotometer (Shimadzu UV-3600) at wavelengths of 350-1800 nm.

Luminescence properties

The X-ray luminescence spectra of glass were measured with the Copper (Cu) target X-ray generator (Inel, XRG3D-E). The power setting X-ray source was operated at 50 kV, 30 mA. X-ray excitation spectra of glass samples were measured with a QE65000 fiber optics spectrometer

Results and Discussions

Physical Properties

The variation of density (g/cm^3) is a function of Sm_2O_3, Eu_2O_3, and Dy_2O_3 concentration as shown in Figure 1. The glass samples density tends to increase with increasing of Sm_2O_3, Eu_2O_3, and Dy_2O_3 concentrations. This means that there is change in the structural arrangement of the dopant concentration that was added to the glass sample network. It also shows that boron oxide is replaced by Sm_2O_3, Eu_2O_3, and Dy_2O_3 concentrations. The increased density of glass samples is due to a higher molecular weight for Sm_2O_3, Eu_2O_3, and Dy_2O_3 than any other composition found in the given glass samples system.

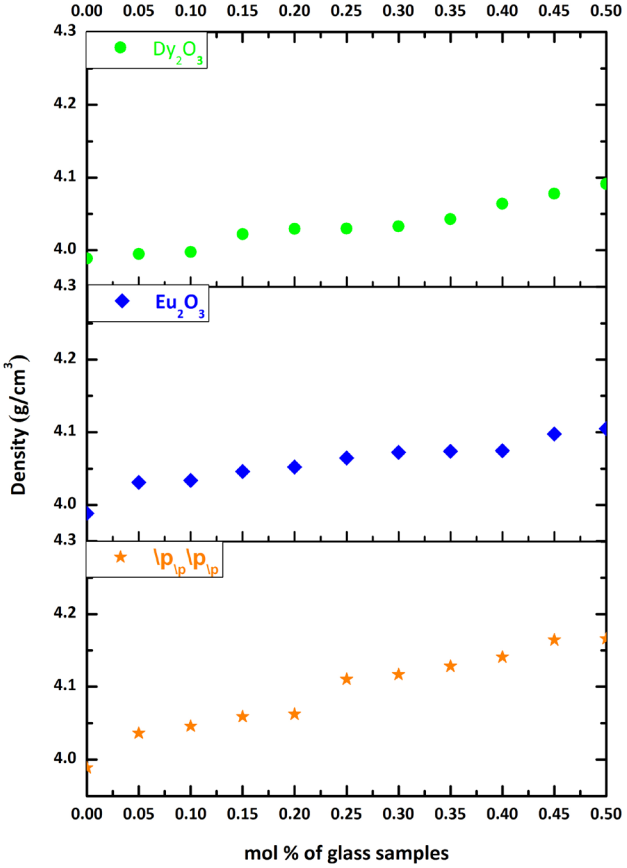

Figure 1. *Density of glass samples.*

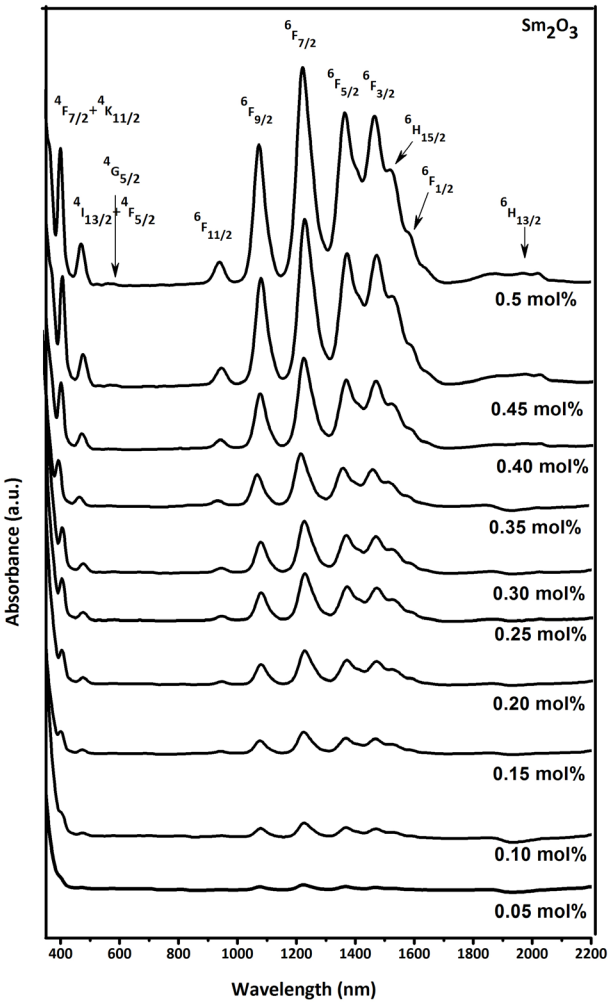

Figure 2. *Absorption spectra of Sm_2O_3 doped GDSB Glass.*

Optical Properties

The absorption spectra for the Sm_2O_3, Eu_2O_3 and Dy_2O_3 doped with CaO: Gd_2O_3: SiO_2: B_2O_3 glass samples. The absorption spectra of Sm^{3+} ions show eleven absorption bands at 360, 373, 403, 475, 944, 1077, 1225, 1368, 1468, 1520, and 1586 nm due to the transition spectra of $^6H_{5/2}$ to $^4D_{3/2}$, $^6P_{7/2}$, $^6P_{3/2}$, $^4I_{11/2}$, $^6F_{11/2}$, $^6F_{9/2}$, $^6F_{7/2}$, $^6F_{5/2}$, $^6F_{3/2}$, $^6H_{15/2}$, and $^6F_{1/2}$ respectively,[10-18] as shown in Figure 2. The absorption spectra of Eu^{3+} ions show two absorption bands at 2100 and 2203 nm due to the transition spectra of $^7F_0$ and $^7F_6$ respectively,[5, 6, 18, 19] as shown in Figure 3. The absorption spectra of Dy^{3+} ions show nine absorption bands at 387, 426, 455, 751, 805, 898, 1085, and 1261 nm due to the transition spectra of ($^4I_{13/2}$ + $^4F_{7/2}$ + $^4M_{21/2}$ + $^4K_{17/2}$), $^4G_{11/2}$, $^4I_{15/2}$, $^6F_{3/2}$, $^6F_{5/2}$, $^6F_{7/2}$, ($^6H_{7/2}$ + $^6F_{9/2}$), ($^6F_{11/2}$ + $^6H_{9/2}$), and $^6H_{11/2}$ respectively,[17, 18, 20-23] as shown in Figure 4.

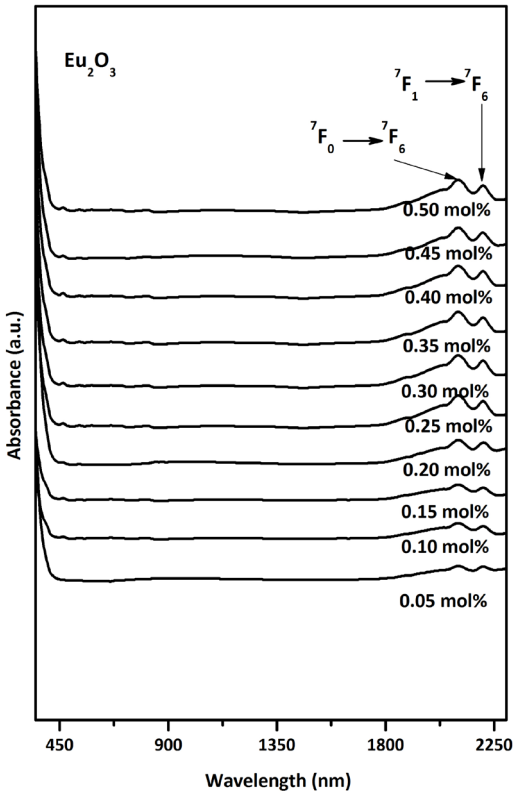

Figure 3. *Absorption spectra of Eu_2O_3 doped GDSB Glass.*

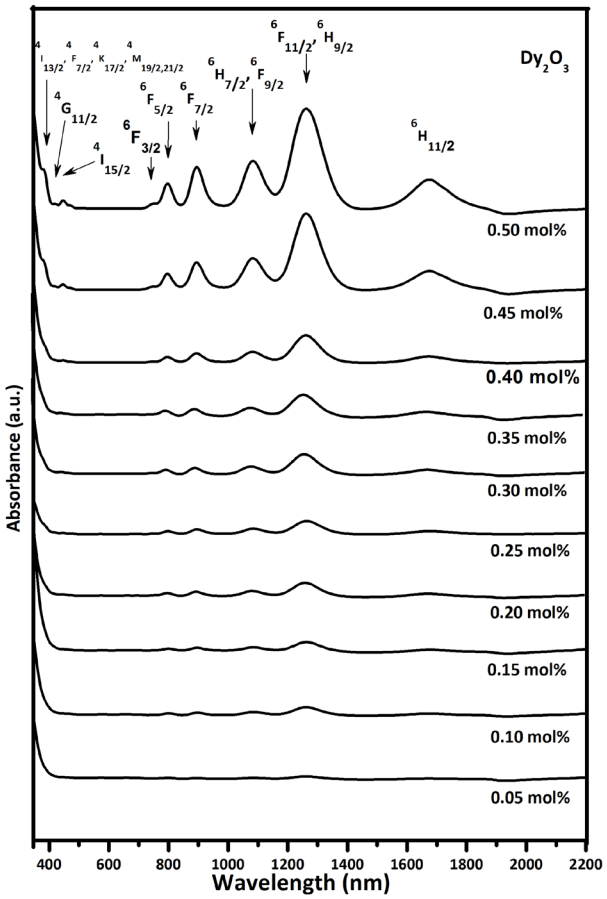

Figure 4. *Absorption spectra of Dy_2O_3 doped GDSB Glass.*

X-ray Luminescence properties

An X-ray of 50 kV and 30 mA were irradiated onto glass samples. The X-rays included an optical luminescence spectra of the Sm_2O_3, Eu_2O_3 and Dy_2O_3 doped with CaO: Gd_2O_3: SiO_2: B_2O_3 glass samples. They were then compared with BGO scintillation crystals having the same size and shape. Glass doped with Sm_2O_3 at 0.35 mol% are shown in Figure 5. The total area under peak of spectrum, the integral scintillation efficiency of 0.35 mol% Sm^{3+} doped glass samples and found that 25% of BGO scintillation crystal. The emission peaks of Sm^{3+} ions show four emission peak at 560 ($^4G_{5/2}\rightarrow{}^6H_{5/2}$), 598 ($^4G_{5/2}\rightarrow{}^6H_{7/2}$), 645 ($^4G_{5/2}\rightarrow{}^6H_{9/2}$) and 705 ($^4G_{5/2}\rightarrow{}^6H_{11/2}$) nm respectively.[10-18] Glass doped with Eu_2O_3 at 0.30 mol% are shown in Figure 6. The total area under peak of spectrum, the integral scintillation efficiency of 0.35 mol% Eu^{3+} doped glass samples were found to be 13% to that of BGO scintillation crystals. The emission peaks of Eu^{3+} ions show five emission peaks at 578 ($^5D_0\rightarrow{}^7F_0$), 590 ($^5D_0\rightarrow{}^7F_1$), 616 ($^5D_0\rightarrow{}^7F_2$), 652($^5D_0\rightarrow{}^7F_3$), and 703 ($^5D_0\rightarrow{}^7F_5$) nm respectively.[5, 6, 18, 19] Glass doped with Dy_2O_3 at 0.45 mol% are shown in Figure 7. The total area under peak of spectrum, the integral scintillation efficiency of 0.45 mol% Dy^{3+} doped glass samples was found to 27% that of BGO scintillation crystals. The emission peaks of Dy^{3+} ions show four emission peaks at 482 ($^4F_{9/2}\rightarrow{}^6H_{15/2}$), 577($^4F_{9/2}\rightarrow{}^6H_{13/2}$), 661 ($^4F_{9/2}\rightarrow{}^6H_{11/2}$), and 751 ($^4F_{9/2}\rightarrow{}^6_{H9/2}+{}^6F_{11/2}$) nm respectively.[17, 18, 20-23]

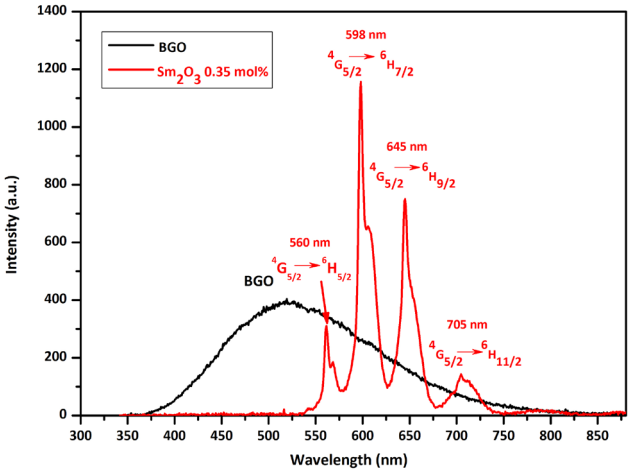

Figure 5. *Comparison of X-ray luminescence of BGO with GCSB doped with Sm_2O_3 at 0.35 mol%.*

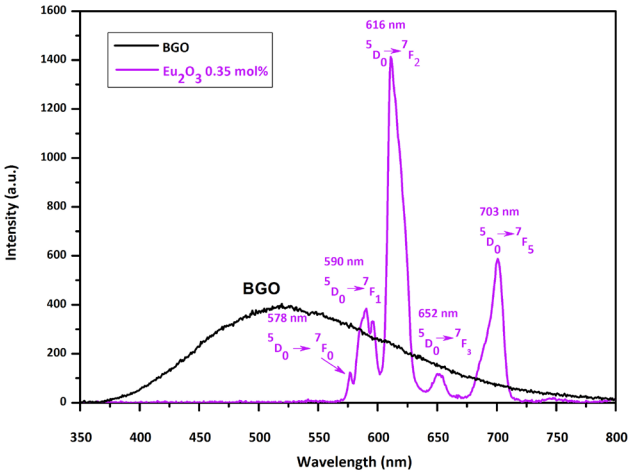

Figure 6. *Comparison of X-ray luminescence of BGO with GCSB doped with Eu_2O_3 at 0.35 mol%.*

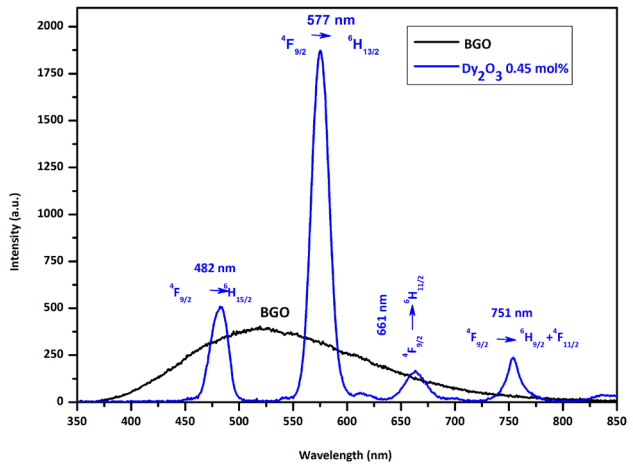

Figure 7. *Comparison of X-ray luminescence of BGO with GCSB doped with Dy_2O_3 at 0.35 mol%.*

Conclusions

The glass concentration in the formula (55-x) B_2O_3–10SiO_2- 25Gd_2O_3–10 CaO- xA_2O_3 when A_2O_3=Sm_2O_3, Eu_2O_3 and Dy_2O_3, where x=0.05, 0.10, 0.15, 0.20, 0.25, 0.30, 0.35, 0.45, and 0.50 respectively have been grouped based on their physical, optical, and luminescence properties. The experimental results show that the glass sample densities tended to increase with an increase in Sm_2O_3, Eu_2O_3, and Dy_2O_3 concentration. Absorption spectra of Sm^{3+} ions show eleven absorption bands at 360, 373, 403, 475, 944, 1077, 1225, 1368, 1468, 1520, and 1586 nm due to the transition spectra of $^6H_{5/2}$ to $^4D_{3/2}$, $^6P_{7/2}$, $^6P_{3/2}$, $^4I_{11/2}$, $^6F_{11/2}$, $^6F_{9/2}$, $^6F_{7/2}$, $^6F_{5/2}$, $^6F_{3/2}$, $^6H_{15/2}$, and $^6F_{1/2}$ respectively. Absorption spectra of Eu^{3+} ions show two absorption bands at 2100 and 2203 nm due to the transition spectra of $^7F_0$ and $^7F_6$ respectively. Absorption spectra of Dy^{3+} ions show nine absorption bands at 387, 426, 455, 751, 805, 898, 1085, and 1261 nm with due to the transition spectra of ($^4I_{13/2}$ + $^4F_{7/2}$ + $^4M_{21/2}$ + $^4K_{17/2}$), $^4G_{11/2}$, $^4I_{15/2}$, $^6F_{3/2}$, $^6F_{5/2}$, $^6F_{7/2}$, ($^6H_{7/2}$ + $^6F_{9/2}$), ($^6F_{11/2}$ + $^6H_{9/2}$), and $^6H_{11/2}$ respectively. Emission peaks of Sm^{3+} ions show four emission peaks at 560 ($^4G_{5/2}\rightarrow{}^6H_{5/2}$), 598 ($^4G_{5/2}\rightarrow{}^6H_{7/2}$), 645 ($^4G_{5/2}\rightarrow{}^6H_{9/2}$), and 705 ($^4G_{5/2}\rightarrow{}^6H_{11/2}$) nm respectively. For glass doped with Sm_2O_3 at 0.35 mol%, the total area under peak of spectrum and the integral scintillation efficiency of 0.35 mol% Sm^{3+} doped glass samples was found to be 25% that of BGO scintillation crystals. The emission peaks of Sm^{3+} ions show four emission peaks at 560 ($^4G_{5/2}\rightarrow{}^6H_{5/2}$), 598 ($^4G_{5/2}\rightarrow{}^6H_{7/2}$), 645 ($^4G_{5/2}\rightarrow{}^6H_{9/2}$), and 705 ($^4G_{5/2}\rightarrow{}^6H_{11/2}$) nm respectively. Glass doped with Eu_2O_3 at 0.30 mol%, the total area under peak of spectrum and the integral scintillation efficiency of 0.35 mol% Eu^{3+} doped glass samples was found to be 13% to that of BGO scintillation crystals. The emission peaks of Eu^{3+} ions show five emission peaks at 578 ($^5D_0\rightarrow{}^7F_0$), 590 ($^5D_0\rightarrow{}^7F_1$), 616 ($^5D_0\rightarrow{}^7F_2$), 652($^5D_0\rightarrow{}^7F_3$), and 703 ($^5D_0\rightarrow{}^7F_5$) nm respectively. In Glass doped with Dy_2O_3 at 0.45 mol%, the total area under peak of spectrum and the integral scintillation efficiency of 0.45 mol% Dy^{3+} doped glass samples was found to be 27% that of BGO scintillation crystals. The emission peaks of Dy^{3+} ions show four emission peaks at 482 ($^4F_{9/2}\rightarrow{}^6H_{15/2}$), 577 ($^4F_{9/2}\rightarrow{}^6H_{13/2}$), 661 ($^4F_{9/2}\rightarrow{}^6H_{11/2}$), and 751 ($^4F_{9/2}\rightarrow{}^6H_{9/2}$+$^6F_{11/2}$) nm, respectively. There is great interest in developing scintillation materials for industrial and medical use in the future.

Acknowledgements

S. Kaewjaeng and S. Kothan would like to thank Department of Radiologic Technology, Faculty of Associated Medical Sciences, Chiang Mai University for partial supports. J. Kaewkhao would like to thank Nakhon Pathom Rajabhat University for use of their facilities and the support they provided.

References

[1] Tsoulfanidis N., Landsberger S., Measurement and Detection of Radiation 3rd United States of America. Taylor and Francis Group; 2011.

[2] Kumar A, Rai DK, Rai SB, Luminescence of Gd^{3+} ions doped in Oxyfluoroborate glass, J Solid State Communications 117 (2001) 387-92.

[3] Rada S, Pascuta P, Bosca M, Culea M, Pop L, Culea E, Structural properties of the boro-bismuthate glasses containing gadolinium ions, Vibrational Spectroscopy 2008; 48: 255–8.

[4] Eilk CE, Inorganic-scintillator development. Nuclear Instruments and Methods in Physics Research Section A: Accelerators, Spectrometers, Detectors and Associated Equipment 2001; 460: 1-14.

[5] Fu J, Parker JM, Brown RM, Flower, PS, Eu^{2+} ions in CaF_2-containing high Gd_2O_3 concentrations. Journal of Non-Crystalline Solids 2003; 326&327: 335–8.

[6] Fu J, Kobayashi M, Sugimoto S, Parker JM, Eu^{3+} -activated heavy scintillating glasses. Materials Research Bulletin 2008; 43(6): 1502-8.

[7] Iltisa A, Mayhugh MR, Mengeb P, Rozsab CM, Sellesc O, Solovyev V, Lanthanum halide scintillators: Properties and Applications. Nuclear Instruments and Methods in Physics Research Section A: Accelerators, Spectrometers, Detectors and Associated Equipment 2006: 359-63.

[8] Martini M, Fasoli M, Villa I, Guibert P. Radioluminescence of synthetic and natural quartz. Radiation Measurements. 2012; 47(9): 846-50.

[9] Jiang HD, Zhang HJ, Wang JY, Xia HR, Hu XB, Teng B, Zhang CQ, Optical and laser properties of Nd:$GdVO_4$ crystal, Optics Communication 2001; 198: 447-52.

[10] Wantana N, Kaewjaeg S, Kothan S, Kim HJ, Kaewkhao J, Energy transfer from Gd^{3+} to Sm^{3+} and luminescence characteristics of CaO–Gd_2O_3–SiO_2–B_2O_3 scintillating glasses, Luminescence 2017; 181: 382–6.

[11] Mares JA, Nikl M, Nitsch K, Solovieva N, Krasnikov A, Zazubovich S, A role of Gd^{3+} in scintillating processes in Tb-doped Na–Gd phosphate glasses. J Luminescence 2001; 94-95: 321-4.

[12] Rodová M, Cihlar A, Kuizek K., Nitch K, Solovieva N., Preparation and properties of Ce-doped Na–Gd phosphate glasses. Radiation Measurements 2004; 38(4–6): 489-92.

[13] Lakshminarayana G, Buddhudu S, Spectral analysis of Sm^{3+} and Dy3+:B2O3–ZnO–PbO glasses, Physica B 2006; 373: 100–6.

[14] Som T, Karmakar B, Infrared-to-red upconversion luminescence in samarium-doped antimony glasses, Journal of Luminescence 208; 128: 1989–96.

[15] Biju PR, Ajithkumar G, Jose G, Unnikrishnan NV, Spectroscopic studies of Sm^{3+}-doped phosphate glasses, Bull. Mater. Sci. 1998; 21: 415-9.

[16] Praveena R, Venkatramu V, Babu P, Jayasankar CK, Fluorescence spectroscopy of Sm^{3+} ions in P_2O_5–PbO–Nb_2O_5glasses, Physica B 2008; 403: 3527.

[17] Zhang J, Wang Y, Wen Y, Zhang F, Liu B, Luminescence properties of $Ca10K(PO_4)_7$:RE^{3+}(RE=Ce, Tb, Dy, Tm and Sm) under vacuum ultraviolet excitation, Journal of Alloys and Compounds 2011; 509: 4649–52.

[18] Mohitkar AS, Kalpana G, Vidyasagar K, Syntheses, structure and rare earth metal photoluminescence of new and known isostructural A2Mo4Sb2O18 (A¼Ce, Pr, Sm, Eu, Gd, Tb, Dy, Ho, Er,Tm, Yb, Lu) compounds, Journal of Solid State Chemistry 2011; 184: 735–40.

[19] Mohan BA, Jamalaiah BC, Suhasini T, Srinivasa RT, Rama MT, Optical properties of Eu^{3+}ions in lead tungstate tellurite glasses, Solid State Sciences 2011; 13: 574-8

[20] Santiago M, Marcazzó J, Grasselli C, Lavat A, Molina P, Spano F, Caselli E, Thermo- and radioluminescence of undoped and Dy-doped strontium borates prepared by sol-gel method. Radiation Measurements 2011; 46(12): 1488-91.

[21] Zhang F, Xiao Z, Yan L, Zhu F, Huang A, Visible luminescence properties of Er^{3+}–Dy^{3+}codoped tellurite glasses, Appl Phys A 2010; 101: 77–80.

[22] Yan Z, Chunhua L, Yaru N, Qitu Z, Zhongzi X,Optical Properties of Dy^{3+} Doped in Boroaluminasilicate Glass, Journal of Rare Earth 2007; 25: 99-103.

[23] Insiripong S, Kaewkhao J, Ratanae T, Limsuwan P, Optical and Structural Investigation of Bismuth Borate Glasses Doped With Dy^{3+}, Procedia Engineering 2011; 8: 195–9.

[24] Chewpraditkul W, Shen Y, Chen D, Yu B, Prusa P, Nik, M, Beitlerova, A., Wanarak, C., Luminescence and scintillation of Ce^{3+}-doped high silica glass. Optical materials 2012; 34 (11): 1762–6.

[25] Chewpraditkul W, Shen Y, Chen D, Beitlerova A, Nik M, Luminescence of Tb^{3+}-doped high silica glass under UV and X-ray excitation. Optical Materials 2013; 35(3): 426-30.

26. Fukabori A, Yanagida, Chani V, Moretti F, Pejchal J, Yokota Y, Kawaguchi N, Kamada K, Watanabe K, Murata T, Arikawa Y, Yamanoi K, Shimizu T, Sarukura N, Nakai M, Norimatsu T, Azechi H, Fujino S, Yoshida H, Yoshikawa A, Optical and scintillation properties of Pr-doped Li-glass for neutron detection in inertial confinement fusion process. Journal of Non-Crystalline Solids 2011; 357(3): 911-4.

[27] He D, Yu D, Cheng J, Li S, Hu L, Effect of Tb^{3+} concentration and sensitization of Ce^{3+} on luminescence properties of terbium doped phosphate scintillating glass. Journal of Alloys and Compounds 2011; 509(5): 1906-9.

[28] Pan Z, James K, Cui Y, Burger A, Cherepy N, Payne SA, Mu R, Morgan SH, Terbium-activated lithium–lanthanum–aluminosilicate oxyfluoride scintillating glass and glass-ceramic. Nuclear Instruments and Methods in Physics Research Section A: Accelerators, Spectrometers, Detectors and Associated Equipment 2008; 594(2): 215-9.

[29] D.A. Kilymis, J.M. Delaye, S. Ispas, Density effects on the structure of irradiated sodium borosilicate glass: A molecular dynamics study, J. Non-Cryst. Solids 2016; 432: 354.

[30] Kirdsiri, K., Kaewkhao, J., Limsuwan, P. Photon Interaction in Borate Glass Doped with Bi_2O_3 at Different Energies. Procedia Engineering 2012; 32: 727-33.

[31] Limkitjaroenporna, P., Kaewkhaoa, J., Chewpraditkuld, W., Limsuwan, P., (2012) Mass Attenuation Coefficient and Effective Atomic Number of Ag/Cu/Zn Alloy at Different Photon Energy by Compton Scattering Technique, Procedia Engineering 2012; 32): 847-54.

Journal of Associated Medical Sciences 2018; 51(1): 32-37

JAMS
Journal of Associated Medical Sciences

Thai-Journal Citation Index Centre (TCI) & ASEAN Citation Index (ACI)

Journal of Associated Medical Sciences

Journal homepage: https://www.tci-thaijo.org/index.php/bulletinAMS/index

Occupations after Stroke in Stroke Survivors' and Their Family Caregivers' Perception: Similarities or differences?

Jananya Panyamee Dhippayom* **Piyawat Trevittaya** **Phuanjai Rattakorn**

Occupational Therapy Department, Faculty of Associated Medical Sciences, Chiang Mai University, Thailand

ARTICLE INFO

Article history:
Received 20 December 2017
Accepted as revised 19 January 2018
Available online 19 January 2018

Keywords:
Occupation, stroke, stroke survivors, family caregivers

ABSTRACT

Background: Stroke is a leading cause of death and disability worldwide. Stroke survivors have to adapt to a life with restrictions on activities of daily living as a consequence of stroke. In Thai culture, family members generally take responsibility in providing help, care, and support to stroke survivors. Being family caregivers has been reported to be a burden. To equip families to promote better quality of life in stroke survivors in Thailand, an investigation of stroke survivors' and their family caregivers' perception on occupational performance after stroke is required.

Objectives: To examine and compare the perception among stroke survivors and their family caregivers on occupational performance of stroke survivors.

Materials and methods: Thirty stroke survivors living in the communities and their primary caregivers were recruited for the study. The 4th Edition Canadian Occupational Performance Measure (COPM) was used to assess stroke survivors' self-perception on occupations. They were asked to identify a maximum of five activities that caused difficulty to stroke participants. Stroke participants' performance and satisfaction of the reported activities were rated on a scale. The identified problems, and rated scores of performance and satisfaction were compared between two groups using Fisher's exact test and Wilcoxon signed-rank test.

Results: After stroke, participants had difficulty performing occupations by themselves, especially in the area of self-care which included personal care, functional mobility, and community management. When comparing the individual pairs, most activities were reported differently. Only 46 activities out of 157 activities (29.3%) were identified by both groups. Their perceptions on performance, and satisfaction scores of the same activities were not statistically different. The results of the study indicated that there were some similarities and discrepancies between the perceptions of the stroke participants and their caregivers on occupations after stroke even though they had close relationship.

Conclusion: For better quality of life among stroke survivors in Thai culture, occupational therapists need to use the client-centered approach focusing on both stroke survivors and their family caregivers in promoting a deeper understanding of stroke survivors' needs of care, what activity they cannot do by themselves and to what extent assistance is required.

* **Corresponding author.**
Author's Address: Occupational Therapy Department, Faculty of Associated Medical Sciences, Chiang Mai University, Chiang Mai Province, Thailand
** **E-mail address:** jananya.p@cmu.ac.th
doi: 10.14456/jams.2018.7
E-ISSN: 2539-6056

Introduction

Stroke is one of the major challenges of health care being the second leading cause of death and the third major cause of disability worldwide.[1] It was also reported to be the leading cause of death in Thailand.[2] The consequences of stroke depend on several factors, including the location and the size of the brain lesion, and personal factors. There are many devastating consequences after stroke, such as paralysis, numbness, perceptual and cognitive deficits, as well as emotional and behavioral changes.[3] Even though all these might improve over time and with rehabilitation, most stroke survivors still have some difficulties in performing occupations.

In occupational therapy, "occupation" means everyday activities that people do as individuals, in families and with communities to occupy time and bring meaning to life.[4] Occupations include things people need to, want to and are expected to do in the area of self-care, work, and leisure.[4] As an impact of stroke, stroke survivors need help and care from their caregivers in what they cannot perform. There are two common types of caregivers, including formal and informal. Formal caregivers are paid for trained care, whereas informal caregivers are not paid for providing care. Traditionally, an informal caregiver has an important role for stroke survivors who live in the community in Thailand.[5] It is generally the responsibility of family members to provide help and care for stroke survivors.[5] They take this duty because of obligation and their subjective choices derived from love, hope, and a sense of reciprocity.[6] Being an informal caregiver is also viewed as a form of suffering due to a lack of full understanding and preparation for the situation.[6, 7] This results in their development of physical symptoms, psychological/emotional problems, and social issues.[6] Also, unmet needs of care have been reported by stroke survivors.[8] However, family appears to increase stroke rehabilitation/outcomes by providing emotional and instrumental support as well as assistance with daily living.[9] Therefore, to preserve rehabilitation gains and the long-term well-being of the stroke survivors, the emphasis on stroke rehabilitation may need to shift from a patient-focused approach to a combined patient-caregiver-focused approach. The study aimed to investigate the perception of informal caregivers on occupations of stroke survivors whether there were similarities or differences when comparing with the perception of stroke survivors.

Materials and methods

This study had three research sites in Chiang Mai, Thailand. Thirty stroke survivors and their family caregivers volunteered to participate in the study. For the stroke participants, they were clients who lived in the service areas of Nakornping Hospital, Nong Pa Krang Rehabilitation Center, and Huay Kieng Rehabilitation Center. Purposive sampling was used to select the stroke participants who met the inclusion criteria, including having an onset of stroke of less than two years, being able to communicate, having no deficits of perceptual and cognitive functions, and having a family member as a primary caregiver. The 4th Edition Canadian Occupation Performance Measure (COPM) was used to measure the stroke participants' self-perception of performance in everyday living. They were asked to identify the priority of five most significant occupations that they could not perform by themselves and rate their performance and satisfaction scores of the identified occupations from 1 to 10, where 1 indicated poor performance and low satisfaction, while 10 indicated very good performance and high satisfaction.[10] Then, their family caregivers were asked to do the same procedure with the stroke participants. The perception of the stroke participants and their family caregivers on the occupations were compared using Fisher's exact test and Wilcoxon signed-rank test.

Even though the COPM was reported to be a suitable outcome measure for assessing patients with stroke in research and clinical settings,[11] there was no evidence of using the 4th edition COPM among Thai stroke survivors and their family caregivers who lived in the community. Therefore, the reliability of the 4th edition COPM had to be examined before it was used in the data collection process. Test-retest reliability was conducted with another group of 30 Thai stoke survivors who met the inclusion criteria as mentioned above and their 30 family caregivers. It was found that 96 and 97 activities were reported by the stroke survivors and by their family caregivers respectively. 100% of the problems reported by both groups were also identified for the second time with two weeks interval. The Spearman's rho correlation coefficient for the test-retest performance and satisfaction scores of the stroke survivors were 0.879 (p<.001) and 0.956 (p<.001) respectively. The Spearman's rho correlation coefficient for the test-retest performance and satisfaction scores of the family caregivers were 0.991 (p<.001) and 0.992 (p<.001) respectively. Therefore, the 4th edition COPM had high test-retest reliability for Thai stroke survivors and their family caregivers.

Results

Demographic data of the stoke participants and their primary caregivers are shown in Table 1. The age of the stroke participants ranged from 33 to 79 years old (Mean 60.33±11.77), and most of them were male (70%). For their family caregivers, their age ranged from 21 to 77 years (Mean 49.54±13.92). There were 20 females (66.7%) and 10 males (33.3%). Two majority groups of their relationship with the stroke participants were spouse (50%) and children (33.33%). All stroke participants and most family caregivers reported restriction on occupations after stroke. However, four family caregivers did not acknowledge any problems. The total numbers of activities reported by the stroke participants and by their family caregivers as an impact of stroke were 80 and 77 activities respectively. The identified activities were classified into three areas of occupation and nine categories of activity according to the COPM as shown in Table 2 and Table 3.

Table 1 Demographic data of the stroke participants and their family caregivers.

Aspects	Stroke participants (n=30)	Family caregivers (n=30)
Age range (Mean±SD)	33-79 years old (60.33±11.77)	21-77 years old (49.54±13.92)
Gender :		
Male	21 (70%)	10 (33.3%)
Female	9 (30%)	20 (66.7%)
Relationship to the stroke participants		13 wives (43.3%) 2 husbands (6.7%) 5 daughters (16.67%) 5 sons (16.67%) 1 sister (3.33%) 1 brother (3.33%) 2 fathers (6.67%) 1 sister-in-law (3.33%)
Numbers of activities as an impact of stroke		
0 activities	0	4
1 activities	12	8
2 activities	6	3
3 activities	1	4
4 activities	2	4
5 activities	9	7
The total number of identified activities	**80**	**77**

Table 2 Examination of the concurrence of identified activities.

Group	Total numbers of identified activities	Areas of occupation			Fisher's Exact Test (*p*)
		Self-care	Work	Leisure	
Stroke participants	80	55 (68.8%)	23 (28.8%)	2 (2.5%)	2.541 (0.265)
Family caregivers	77	61 (79.2%)	14 (18.2%)	2 (2.60%)	
Total	**157**	**116**	**37**	**4**	

Table 3 Classification of identified activities according to the areas of occupation and categories of activity.

Group	The numbers of identified activities									Total
	Self-care			Productivity			Leisure			
	Personal care	Functional mobility	Community management	Paid/Unpaid work	Household management	Play/school	Quiet recreation	Active recreation	Socialization	
Stroke participants	22	16	17	11	12	0	2	0	0	80
Family caregivers	32	14	15	8	6	0	2	0	0	77
Total	**54**	**30**	**32**	**19**	**18**	**0**	**4**	**0**	**0**	**157**

In Table 2, both stroke participants and their family caregivers had the same point of view that the stroke participants were confronted with difficulty in performing activities in all areas of occupation. Most limitation was in the area of self-care, followed by work, and leisure being least. There was no significant difference (Fisher's Exact Test=2.541, $p>0.05$) between the perception of stroke participants and their family caregivers on occupation restriction regarding the areas of occupation. In Table 3, personal care, community management, and functional mobility were the top three categories of activity that the stroke participants struggled with.

The numbers of similar activities between the individual pairs and the percentage of the similar activities according to the categories of occupation are shown in Table 4 and 5.

Table 4 Numbers of individual pairs according to the numbers of the same activities.

Numbers of the same activities (Activities)	Numbers of individual pairs (Pairs)
0	10
1	9
2	4
3	1
4	4
5	2

Table 5 Percentage of similar and different problems according to the categories of occupation.

Category of activity	Total activities	Similar activities	Different activities	% the same within the category	% the difference within the category
Personal care	54	19	35	35.18	64.82
Functional mobility	30	8	22	26.67	73.33
Community management	32	9	23	28.13	71.87
Paid/Unpaid work	19	6	13	31.57	68.43
Household management	18	3	15	16.67	83.33
Quiet recreation	4	1	3	25	75
Total	**157**	**46 (29.30%)**	**111 (70.70%)**		

When compare the identified activities between the individual pairs, most of the individual pairs tended to perceive a few of the same problems (0-2 activities). (See Table 4) Also, there were 10 out of 30 pairs reporting none of the same problems. In Table 5, there were only 46 out of 157 activities (29.30%) that the stroke participants and their family caregivers reported the same. The top three categories of activity being reported the same were personal care, paid/unpaid work, and community management with the percentage of the same problems of 35.18, 31.57, 28.1 respectively. For those 46 activities, the perceptions on occupational performance and satisfaction of occupational performance between the stroke participants and their primary caregivers were not statistically different as shown in Table 6 and 7.

Table 6 The comparison of occupational performance of stroke survivors between the perception of the stroke participants and their family caregivers (n=46 activities).

Group	Min/Max	Mean±SD	Wilcoxon Signed Ranks Test Z (*p*)
Stroke participants	1/9	3.78±2.42	-0.326 (.744)
Family caregivers	1/8	3.61±2.18	

Table 7 The comparison of satisfaction with occupational performance of stroke survivors between the perception of the stroke participants and their family caregivers. (n=46 activities).

Group	Min/Max	Mean±SD	Wilcoxon Signed Ranks Test Z (*p*)
Stroke participants	1/9	3.61±2.74	-1.252 (.211)
Family caregivers	1/8	4.35±2.49	

Discussion

This study's was aimed to investigate and compare the perception of 30 stroke survivors and their family caregivers on occupations after stroke. From the demographic data, most of the family caregivers were female. Most of them were spouses, and children were the next highest category.[6] This was in accordance with other studies.[5, 6] The COPM was an individualized, client-centered outcome measure.[10] It was designed to capture a client's self-perception of occupation performance in everyday living.[10] It could be used with family members or caregivers.[11] The results of assessment by the 4th edition COPM showed that the stroke participants and their family caregivers shared some similarities and differences in the perception of occupations after stroke.

Regarding similarity, both groups perceived that stroke had an impact on occupations, especially in terms of self-care activities (Table 2), including personal care, community management, and functional mobility (Table 3). Concerning occupational therapy, occupations occur in context and are influenced by the interplay among client factors, performance skills, and performance patterns.[12] Values, beliefs, and spirituality are the client factors influencing a person's motivation to engage in occupations and give his or her life meaning.[12] As self-care activity has an important role in maintaining health and wellness,[12, 13] people expect to regularly perform their self-care activities by themselves. Therefore, it is not surprising that the stroke participants and their primary caregivers expressed most of the problems in the area of self-care activity. However, there were some categories of activity that the stroke participants and their family caregivers did not report to have caused any problem. These included play/school activity, active recreation, and socialization. In the study, the stroke participants were adults or elders, and they did not need to do any activity in the play/school category. With regard to active recreation and socialization, this might be a result of the fact that the stroke participants and their family caregivers were asked to identify a maximum of five most significant occupations at the time of interview. Therefore, less significant activities were not reported. Moreover, having disability led to limitation of participation that was less diverse, limited in the home, involved fewer social relationships, and included less active recreation.[14] Thus, it might be possible that the stroke participants had significant disabilities that prevented them from doing less significant activities such as active recreation and socialization.

Even though the stroke participants and their family caregivers had close relationship (couples and parents-children), most of the stroke participants and their family caregivers perceived a few of the same problems (0-2 activities for each individual pair) (Table 4), or 46 activities out of total 157 identified activities (29.30%) (Table 5). When considering each category of activity (Table5), the highest three categories that both groups reported the same were personal care, paid/unpaid work, and community management. According to the nature of the activities in these categories, the stroke participants might not be able to perform them independently due to their decreased performance skills and physical barriers. They might need a great deal of assistance, or even had to ask their family caregivers for help. Therefore, both stroke participants and their family caregivers might perceive these activities much more the same than other groups of activity.

As the results of the study indicated the discrepancy of perception on occupations after stroke between the stroke participants and their family caregivers, this might lead to unmet care needs. The stroke participants might not receive any help in the significant activities that they needed or could not perform by themselves, or the family caregivers might provide the stroke participants with assistance in the activities that they did not want. Moreover, the discrepancy of perception of occupations after stroke might make their family caregivers overestimate or underestimate the performance and satisfaction of the stroke participants on those occupations. Unfortunately, the study did not design the methodology to proof this. There was only an analysis of the performance and satisfaction scores of the same activities reported by the stroke participants and their family caregivers (Table 6 and 7) indicating no differences of their perception on those scores.

Our finding confirmed the importance of understanding the needs of care in enabling the family caregivers to know the remaining functional capacity and satisfaction of the stroke survivors on those activities. Consequently, the family caregivers could provide the stroke survivors with appropriate and accordant assistance. Understanding the stroke participants' needs of care using occupations as a tool is not only beneficial to the stroke participants, but it can also relieve suffering among the family caregivers. The results of this study indicating the importance of understanding the needs of care in the family caregivers were in line with other studies concerning the uncertainty about stroke patients' care needs that caused a feeling of caregiving burden in the family caregivers.[5, 15] They did not have a good understanding of the role to which they were committed, and they were not well prepared to take on

even the basic tasks to meet the stroke patients' needs on discharge.[16] Therefore, early clarification of the stroke survivors' care needs is recommended for promoting better quality of life for the stroke survivors and their family caregivers. Thai occupational therapists should extend their expertise to the community to drive this crucial mechanism. The client-centered approach seemed to work well for promoting the understanding of occupations among Thai stroke survivors and their family caregivers. The outcomes of promoting the understanding about occupations among Thai stroke survivors and their family caregivers require further investigation.

Conclusion

The stroke survivors and their family caregivers had both similarities and discrepancies of the perception on occupations after stroke. To promote better health and well-being in the stroke survivors, the stroke survivors' and their family caregiver's perception should be adjusted to meet the same perception on occupations.

Conflict of interest

The researchers claimed no conflicts of interest.

Acknowledgements

This study was supported by grant from Chiang Mai University. All stroke participants and their care givers who lived in the service areas of Nakornping Hospital, Nong Pa Krang Rehabilitation Center, and Huay Kieng Rehabilitation Center were gratefully acknowledged.

References

[1] Johnson W, Onuma O, Owolabi M & Sachdev S. Stroke: a global is needed. Bull. World Health Organ 2016; 94: 634-634A. doi: http://dx.doi.org/10.2471/BLT.16.181636.

[2] Porapakkha Y, Rao C, Pattaraarchachai J, Polprasert W, Vos T, Adair T, and Lopez AD. Estimated causes of death in Thailand, 2005: Implications for health policy. Pop Health Metr 2010; 8(14): 1-11.

[3] Radomski MV, Trombly Latham CA. Occupational therapy for physical dysfunction. 7th ed. Philadelphia: Wolters Kluwer Health/Lippincott Williams & Wilkins; 2014.

[4] Christiansen CH., Baum CM. Occupational therapy: performance, participation, and well-being. 3rd ed. Thorofare, NJ: Slack; 2005.

[5] Zhang J, Lee DTF. Meaning in stroke family caregiving: a literature review. Geriatric Nursing 2017; 38(1): 48-56.

[6] Jullamate P, de Azeredo Z, Paul C, & Subgranon R. Thai stroke patient caregivers: who they are and what they need. Cerebrovascular Disease 2006; 21(1-2): 128-133. doi:10.1159/000090211.

[7] Ostwald SK, Bernal MP, Cron SG. Stress experienced by stroke survivors and spousal caregivers during the first year after discharge from inpatient rehabilitation. Top Stroke Rehabilitation 2009; 16(2): 93-104.

[8] Camicia M, Lutz BJ, Markoff N, & Catlin A. Determining the needs of family caregivers of stroke patients during inpatient rehabilitation using interview, art, and survey. Rehabil Nurs 2018; Jan 3: doi: 10.1097/RNJ.0000000000000129.

[9] Palmer S, & Glass TA. Family function and stroke recovery: a review. Rehabilitation Psychology 2003; 48(4): 255-65.

[10] Law M, Beptiste S, Carswell A, McColl MA, Polatajko H, & Pollock N. Canadian Occupational Performance Measure manual. Ottawa: CAOT Publication; 1999.

[11] Yang SY, Lin CY, Lee YC, Chang JH. The Canadian Occupational Performance measure for patients with stroke: a systematic review. J Phys Ther Sci 2017 Mar; 29(3): 548-55

[12] The American Occupational Therapy Association. Occupational therapy practice framework: domain and process. 3rd ed. Am J Occup Ther 2002; 56: 609-39.

[13] Reed K. Models of practice in occupational therapy. Baltimore: Williams & Wilkins; 1984

[14] Law M. Participation in the occupations of everyday life. Am J Occup Ther 2002; 56(6): 640-9.

[15] Scholte op Reimer WJ, de Haan RJ, Rijnders PT, Limburg M, & van den Bos GA. The burden of caregiving in partners of long-term stroke survivors. Stroke 1998; 29(8): 1605-11.

[16] Lutz BJ, Young ME, Cox KJ, Martz C, & Creasy KR. The crisis of stroke: experiences of patients and their family caregivers. Top Stroke Rehabil 2011; 18(6): doi: 10.1310/tsr1806-786.

Journal of Associated Medical Sciences 2018; 51(1): 38-44

JAMS
Journal of Associated Medical Sciences

Thai-Journal Citation Index Centre (TCI) & ASEAN Citation Index (ACI)

Journal of Associated Medical Sciences

Journal homepage: https://www.tci-thaijo.org/index.php/bulletinAMS/index

Study of leukemic stem cell population ($CD34^+/CD38^-$) and WT1 protein expression in human leukemic cell lines

Pawaret Panyajai **Noppadet Amnajphook** **Sommawan Keawsangthongcharoen** **Sawitree Chiampanichayakul** **Singkome Tima** **Songyot Anuchapreeda***

Department of Medical Technology, Faculty of Associated Medical Sciences, Chiang Mai University, Chiang Mai Province, Thailand

ARTICLE INFO

Article history:
Received 15 October 2017
Accepted as revised 12 January 2018
Available online 19 January 2018

Keywords:
Leukemic stem cell, leukemia, $CD34^+/CD38^-$, Wilms' tumor 1

ABSTRACT

Background: Leukemic stem cells (LSCs) play a central role in relapse and refractory cases of leukemia patients. This cell has been found to resist to a conventional chemotherapy more than leukemic cells. Novel therapeutic strategy directly targets to eliminate the LSCs for eradication of the disease. Abnormal of leukemic cell proliferation is the main problem. The mechanism is involved in many proteins in cell signaling pathway. Wilms' tumor 1 protein (WT1) is the transcription factor protein. It overexpresses and relates to leukemic cell proliferation but there is no report of WT1 protein expression in the LSCs.

Objectives: To compare the percent of LSC ($CD34^+/CD38^-$) population and WT1 protein expression levels in KG-1a, KG-1, and K562 cell lines.

Materials and methods: Leukemic cells were determined percent of LSC population and WT1 protein level by flow cytometry and Western blot analysis.

Results: The result showed that LSC population in KG-1a, KG-1, and K562 cells were 92.82±3.28, 75.95±4.83, and 0.44±0.51%, respectively. Almost cell population (over than 99%) in K562 cells was leukemic blast cells ($CD34^-$). WT1 protein levels by mean fluorescent intensity (MFI) analysis in LSCs of KG-1a, KG-1, and K562 cells were 46.8±5.92, 59.54±4.65, and 183.42±17, respectively. By Western blot analysis, KG-1a cells showed the highest CD34 protein level while KG-1 and K562 cells were 35.68±11.01 and 3.56±3.56%, respectively, when compared to that of KG-1a (100%). Moreover, K562 cells showed the highest WT1 protein level (100%), followed by KG-1 and KG-1a cells with the expression values of 67.23±6.86 and 42.52±5.84%, respectively.

Conclusion: WT1 protein expression levels in LSCs of KG-1a cells was less than KG-1 and K562 cells. WT-1 expression is related with the leukemic cell proliferation rate.

Introduction

Cancer is a public health problem in the world which is approximately 13% of death cause. In 2012, there are more than 8.2 million of cancer patients and the World Health Organization (WHO) has predicted that there will be an additional 70% of cancer patients and will occur in developing countries in the next 20 years.[1] In Thailand, cancer is the first cause of death for several decades. In 2011, there were approximately 35,000 patients who died with cancers. Leukemia is a type of cancer that can be found throughout the world and in people of all ages, including Thailand. Leukemia is a well-known cancer which is 1 of the most top 10 common cancers. Currently, there are more leukemia patients which can be occurred in all ages. There were 2.65 million of patients who died with leukemia in 2012.[1] While there are estimated to die with leukemia about 2,500 patients in Thailand. Especially in

* **Corresponding author.**
Author's Address: Department of Medical Technology, Faculty of Associated Medical Sciences, Chiang Mai University, Chiang Mai 50200, Thailand
** **E-mail address:** songyot.anuch@cmu.ac.th
doi: 10.14456/jams.2018.5
E-ISSN: 2539-6056

children, the incidence of leukemia was found in 53% of all cancers. Moreover, 74% of leukemia is a type of acute lymphoblastic leukemia (ALL).[1] Nowadays, chemotherapy is the most popular for many cancer treatments, including leukemia. However, there are many leukemia patients who do not respond to chemotherapy because anti-cancer drugs cannot completely eliminate all of leukemic cells in patients. The remaining cells in the patients during treatment or after treatment is known as minimal residue disease (MRD). Leukemic stem cell (LSC) is always found in MRD. Previous reports showed that LSCs resisted to chemotherapeutic drugs more than normal leukemic cells after chemotherapeutic induction. They express $CD34^+$ and $CD38^-$ on their cell surfaces.[2-4] Moreover, LSCs ($CD34^+/CD38^-$) could also self-renew and differentiate into leukemic blasts in the recipient mice.[4,5] Cell surface proteins in LSCs are different from hematopoietic stem cells (HSCs) even if they are $CD34^+/CD38^-$. LSCs show different cell surface markers such as, CD44[6], CD96[7], and CD123[8]. High frequencies of $CD34^+/CD38^-$ LSC at diagnosis and after treatment help to predict relapse in AML.[9]

In leukemic cells, Wilms' tumor 1 (WT1) protein is expressed as a biological marker and plays an important role in cell proliferation.[10] It is overexpressed in leukemic cells when compared to normal blood cells. The decreasing of WT1 protein expression results in decreasing of leukemic cell proliferation.[11,12] Thus, WT1 protein plays a key role in leukemogenesis. However, there is no report about WT1 in LSCs. We believed that all cell population mixtures of cell lines have LSCs, but the cell number population may be varied by the type of leukemic cell line. This study was to investigate percent population of LSCs in three leukemic cell lines and determine percent of WT1 expression in LSCs. KG-1, KG-1a, and K562 cells are leukemic cell lines to be used as the leukemic cell model in this study.

Materials and methods

Cell culture and condition

KG-1 (acute myeloblastic leukemia cell line), KG-1a (subline of KG-1 cell line), and K562 (chronic myelogenous leukemia cell line) were used as human leukemic cell line models in this study. K562 cells were cultured in RPMI-1640 medium (GIBCO™, Thermo Fisher Scientific, MA, USA) supplemented with 10% fetal bovine serum (Capricon, Ebsdorfergrund, Germany), 2 mM L-glutamine, 100 units/mL penicillin and 100 µg/mL streptomycin (GIBCO™, Thermo Fisher Scientific, MA, USA). KG-1a and KG-1 cells were cultured in IMDM medium (GIBCO™, Thermo Fisher Scientific, MA, USA) supplemented with 20% fetal bovine serum, 2 mM L-glutamine, 100 units/mL penicillin and 100 µg/mL streptomycin. All leukemic cell lines were cultured at 37 °C in a humidified incubator with 5% CO_2.

Growth rate analysis of leukemic cell lines

KG-1a, KG-2, and K562 cells were seeded with complete medium in 24-well plate with the concentration of 1.0×10^4 cells/well. Then, cells were counted with trypan blue dye exclusion method (0.4% trypan blue solution, Amresco®, OH, USA) for 6 days. Values for the measured property are plotted on a graph between total viable cell number and times.

Trypan blue dye exclusion method

After leukemic cells were harvested, cells were washed with ice-cold PBS, pH 7.4 for 3 times. Then, cells were resuspended with PBS, pH 7.4 and stained with 0.4% trypan blue solution at 1:2 dilution for counting cells on hemocytometer. The viable cell shows a clear cytoplasm because it can exclude trypan blue, while dead cells show a blue cytoplasm and vice versa in mechanism.

$CD34^+/CD38^-$ cell analysis by flow cytometry

KG-1a, KG-1, and K562 cells were harvested after cell concentrations reached 80% cell confluency. Then, cells were adjusted the concentration to 1.0×10^7 cells/mL and blocked non-specific antibody binding with 10% AB serum in PBS for 30 min at 4 °C. After that, leukemic cell lines were incubated with FITC conjugated anti-CD34 and PE conjugated anti-CD38 monoclonal antibodies for 30 min at 4 °C. Cells were then washed with 1% BSA-PBS for 3 times and re-suspended with 1% paraformaldehyde. $CD34^+/CD38^-$ cells were analyzed by flow cytometer (FC500, Beckman coulter, CA, USA).

WT1 protein expression by flow cytometry

The leukemic cell lines were examined WT1 by flow cytometry. Briefly, leukemic cell lines (1.0×10^7 cells) were blocked non-specific antibody binding with 10% human AB serum in PBS, pH 7.4 for 30 min at 4 °C. After that, cells were fixed with 4% paraformaldehyde for 20 min exactly. Then, cells were washed and permeabilized by permeabilization buffer (0.02% NaN_3, 0.1% saponin, and 5% FBS in PBS, pH 7.4) and incubated with anti-WT1 antibody for 30 min at 4 °C. Cells were washed with permeabilization buffer and incubated with PE-Cy5.5 conjugated secondary antibody for 30 min at 4 °C. Finally, cells were washed and re-suspended with 1% paraformaldehyde for flow cytometry analysis.

Protein extraction and Western blotting

KG-1a, KG-1, and K562 cells were harvested after cells reached 80% cell confluency. Leukemic cells were harvested. The number of viable cells was determined using 0.4% trypan blue dye solution. Thereafter, total protein was extracted using RIPA buffer. Protein concentration was measured by the Folin-Lowry method. Protein was separated by 12% SDS-PAGE and then transferred to PVDF membranes. Membranes were blocked in 5% skim milk and probed by rabbit polyclonal anti-WT1 antibody (Santa Cruz Biotechnology, TX, USA), rabbit monoclonal anti-CD34 antibody (Santa Cruz Biotechnology, TX, USA) and rabbit polyclonal anti-GAPDH antibody (Santa Cruz Biotechnology, TX, USA) at dilution 1:1,000. The reaction was followed by HRP-conjugated goat anti-rabbit IgG (Invitrogen™, CA, USA) at 1:20,000 dilution. The proteins were visualized using Luminata™ Forte Western HRP substrate (Millipore Corporation, MA, USA). Finally, the protein band signal was quantified by using a scan densitometer (Bio-Rad, CA, USA).

Statistical analysis

Data are expressed as the mean±SD from triplicate samples of three independent experiments. The statistical differences between the means were determined using independent t-test. The differences were considered significant when the probability value obtained was found to be less than 0.05 (p<0.05) and 0.001 (p<0.001).

Results

Cell growth of KG-1, KG-1a, and K562 leukemic cell lines

Figure 1 shows the different patterns of leukemic cell growths. The growth rate of all leukemic cells showed lag phase in the first 3 days. After day 3, KG-1a and KG-1 cells showed low proliferation rate as compared to K562 cells.

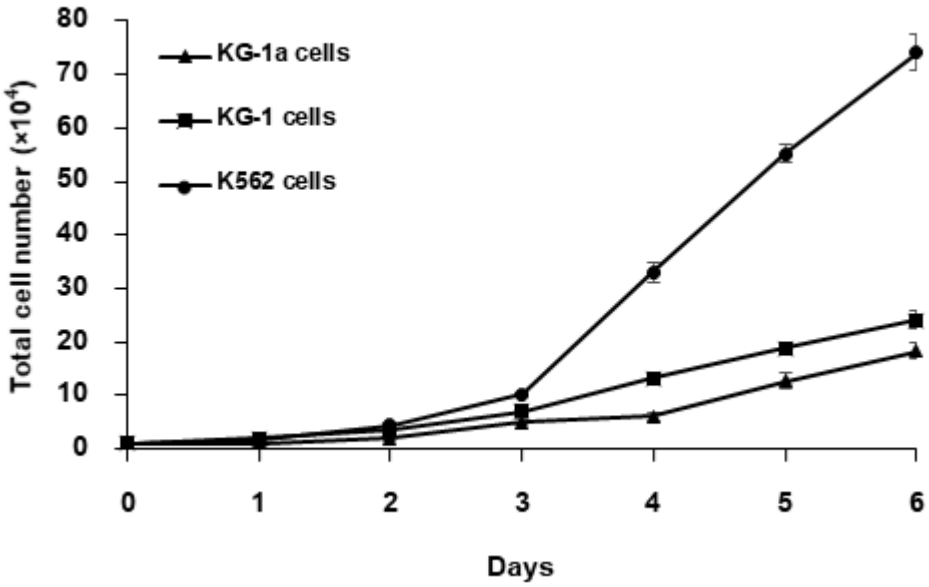

Figure 1. *Growth curves of leukemic cell lines. KG-1a, KG-1, and K562 cells were seeded in 24 well-plates with the concentration of 1.0×10⁴ cells/well. Cells were counted with trypan blue exclusion method for 6 days.*

Leukemic stem cell population in leukemic cell lines by flow cytometry

In this study, KG-1a cells had the highest LSC ($CD34^+/CD38^-$) population with 92.82±3.28% by flow cytometry followed by KG-1 cells with 75.95±4.83%, while leukemic stem cell population in K562 cells were less than 0.5%. The K562 cell population mostly were blast cells ($CD34^-$) which showed more than 99%. The result showed significantly different of LSC population among KG-1a cells and others two cell lines (p<0.001) (Table 1 and Figure 2).

Table 1 Percentage of leukemic stem cell populations in cell lines.

Cell lines	% Cell populations (Mean±SD)			
	$CD34^+/CD38^-$	$CD34^+/CD38^+$	$CD34^-/CD38^-$	$CD34^-/CD38^+$
KG-1a	92.82±3.28	1.60±1.18	3.54±2.28	0.06±0.03
KG-1	75.95±4.83	13.62±5.24	6.58±3.90	1.85±1.43
K562	0.44±0.51	0.26±0.16	98.27±0.59	1.30±0.28

Data represents the mean±standard deviation (SD) of three independent experiments.

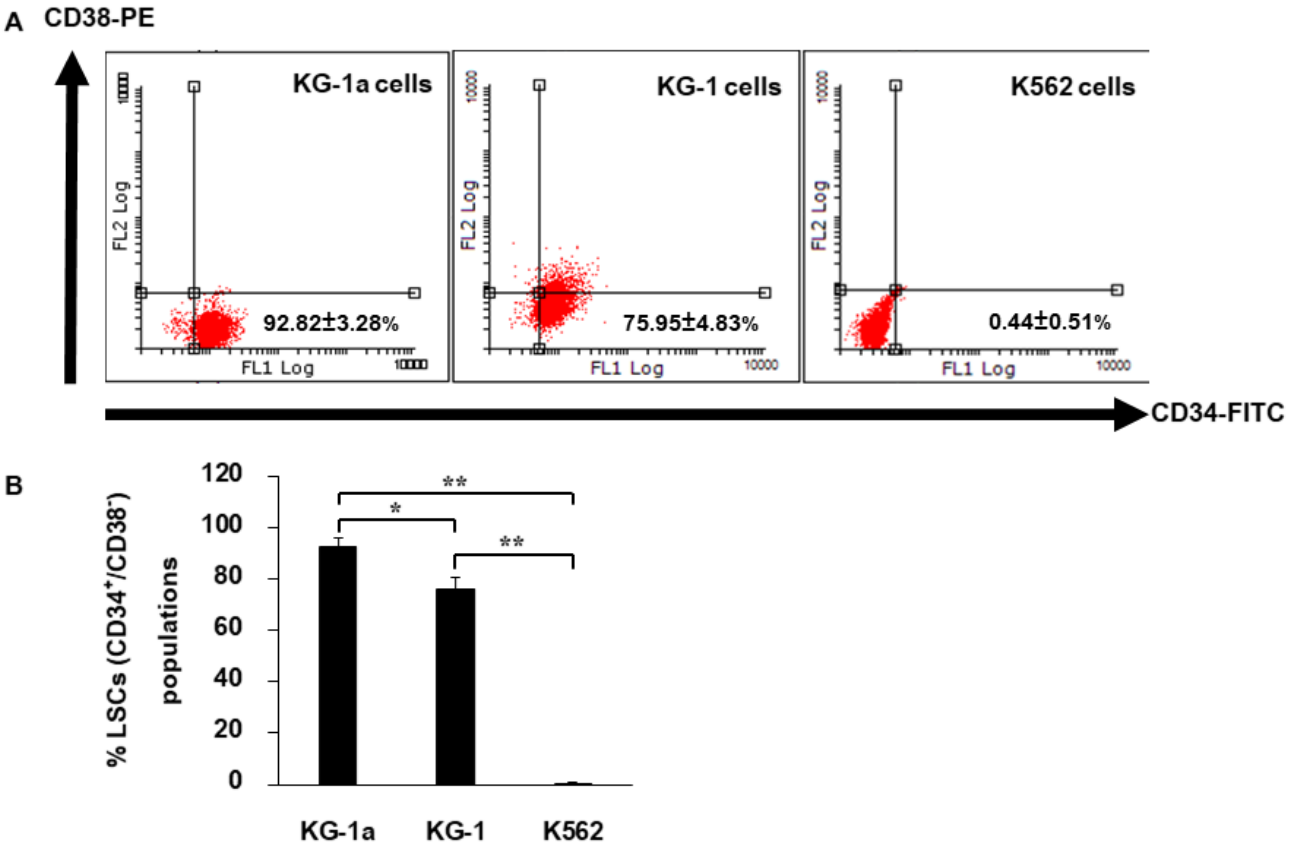

Figure 2. *Leukemic stem cell populations in each cell line. (A) Flow cytometry analysis show cell populations in each quadrant region. Each cell line was stained with FITC conjugated anti-CD34 antibody and PE conjugated anti-CD38 antibody. (B) Data of LSC populations were represented as the mean values±SD of three independent experiments. Single asterisk (*) denotes a significant difference from each group at p-value<0.05 and double asterisk (**) denotes a significant difference in each group at p-value<0.001.*

WT1 protein expression in leukemic cells by flow cytometry

To determine WT1 protein expressions in LSCs, all leukemic cell lines were determined and compared WT1 protein expression levels by flow cytometry. The result showed that K562 cells had the highest mean fluorescence intensity (MFI) of WT1 in leukemic cells with 183.42±17.44, followed by KG-1 and KG-1a with the MFIs of 59.54±4.65 and 46.8±5.92, respectively (Figure 3).

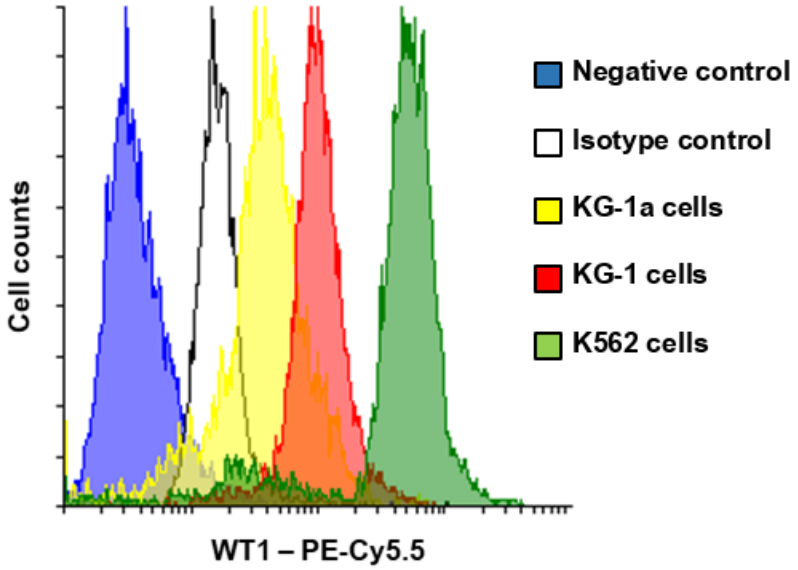

Figure 3. *WT1 expression in leukemic cell lines. Each cell line was stained with FITC conjugated anti-CD34 antibody, PE conjugated anti-CD38 antibody, and anti-WT1 antibody with PE-Cy5.5 conjugated secondary antibody.*

CD34 and WT1 protein expressions in leukemic cell lines by Western blotting

KG-1a cells showed the highest CD34 protein expression after determining by Western blotting (100%), while CD34 protein levels of KG-1 and K562 cells were significantly lower than KG-1a cells with the values of 35.68±11.01 and 3.56±3.56%, respectively (Figure 4). The WT1 protein levels showed that K562 cells had the highest WT1 protein level (100%), followed by KG-1 and KG-1a cells with 67.23±6.86 and 42.52±5.84%, respectively, compared to K562 cells (Figure 5). The results showed significantly different of WT1 protein expression between K562 cells and others two cell lines (p<0.05). Moreover, WT1 protein level of KG-1 cells was significantly higher (24.71%) than KG-1a cells (p<0.05).

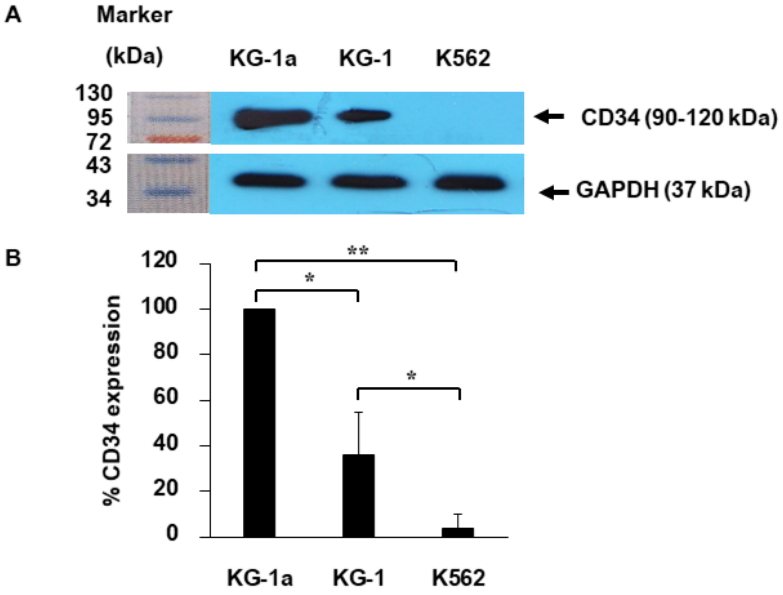

Figure 4. *CD34 protein expression levels in leukemic cell lines. (A) The levels of CD34 protein from KG-1a, KG-1, and K562 cell lines after incubation for 48 h were assessed by Western blotting; GAPDH was used as the loading control. (B) The protein levels were analyzed with a scan densitometer. Data are the mean values±SD of three independent experiments. Single asterisk (*) denotes a significant difference from each group at p-value<0.05 and double asterisk (**) denotes a significant difference in each group at p-value<0.001.*

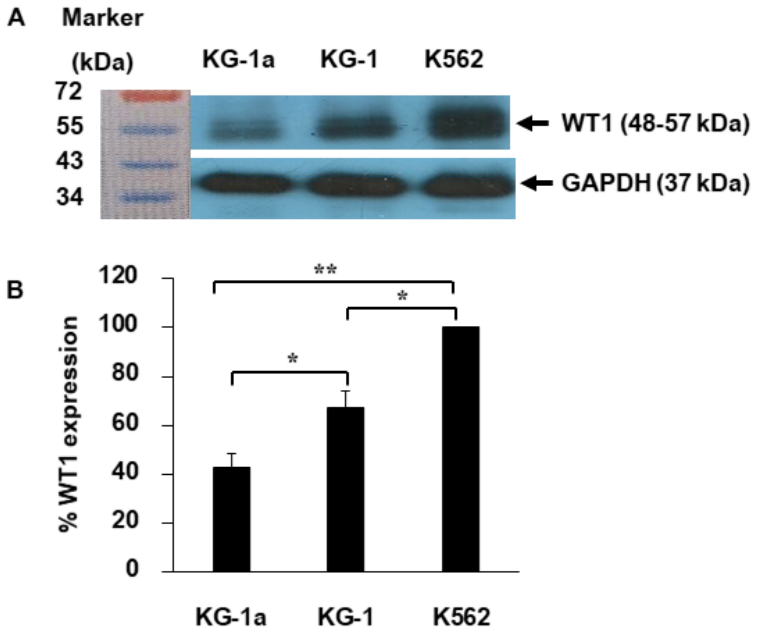

Figure 5. *WT1 protein expression levels in leukemic cell lines. (A) The levels of WT1 protein form KG-1a, KG-1, and K562 cell lines after incubation for 48 h were assessed by Western blotting; GAPDH was used as the loading control. (B) The protein levels were analyzed with a scan densitometer. Data are the mean values±SD of three independent experiments. Single asterisk (*) denotes a significant difference from each group at p-value<0.05 and double asterisk (**) denotes a significant difference in each group at p-value<0.001.*

Discussion

Nowadays, there are many reports which indicated both of acute myeloid leukemia (AML) and chronic myeloid leukemia (CML) contain LSCs.[4,5,13] LSCs are responsible for relapse and refractory cases to leukemia chemotherapy.[14] Thus, remaining LSC in leukemia patient (minimal residual disease or MRD) is the main problem for leukemia treatment. LSCs are also very difficult to get rid of due to drug resistance and absence of drug response phenotypes. However, LSC population rarely presented in AML patient was found only 0.01-0.09%.[4] This study is the first report to show the percent of LSCs in leukemic cell lines and relationship between LSCs and WT1 protein expression in leukemic cell lines.

In present study, three leukemic cell lines were used as model and investigated their growth rates and LSC populations for WT1 protein expression. LSC population in both KG-1a and KG-1 cells were more than 50% while LSC population in K562 cells were less than 0.5%. KG-1a cells had LSC population more than 90%. This result relates to the rate of cell growth in three cell lines.

WT1 protein have been reported as an oncoprotein which is involved in leukemic cell proliferation.[15] Increase level of WT1 protein results in high rate of cell proliferation. This study, WT1 expression levels in KG-1a, KG-1, and K562 cells were different. WT1 expression level in K562 cells after flow cytometry and Western blotting showed the highest levels whereas, the lowest was found in KG-1a cells. This phenomenon relates to the growth rates of both cell lines. K562 cells demonstrated higher rate of cell proliferation than KG-1a cells from day 4 to 6. Furthermore, KG-1a cells showed the different LSC populations (92.82±3.28%) with 211-fold when compared to K562 cells (0.44±0.51%). LSC itself has lower activity when compared to leukemic blast cells.[16-18] Almost cell population of K562 cell line is leukemic blast cells ($CD34^-$). Thus, cell proliferation rate is higher than that of KG-1a cells ($CD34^+/CD38^-$). However, KG-1 cells showed the rate of cell proliferation and LSC population between KG-1a and K562 cells. KG-1a cell is less differentiated variant of KG-1 cell.[19] Moreover, previous reports also indicated that LSCs expressed *Bmi-1* gene which involved in the regulation of self-renewal and differentiation in LSCs.[20-22] High level of *Bmi-1* gene expression could lead to LSCs are mostly quiescent cell cycle[23] which suggested that conventional anti-proliferative cytotoxic agents are minimally impacted against LSCs. In hematopoietic cell differentiation, HSCs ($CD34^+/CD38^-$) differentiate to be multipotent progenitor ($CD34^+/CD38^-$) and committed cells ($CD34^+/CD38^+$).[24] HSC resides in the $Lin^-/CD34^+/CD38^{-/lo}/CD90^+$ fraction in bone marrow and $CD34^+/CD38^+$ cells contained multiple progenitors while leukemia stem cells resided in an early $CD34^+/CD38^-/CD90^-$ progenitor, while leukemic blasts were $CD34^+/CD38^+$ phenotype.[25,26] Recently, there are previous reports demonstrated that the distinct surface protein expressions on LSCs as compared to normal HSCs, such as CD44[6], CD96[7], and CD123[8]. These antigens are useful for the isolation and identification of LSCs which required further study for investigation in KG-1a cells. Previous study showed that normal HSC-enriched population ($Lin^-/CD34^+/CD38^-/CD90^+$) expressed CD96 weakly, while $CD96^+$ AML cells are enriched for LSC activity.[7] Thus, CD96 was reported as a LSC-specific marker in AML. However, WT1 protein have been reported as a biological marker in leukemia. This study reveals that WT1 protein expression also presents in LSCs even if lower than that of leukemic cells.

This is the first report to show the WT1 protein expression levels in LSCs. In present study, the result indicated that WT1 protein expression is inversely proportional to LSC population. Thus, KG-1a cells showed a low proliferative rate than KG-1 and K562 cells.

Conclusion

KG-1a cell represents LSC of leukemia patient. Furthermore, KG-1a cells also had WT1 expression which was a suitable target protein for further study. This study reveals the LSC population and WT1 protein levels in distinct phenotypes of 3 leukemic cell lines are different. These two factors (LSC population and WT1 protein) were found to relate to rate of cell proliferations. High level of WT1 protein indicates the high rate of cell proliferation as presented in K562 leukemic blast cells. On the other hand, low level was found in KG-1a leukemic stem cells. However, WT1 can be used as biological marker in LSCs. This research provides a basic knowledge for studying LSCs target therapy. In addition, there are some other proteins that also effect to proliferation and function of LSCs which should be investigated in further study.

Acknowledgements

The authors are grateful for grants received from the Thailand Research Fund (TRF) and Chiang Mai University grant, and the National Research Council (NRC) and Chiang Mai University Research Fund under Grant number 348438.

References

[1] Jaffe ES, Swerdlow SH, Vardiman JW. Haematopoietic and lymphoid malignancies. In: Stewart BW, Wild CP, editors. World Cancer Report 2014. 150 Cours Albert Thomas, 69372 Lyon CEDEX 08, France: International Agency for Research on Cancer (IARC); 2014. p. 482-94.

[2] Sikic BI. Multidrug resistance and stem cells in acute myeloid leukemia. Clin Cancer Res 2006; 12(11 Pt 1): 3231-2.

[3] Wang F, Wang XK, Shi CJ, Zhang H, Hu YP, Chen YF, et al. Nilotinib enhances the efficacy of conventional chemotherapeutic drugs in $CD34^+CD38^-$ stem cells and ABC transporter overexpressing leukemia cells. Molecules 2014; 19(3): 3356-75.

[4] Lapidot T, Sirard C, Vormoor J, Murdoch B, Hoang T, Caceres-Cortes J, et al. A cell initiating human acute myeloid leukaemia after transplantation into SCID mice. Nature 1994; 367(6464): 645-8.

[5] Bonnet D, Dick JE. Human acute myeloid leukemia is organized as a hierarchy that originates from a primitive hematopoietic cell. Nat Med 1997; 3(7): 730-7.

[6] Jin L, Hope KJ, Zhai Q, Smadja-Joffe F, Dick JE. Targeting of CD44 eradicates human acute myeloid leukemic stem cells. Nat Med 2006; 12(10): 1167-74.

[7] Hosen N, Park CY, Tatsumi N, Oji Y, Sugiyama H, Gramatzki M, et al. CD96 is a leukemic stem cell-specific marker in human acute myeloid leukemia. Proc Natl Acad Sci U S A 2007; 104(26): 11008-13.

[8] Jordan CT, Upchurch D, Szilvassy SJ, Guzman ML, Howard DS, Pettigrew AL, et al. The interleukin-3 receptor alpha chain is a unique marker for human acute myelogenous leukemia stem cells. Leukemia 2000; 14(10): 1777-84.

[9] Schuurhuis GJ, Meel MH, Wouters F, Min LA, Terwijn M, de Jonge NA, et al. Normal hematopoietic stem cells within the AML bone marrow have a distinct and higher ALDH activity level than co-existing leukemic stem cells. PLoS One 2013; 8(11): e78897.

[10] Scharnhorst V, van der Eb AJ, Jochemsen AG. WT1 proteins: functions in growth and differentiation. Gene 2001; 273(2): 141-61.

[11] Anuchapreeda S, Tima S, Duangrat C, Limtrakul P. Effect of pure curcumin, demethoxycurcumin, and bisdemethoxycurcumin on WT1 gene expression in leukemic cell lines. Cancer Chemother Pharmacol 2008; 62(4): 585-94.

[12] Anuchapreeda S, Limtrakul P, Thanarattanakorn P, Sittipreechacharn S, Chanarat P. Inhibitory effect of curcumin on WT1 gene expression in patient leukemic cells. Arch Pharmacal Res 2006; 29(1): 80-7.

[13] Sirard C, Lapidot T, Vormoor J, Cashman JD, Doedens M, Murdoch B, et al. Normal and leukemic SCID-repopulating cells (SRC) coexist in the bone marrow and peripheral blood from CML patients in chronic phase, whereas leukemic SRC are detected in blast crisis. Blood 1996; 87(4): 1539-48.

[14] de Figueiredo-Pontes LL, Pintao MC, Oliveira LC, Dalmazzo LF, Jacomo RH, Garcia AB, et al. Determination of P-glycoprotein, MDR-related protein 1, breast cancer resistance protein, and lung-resistance protein expression in leukemic stem cells of acute myeloid leukemia. Cytometry B Clin Cytom 2008; 74(3): 163-8.

[15] Yamagami T, Sugiyama H, Inoue K, Ogawa H, Tatekawa T, Hirata M, et al. Growth inhibition of human leukemic cells by WT1 (Wilms tumor gene) antisense oligodeoxynucleotides: implications for the involvement of WT1 in leukemogenesis. Blood 1996; 87(7): 2878-84.

[16] Holyoake T, Jiang X, Eaves C, Eaves A. Isolation of a highly quiescent subpopulation of primitive leukemic cells in chronic myeloid leukemia. Blood 1999; 94(6): 2056-64.

[17] Won EJ, Kim H-R, Park R-Y, Choi S-Y, Shin JH, Suh S-P, et al. Direct confirmation of quiescence of $CD34^{+}CD38^{-}$ leukemia stem cell populations using single cell culture, their molecular signature and clinicopathological implications. BMC Cancer 2015; 15: 217.

[18] She M, Niu X, Chen X, Li J, Zhou M, He Y, et al. Resistance of leukemic stem-like cells in AML cell line KG1a to natural killer cell-mediated cytotoxicity. Cancer Lett 2012; 318(2): 173-9.

[19] Mrózek K, Tanner SM, Heinonen K, Bloomfield CD. Molecular cytogenetic characterization of the KG-1 and KG-1a acute myeloid leukemia cell lines by use of spectral karyotyping and fluorescence in situ hybridization. Genes Chromosomes Cancer 2003; 38(3): 249-52.

[20] Lessard J, Sauvageau G. Bmi-1 determines the proliferative capacity of normal and leukaemic stem cells. Nature 2003; 423(6937): 255-60.

[21] Raaphorst FM. Self-renewal of hematopoietic and leukemic stem cells: a central role for the Polycomb-group gene Bmi-1. Trends Immunol 2003; 24(10): 522-4.

[22] Yuan J, Takeuchi M, Negishi M, Oguro H, Ichikawa H, Iwama A. Bmi1 is essential for leukemic reprogramming of myeloid progenitor cells. Leukemia 2011; 25(8): 1335-43.

[23] Saito Y, Kitamura H, Hijikata A, Tomizawa-Murasawa M, Tanaka S, Takagi S, et al. Identification of therapeutic targets for quiescent, chemotherapy-resistant human leukemia stem cells. Sci Transl Med 2010; 2(17): 17ra9.

[24] Seita J, Weissman IL. Hematopoietic stem cell: self-renewal versus differentiation. Wiley Interdiscip Rev Syst Biol Med 2010; 2(6): 640-53.

[25] Majeti R, Weissman IL. Human acute myelogenous leukemia stem cells revisited: there's more than meets the eye. Cancer Cell 2011; 19(1): 9-10.

[26] Majeti R, Becker MW, Tian Q, Lee T-LM, Yan X, Liu R, et al. Dysregulated gene expression networks in human acute myelogenous leukemia stem cells. Proc Natl Acad Sci U S A 2009; 106(9): 3396-401.

Journal of Associated Medical Sciences 2018; 51(1): 45-50

JAMS
Journal of Associated Medical Sciences

Thai-Journal Citation Index Centre (TCI) & ASEAN Citation Index (ACI)

Journal of Associated Medical Sciences

Journal homepage: https://www.tci-thaijo.org/index.php/bulletinAMS/index

The diagnostic X-ray exposure technique guidelines for elephants' limbs in Elephant Hospital, Thai Elephant Conservation Center, Thailand

Chatchanok Udomtanakunchai[1*] Sirijan Lawongwan[1] Sasithorn Tasomkan[1] Pornsawan Pongsopawijit[2] Warangkhana Langkaphin[3]

[1]Department of Radiologic Technology, Faculty of Associated Medical Sciences, Chiang Mai University, Chiang Mai Province, Thailand
[2]Department of Companion Animal and Wildlife Clinic, Faculty of Veterinary Medicine, Chiang Mai University, Chiang Mai Province, Thailand
[3]National Elephant Institute, Forest Industry Organization, Lampang Province, Thailand

ARTICLE INFO

Article history:
Received 1 December 2017
Accepted as revised 28 January 2018
Available online 30 January 2018

Keywords:
Asian elephant, limb, diagnostic X-ray, Sante's rule

ABSTRACT

Background: Radiographic image is the first of choice for diagnosing complications involving elephants' limbs. The extreme thickness of their limbs causes inaccurate image quality. Therefore, an appropriate procedure is hereby investigated as a matter concerned. Because of difference of X-ray absorption in elephant tissue from human tissue, the Sante's rule cannot be directly applied.

Objectives: This study sought to acquire the appropriate equation by modifying the Sante's rule with a tissue factor for calculating the exposure technique for Asian elephants' limbs.

Materials and methods: Firstly, capacity of a mobile X-ray machine was evaluated in terms of dose rate, precision, and accuracy of radiation. The exposure techniques were then designed using the modified Sante's rule and tested with the hind limbs of 10 live elephants.

Results: Output of X-ray machine revealed the dose rate in milli-Rontgen per milli-Ampere-sec equal to 4×10^{-4} of kVp^2, and the machine factor equal to 6.4. The radiographic images taken using the calculated exposure techniques showed good quality, and so, it is possible to differentiate between the medullar and the cortex of the bone.

Conclusion: Equations suitable for designing the exposure technique are kVp equal to two times of sample thickness in centimeter plus source image distance in inche and the tissue correcting factor 5, and mAs equal to two-fifths of the sample thickness in centimeters.

Introduction

Elephant is the national animal of Thailand. Some elephants have an elevated position as companions to humans. The Thai Elephant Conservation Center's Elephant Hospital offers free treatment to elephants all over Thailand. The treatments are offered through mobile clinics operated by various organizations.[1] In the past decade, injury has been the cause of most Thai and Asian elephants' health problems.[2,3] When zoo animals such as elephants have a medical condition, radiological imaging is required as an important tool for diagnosis.[4] Because of their thick limbs and uncontrolled complications, exposure technique guidelines are required for good quality images. Past studies have sought to develop effective radiographic techniques for large animals such as elephants and white rhinoceroses for monitoring bone maturation, ossification, mineralization, and injury.[5-10] However, no explanation has been stated for those acquired techniques. Image quality depends on the variation of the influencing factors, such as kVp, mAs, time, source image distance (SID), and tissue absorption factor.

* **Corresponding author.**
Author's Address: Department of Radiologic Technology, Faculty of Associated Medical Sciences, Chiang Mai University, 110 Intawaroroj Road, Sripoom, Chiang Mai Province, Thailand
** **E-mail address:** chatchanok.u@cmu.ac.th
doi: 10.14456/jams.2018.8
E-ISSN: 2539-6056

In general, radiographic techniques (kVp and mAs) are calculated based on the principles of Sante's rule which includes parameters such as tissue thickness, source image distance and grid factor.[11] In fact, tissue density which is one of the important factors that affect X-ray absorption by a medium should be an factor of concern.[12] Current available known data strongly indicated only X-ray absorption on human tissue.[13,14] The radiographic technique calculated based on information on human characteristics cannot be used for elephants because of the main difference in physical characteristic of elephant skin. Lacking of knowledge has led to imprecise radiographic techniques for diagnosing elephants and is a cause for misdiagnosis. Hence, this work aims to design the equation of exposure factors (kVp and mAs) of a mobile X-ray machine for calculating the exposure technique guidelines that use for elephant limbs.

Materials and methods

This study was approved by the Animal Ethics Committee, Faculty of Veterinary Medicine, Chiang Mai University, Thailand, in 2017 (R4/2560). Live Asian elephants residing in The National Elephant Institute, Forest Industry Organization, Lampang Province, Thailand, were joined in this experiment. A mobile X-ray machine (Hitachi, model Sirius 130HP, 250 mA, Japan) and a computed radiograph of Fuji model FCR PRIMA II (IP cassette type CC with CR imaging plate type ST-VI size 14"×17", Japan) were used for image recording. All radiographic images were recorded using digital image plates as DICOM files. Histogram of intensity was obtained by a freeware ImageJ program[15] (version 1.51p) for image evaluation.

Evaluation of X-ray machine

Capacity of the X-ray machine was assessed by triplicate determination of dose rate at three different mAs of each kVp (60, 80, 90, 100, 110, 120 and 130) at source image distance of 25 inch and field size of 14×14 square inches. Line voltage (kVp), mAs, and dose rate of X-ray were determined by using a solid state multisensor for diagnostic range (Radcal model AGMS-D+, CA, USA) size 35.6 mm × 20.0 mm × 11.8 mm. The machine factor (P) of the X-ray machine can be calculated from the relationship between the dose, the kVp, and mAs as the following equation: Dose (mR) = $P(kVp)^2.mAs/(SID)^2$.[16]

Exposure technique designing

For radiographic imaging, factors affecting the exposure technique included capacity of the X-ray machine, source image distance, grid, and image acquisition system. Firstly, the estimated exposure technique was modified based on Sante's rule which includes equations for calculating the kVp and the mAs value.[17] One hind limb of a live elephant was measured for thickness and subjected to three trial exposures: (1) estimated technique, (2) lower technique, and (3) higher technique. Three images were evaluated. Exposure technique was then recalculated using the modified Sante's rule equation, and used to expose ten live elephants' hind limbs. Evaluation of the image quality was based on veterinary opinions and density plot profil. Statistical analysis was performed by authors. Microsoft Excel (2016) program was used for descriptive statistics to estimate the central tendency. All data were established as normal distributions; then, the mean and the standard deviation were calculated.

Results

Evaluation of X-ray machine

In order to draw the exposure technique chart, the X-ray machine was assessed for exposure properties by testing the precision and accuracy of kVp and the output of X-ray. The kVp value was evaluated by setting kVp (60, 80, 90, 100, 110, 120, and 130) for three various mAs values in each kVp. The accuracy and precision of kVp are, respectively, presented in %Error (between 1.72 and 2.59) and %CV (lower than 1 for all kVp) (Table 1). The result of the output of the X-ray machine is shown in dose rate in milli-roentgen per milli-ampere second (mR/mAs) at each kVp, as shown in Figure 1. The relation between the dose rate and kVp was defined by the equation mR/mAs $=6.4\times10^{-4}*kVp^2$, which gave the machine factor (P) as equal to 6.4.

Table 1 Accuracy (%Error) and precision (%CV) of kVp values between 60 and 130 of X-ray machine at source image distance of 100 cm and field size of 14"×14"

Setting kVp (mAs)	Measured kVp Mean±SD	%Error	%CV
60 (50, 160, 200)	61.30±0.06	2.17	0.09
80 (40, 100, 160)	81.55±0.07	1.94	0.09
90 (40, 80, 120)	92.28±0.04	2.53	0.05
100 (40, 80, 120)	102.59±0.03	2.59	0.03
110 (40, 80, 100)	112.26±0.05	2.05	0.05
120 (20, 50, 80)	122.07±0.10	1.72	0.08
130 (20, 50, 80)	132.57±0.16	1.97	0.12

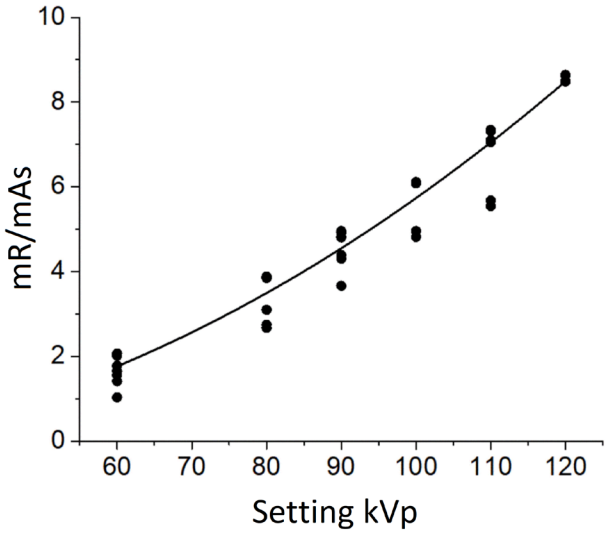

Figure 1 *Plot of exposure rate per mAs at various setting kVp values; the relation was fitted with the equation mR/mAs = $6.4\times10^{-4}*kVp^2$ (machine factor, P=6.4).*

Exposure technique designing

According to the principal of the Beer-Lambert Rule which descript the attenuation properties of X-ray in the medium as the following equation.[12]

$$I=I_0e^{-\mu X}$$

Where μ is the linear attenuation coefficient (cm^{-1})
I_0 is the initial intensity that is related to the X-ray flux before passing through
I is the transmitted intensity that passes through the medium at the measured thickness position
X is the thickness of the medium that the X-ray flux passes through (cm)

For human (subscript H) $$\frac{I_{0H}}{I_H}=e^{\mu_H X} \quad (1)$$

For elephant (subscript E) $$\frac{I_{0E}}{I_E}=e^{\mu_E X} \quad (2)$$

(2)/(1) $$\frac{I_{0E}}{I_E}\frac{I_H}{I_{0H}}=\frac{e^{\mu_E X}}{e^{\mu_H X}} \quad (3)$$

$$\frac{I_{0E}}{I_E}\frac{I_H}{I_{0H}}=e^{(\mu_E X-\mu_H X)} \quad (4)$$

By the condition of transmitted intensity from human tissue and elephant tissue are the same $I_H = I_E$ and the linear attenuation coefficient of elephant tissue (μ_E) which obtained by previous studies is about 1.2 time of human tissue ($\mu_E=1.2\mu_H$) so the initial intensity for elephant tissue (I_{0E}) at the same thickness as human tissue can be simplified as follow.

$$I_{0E}=e^{(0.2\mu_H X)}.I_{0H} \quad (5)$$

By using the equation (5), the estimated value of $e^{(0.2\mu_H X)}$ are ranging from 2-3 when the kVp value are ranging from 40-150 kVp and the thickness of subject is 20 cm. According to the machine factor of X-ray machine is in the lower range that is about 5 times lesser than the maximum value, so the first estimation of the kVp value was obtained by using Sante's rule plus the factor 10.

Test exposure

The capacity of the X-ray machine was such that it showed good accuracy and precision of the kVp value, and the exposure rate was found to theoretically correlate with kVp2. Because of the machine factor and the effect of the high density of the soft tissue of elephants, the radiographic image of the hind limb in the projection of the lateral view (20 cm thickness and the factor considered as 10) was taken using the estimated technique (90 kVp 8 mAs) which was modified from Sante's rule, in comparison with the lower kVp technique (70 kVp 30 mAs) and the higher kVp technique (130 kVp 8 mAs). Among the three techniques, the radiographic image obtained using 90 kVp, 8 mAs, was found to be the best (Figure 2). The plot of density along the transverse image (cross lines) showed no difference in density between the bone tissue and the soft tissue in the lower technique. Regarding the other techniques, the difference between the bone tissue and the soft tissue can be identified using the plot of density, but it lacks some details in the bone part. The new exposure technique was recalculated. The factor 5 was added for the kVp instead and the mAs value was equal to two-fifths of the subject thickness. The equation can be finalized as follows.

kVp = (2 × Tissue thickness [in cm]) + SID (in inch)+5
mAs = Tissue thickness (in cm)/2.5

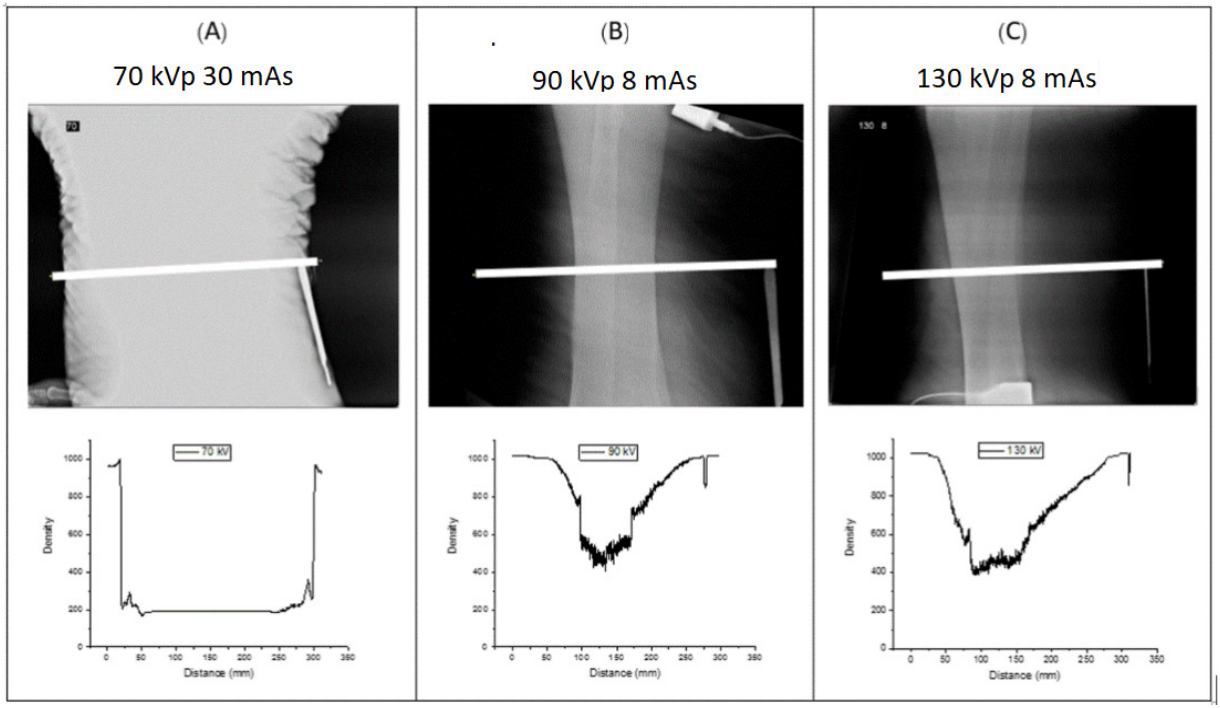

Figure 2 *Radiographic images of lateral view of the elephant's hind limb (upper row) and density plot profile of each image at the white level (lower row) at the lower technique (A), expected technique (B) ,and higher technique (C).*

The exposure technique was recalculated (Table 2) and used to expose the hind limbs of the 10 live elephants which consisted of five males (5, 33, 42, 59, and 67 years) and five females (4, 21, 23, 32, and 72 years) with thicknesses at the middle level of tibia in the range of 19-25 cm. The radiographic images with no post-processing were observed to have good detail in both tibia and fibula except M4 and F3 which have the thick tibia (Figure 3). The quality of the radiographic image in the density plot was extremely good, and the image revealed considerable detail with good distinction between the medullar and the cortex of the bone (Figure 4).

Table 2 Exposure technique guidelines for Asian elephants' limb at various thicknesses (in cm) (kVp = 2 × Tissue thickness [in cm] + SID [in inch]) + 5, and mAs = Tissue thickness (in cm)/2.5, SID 40 inch, no grid, and IP cassette type CC with CR imaging plate type ST-VI size 14"x17"

Thickness (cm)	kVp	mAs	Thickness (cm)	kVp	mAs
16	77	6.3	26	97	12
17	79	6.3	27	99	12
18	81	8	28	101	12
19	83	8	29	103	12
20	85	8	30	105	12
21	87	8	31	107	16
22	89	10	32	109	16
23	91	10	33	111	16
24	93	10	34	113	16
25	95	12	35	115	16

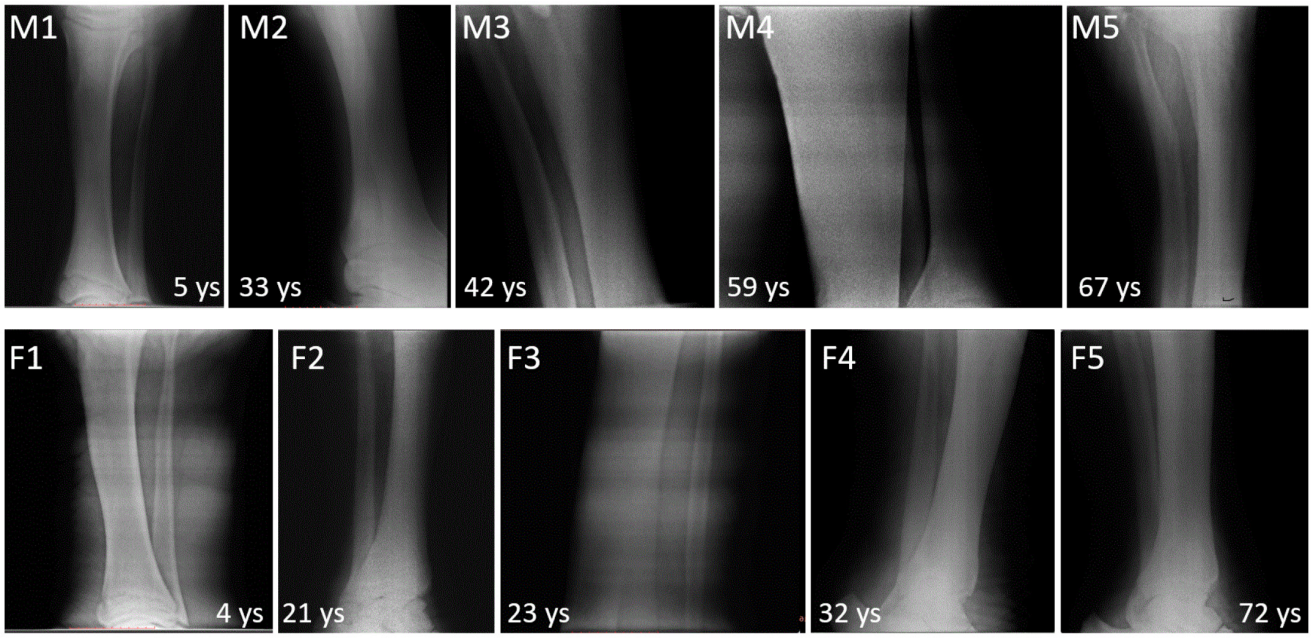

Figure 3 *Radiographic images of the lateral view of the hind limb from ten elephants; the upper row are images from five male elephants (M1 -M5) and the lower row from five female elephants (F1–F5). Thickness and exposure technique of each image are as follows: M1 (19 cm), 83 kVp, 8 mAs; M2 (22 cm), 89 kVp, 10 mAs; M3 (20 cm), 85 kVp, 8 mAs; M4 (22 cm), 89 kVp, 10 mAs; M5 (23 cm), 91 kVp, 10 mAs; and F1 (19 cm), 83 kVp, 8 mAs; F2 (20 cm), 85 kVp, 8 mAs; F3 (25 cm), 95 kVp, 12 mAs; F4 (21 cm), 87 kVp, 8 mAs; and F5 (21 cm), 87 kVp, 8 mAs.*

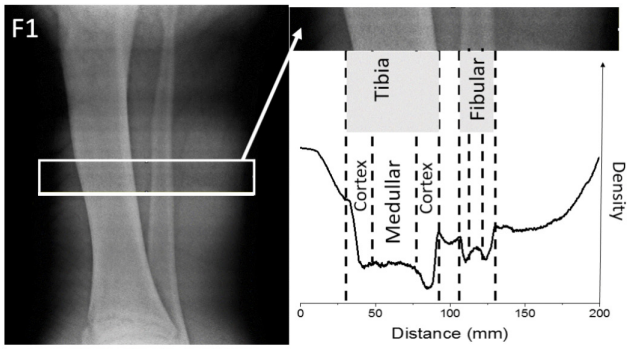

Figure 4 *Density plot profile of the transverse axial region (white block) (right) of the lateral view of the hind limb of an elephant (F1: age 4 years, 83 kVp, 8 mAs) (left).*

Discussion and Conclusion

The assignment of the exposure technique for elephants' hind limb is dependent on many factors, such as output of X-ray machine, image recorder system, and tissue absorption. In general, the grid is usually applied for the X-ray image of the organ with a thickness greater than 20 cm, but in this case, the grid cutoff effect can be easily found by the movement of the animal. In this study, the output of a mobile X-ray machine was reported in terms of mR/mAs as a function of kVp^2 with the constant of 6.4×10^{-4}, which caused the machine factor (P) to be equal to 6.4. In general, the P value ranges from 5 up to 30.[18] In order to assign the exposure technique, it has to be taken into consideration that the kVp and the mAs values depend not only on the capacity of the X-ray machine but also on the absorbability of the elephant tissue. The previous study of authors on the linear attenuation coefficient of elephant soft tissue showed it to be about 1.2 times more than that of the human muscle. Results suggested that elephants required 2–3 times amount of the primary radiation exposed in order to receive the same image quality as that of human. The first trial technique for the hind limb of elephants was estimated based on Sante's rule plus a factor of 10 for the kVp value. This image was of moderate quality since it lacked bony detail because of low contrast image, which was caused by high kVp. A small adjustment was given to the kVp value for estimation, and it was used for the exposition. In practice, the limitation of the mobile X-ray machine was that the mAs setting values were fixed values such as 2, 2.5, 3.2, 4, 5, 6.3, 8, 10 up to 200 such that the mAs value had to be selected from the adjacent value of calculation. When the image showed up too light which was caused by high bone density or plaque addition, increasing the value of mAs by 30–50% or the value of kVp by 10–15% was recommended. Because of the restlessness of the elephant, the shortest exposure time is recommended, and so, increasing of kVp is the first choice. In conclusion, the exposure technique guidelines for Asian elephant limbs can be designed by using the equations of kVp = (2 × Tissue thickness [in cm]) + SID (in inches) + 5 and mAs = Tissue thickness (in cm)/2.5.

Conflict of interest

The authors declare that they have no conflict of interest.

Acknowledgements

This work was supported by Department of Radiologic Technology, Faculty of Associated Medical Sciences, Chiang Mai University, Thailand; and National Elephant Institute, Forest Industry Organization, Lampang Province, Thailand.

References

[1] Angkawanish T, Boonprasert K, Homkong P, Sombutputorn P, Mahasawangkul S, Jansittiwate S, et al. Elephant Health Status in Thailand: The Role of Mobile Elephant Clinic and Elephant Hospital. Gajah. 2009; 31: 15-20.

[2] Sukklad S, Sommanustweechai A, Pattanarangsan R, editors. A retrospective study of elephant wound, wound management from Thai veterinarians 2006 26-29 Oct 2006 Chulalongkorn Uni. Fac. of Vet. Sc., Bangkok, Thailand.

[3] Miller D, Jackson B, Riddle HS, Stremme C, Schmitt D, Miller T. Elephant (Elephas maximus) Health and Management in Asia: Variations in Veterinary Perspectives. Vet Med Int. 2015; 2015: 19.

[4] Freedman MT, Bush M, Novak GR, Heller RM, James AE. Nutritional and metabolic bone disease in a zoological population. Skeletal Radiol. 1976; 1(2): 87-96.

[5] Kaulfers C, Geburek F, Feige K, Knieriem A. Radiographic imaging and possible causes of a carpal varus deformity in an Asian elephant (Elephas maximus). J Zoo Wildl Med. 2010; 41(4): 697-702.

[6] Mumby C, Bouts T, Sambrook L, Danika S, Rees E, Parry A, et al. Validation of a new radiographic protocol for Asian elephant feet and description of their radiographic anatomy. Vet Rec. 2013; 173(13): 318.

[7] Siegal-Willott J, Isaza R, Johnson R, Blaik M. Distal limb radiography, ossification, and growth plate closure in the juvenile Asian elephant (Elephas maximus). J Zoo Wildl Med. 2008; 39(3): 320-34.

[8] Theerapan W. Radiographic study on bone maturation of distal limbs in Asian elephans: Chulalongkorn University. Bangkok. (Thailand). Graduate School.; 2003.

[9] Tongtip N, Thengchaisri N, Viriyarumpa J, editors. Estimation of radiographic exposure in Asian elephant limbs. 37th Kasetsart University Annual Conference; 1999; Bangkok (Thailand): Kasetsart University, Bangkok (Thailand).

[10] van der Kolk JH, van Leeuwen JP, van den Belt AJ, van Schaik RH, Schaftenaar W. Subclinical hypocalcaemia in captive Asian elephants (Elephas maximus). Vet Rec. 2008; 162(15): 475-9.

[11] Holtgrew-Bohling K. Large Animal Clinical Procedures for Veterinary Technicians, 3e. 3 edition ed. St. Louis, MO: Mosby; 2015 October 13, 2015, 704 p.

[12] IAEA. Diagnostic Radiology Physics 2014, 681 p.

[13] David RL. CRC Handbook of Chemistry and Physics, 89th Edition - CRC Press Book. 89th ed: CRC Press; 2008 2008-2009, 2736 p.

[14] IAEA. Dual Energy X Ray Absorptiometry for Bone Mineral Density and Body Composition Assessment. 2011.

[15] Schneider CA, Rasband WS, Eliceiri KW. NIH Image to ImageJ: 25 years of image analysis. Nat Meth. 2012;9(7): 671-5.

[16] Ayad M, Bakazi A, Elharby H, editors. Dosimetry measurements of X-Ray machine operating at ordinary radiology and fluoroscopic examinations. The Third Nuclear and Particle Physics Conference (NUPPAC-2001); 2002; Egypt.

[17] Lavin LM. Radiography in veterinary technology. 2nd ed. Philadelphia, Pa.: W.B. Saunders; 1999.

[18] Dudley RJ, Wood SP, Hutchinson JR, Weller R. Radiographic protocol and normal anatomy of the hind feet in the white rhinoceros (Ceratotherium simum). Vet Radiol Ultrasound. 2015; 56(2): 124-32.

Journal of Associated Medical Sciences 2018; 51(1): 51-56

JAMS
Journal of Associated Medical Sciences

Thai-Journal Citation Index Centre (TCI) & ASEAN Citation Index (ACI)

Journal of Associated Medical Sciences

Journal homepage: https://www.tci-thaijo.org/index.php/bulletinAMS/index

Volumetric and dosimetric comparison of helical tomotherapy treatment planning using different strategies of four dimensional computed tomography images for target volume definition in non-small cell lung cancer patients

Kanyawee Payungkulanan[*1] **Pitchayaponne Klunklin** **Somsak Wanwilairat**

Division of Therapeutic Radiology and Oncology, Department of Radiology, Faculty of Medicine, Chiang Mai University, Chiang Mai Province, Thailand

ARTICLE INFO

Article history:
Received 16 November 2017
Accepted as revised 28 January 2018
Available online 30 January 2018

Keywords:
Four-dimensional computed tomography, non-small cell lung cancer, helical tomotherapy, maximum intensity projection, internal target volume

ABSTRACT

Background: Four-dimensional computed tomography (4DCT) images were used to generate internal target volume (ITV) in lung cancer. However, the drawback is time consumed to delineate all sets of CT scans. Maximum intensity projection (MIP) and select phases of 4DCT datasets were used to reduce time consumed to delineate the ITV.

Objectives: To compare the volume of ITV and dosimetric parameters of planning target volume (PTV) based on three different 4DCT datasets in non-small cell lung cancer (NSCLC) patients of helical tomotherapy treatment planning.

Materials and methods: The 4DCT image datasets of 7 patients diagnosed with stage I-III NSCLC were used. All gross target volumes (GTVs) were delineated by the same radiation oncologist in 3 different 4DCT datasets (10 phases, 3 phases, and MIP image) using Oncentra Master Plan v.4.3 contouring software. $PTV_{10phases}$, $PTV_{3phases}$ and PTV_{MIP} were generated and treatment planning were performed. From PTVs contour, volume and ratio of ITV as well as matching index (MI) were compared. Helical tomotherapy planning was done for each PTV then dosimetric parameters for PTVs and organs at risk (OARs) were evaluated. Statistical analysis was performed using Pair t- test and a $p<0.05$ was considered to be statistically significant.

Results: Mean volume of ITVs were 64.09±63.05 cc, 60.40±60.99 cc, 59.85±60.23 cc for $ITV_{10phases}$, $ITV_{3phases}$ and ITV_{MIP}, respectively. The $ITV_{3phases}$ and ITV_{MIP} were significantly smaller than the $ITV_{10phases}$ ($p<0.05$). The mean ratios between $ITV_{3phases}$ and $ITV_{10phases}$ and between ITV_{MIP} and $ITV_{10phases}$ were 0.93 and 0.92, respectively. The mean MI between $ITV_{3phases}$ and $ITV_{10phases}$ and between ITV_{MIP} and $ITV_{10phases}$ were 0.90 and 0.87, respectively. For the mean MI and the mean ratios of ITVs, there was no significant difference between $ITV_{3phases}$ versus $ITV_{10phases}$ and ITV_{MIP} versus $ITV_{10phases}$. For dosimetric parameters of PTVs, the average V95 of $PTV_{10phases}$, $PTV_{3phases}$ and PTV_{MIP} were 99.51%, 99.65% and 99.68%, respectively. The average V107 of $PTV_{10phase}$, $PTV_{3phases}$ and PTV_{MIP} were 0.24%, 0.22% and 0.23%, respectively. About OARs dose, only statistically significant difference was found in the Ipsilateral lung dose (V20 and V30) of $PTV_{10phases}$ and PTV_{MIP}.

Conclusion: MIP images are reliable for creating ITVs in early stage patients. The 3 phases images data sets are reliable for generating ITVs for all stages of NSCLC

* **Corresponding author.**
Author's Address: Division of Therapeutic Radiology and Oncology, Department of Radiology, Faculty of Medicine, Chiang Mai University, Chiang Mai Province, Thailand
** **E-mail address:** kanyaweepoon@gmail.com
doi: 10.14456/jams.2018.9
E-ISSN: 2539-6056

in which tumor moves straightforward superoinferior (SI) direction and that tumor deformation during breathing are minimal. Dosimetric parameters of all 3 PTVs generated by using 3 different ITV definitions are similar.

Introduction

Respiration is the major cause of intrafraction motion in radiotherapy treatment delivery especially in Non small cell lung cancer (NSCLC)[1]. In radiotherapy treatment planning, to ensure the target volume was covered by prescription dose, the margin needs to be added to clinical target volume (CTV) for forming Internal target volume (ITV) to account intrafraction motion. Four-dimensional computed tomography (4DCT) is an advance technique to create many data sets images tag with respiration movement. This technique is suitable for tumor that move due to respiration especially lung cancer. The 4DCT images can be used to create Internal target volume (ITV) of tumor. Various methods for generating an ITV from 4DCT dataset have been reported. Ideally, the method to create an ITV is contouring all individual CT dataset but the drawback for this method is the time required to delineate all sets of CT scans. To reduce the workload and time consuming, the Maximum intensity projection (MIP) and selected phases images were used to generate ITV. Briefly, the MIP is the post processing tool that reflects the maximum CT number value in each voxel and displays in full intensity with brightest object on projection image[2]. In this study, the MIP image was created from 10 phases of 4DCT datasets. There were several researches[2-8] studied about these methods (MIP and selected phases) compared to all 10 phases images method in terms of the accuracy and efficiency to generate ITV. Therefore, this study studied about MIP and 3 phases methods compared to all 10 phases images method in term of the accuracy and efficiency to generate ITV. This study purpose to compare volume of ITV and dosimetric parameters of different target volume that were created by MIP images and selected phases (3 phases) images with 10 phases images (standard method) in Non small cell lung cancer (NSCLC).

Materials and methods

1. Patient characteristics

Prospective analysis performed on 4DCT datasets from 7 patients who were diagnosed stage I-III with Non-small cell lung cancer (NSCLC) who received external radiotherapy in Radiotherapy Department of Maharaj Nakhon Chiangmai hospital from March - May 2017. The patient characteristics are summarized in Table 1.

Table 1 Patients characteristics

No.	Sex	Age (years)	TNM Staging	Stage grouping	Tumor site
1	Male	61	T3N3M0	Stage IIIB	LUL
2	Male	70	T2aN2M0	Stage IIIA	RML
3	Female	62	T3N2M0	Stage IIIA	LUL
4	Female	56	T4N3M0	Stage IIIB	RUL
5	Male	54	T4N2M0	Stage IIIB	RUL,RLL
6	Male	60	T4N3M0	Stage IIIB	RUL,RML
7	Male	79	T1bN0M0	Stage IA	LLL

TNM = Tumor, Node, Metastasis; RUL = Right Upper Lobe; RML=Right Middle Lobe; RLL= Right Lower Lobe; LUL= Left Upper Lobe; LLL = Left Lower Lobe

2. CT simulation and image acquisition

All patients were immobilized with wing board in supine position with arms above the head during simulation. The 4DCT scanning was performed during free breathing on 64-slice CT scanner (Sensation Open AS, Siemens, Erlangen, Germany). The respiratory signal for the 4DCT was generated by the respiratory gating system AZ-733VI (AZ-733V, Anzai Medical Co. Tokyo, Japan). The 3DCT with intravenous contrast was performed with scanning parameters as shown in Table 2.

After that, 4DCT imaging acquired with scanning parameters are shown in Table 3. Then, the 4DCT datasets were sorted according to phases in 10 CT volumes (CT0%, CT 10%,...,CT90%). The 0% is full maximum inspiration and 50% correspond to full maximum expiration. Moreover, post processing tool, MIP image dataset was created by the software using raw data of all 10 scan phases. All CT datasets were transferred to Oncentra master plan (v 4.3) for contouring target volumes and organs at risk (OARs)

Table 2 Scanning parameters of 3DCT acquisition.

Acquisition Parameters	3D CT
Voltage (kV)	120 kV
Effective current (mAs)	CARE DOSE
Slice thickness (mm)	5 mm
Gantry rotation time (s)	0.5 s (default)
Pitch	0.83

Table 3 Scanning parameters of 4DCT acquisition.

Acquisition Parameters	4D CT
Voltage (kV)	120 kV
Effective current (mAs)	CARE DOSE
Slice thickness (mm)	5 mm
Gantry rotation time (s)	0.5 s (default)
Pitch	0.09

3. Target volume generation

All 4DCT image datasets and MIP image dataset were transferred to the Oncentra Master Plan v.4.3 contouring software. For each patient, the Gross tumor volumes (GTVs) were delineated on each of the 10 phases of 4DCT datasets ($GTV_{10phases}$), $GTV_{3phases}$ was delineated on 3 phases image (full-maximum inspiration, mid-expiration, full-maximum expiration) of 4DCT datasets and GTV_{MIP} was delineated on MIP image dataset by the same radiation oncologist using lung window setting (WW1600, WL-600). The 5 mm expansion was added around $GTV_{10phases}$, $GTV_{3phases}$ and GTV_{MIP} to account the microscopic disease extent and defined as $CTV_{10phases}$, $CTV_{3phases}$ and CTV_{MIP}, respectively. Then three different Internal target volumes (ITVs) and Planning target volumes (PTVs) were generated as follow,

i) $ITV_{10phases}$ derived from combining all CTVs (CTV0% - CTV90%) in the 10 respiratory phases. PTV was created by adding 5 mm isotropic margin around $ITV_{10phases}$ for set up error and determined as $PTV_{10phases}$.

ii) $ITV_{3phases}$ derived from combining 3 CTVs that encompassed CTV0% (full-maximum inspiration), CTV20% (mid-expiration) and CTV50% (full-maximum expiration). The PTV was created by adding 5 mm isotropic margin around $ITV_{3phases}$ for set up error and determined as $PTV_{3phases}$.

iii) ITV_{MIP} was equivalent to CTV_{MIP}. The reason why ITV_{MIP} was equivalent to CTV_{MIP} because the disease outlined on MIP image includes all movement of tumor. For the PTV was created by adding 5 mm isotropic margin around ITV_{MIP} for set up error and determined as PTV_{MIP}.

iv)

4. Analysis of internal target volume (ITV)

Three different ITV definitions were measured and compared using ratio of ITVs and matching index(MI). In this study, $ITV_{10phases}$ was set as a reference volume.

4.1 Ratio of ITVs

The ratio of ITV is defined as the ratio volume of $ITV_{10phases}$ to ITVtest ($ITV_{3phases}$ and ITV_{MIP}). The formula is as follow,

$$\frac{ITV_{test}}{ITV_{10phases}}$$

The ideal value of the ratio of ITV is 1 if two volumes are identical.

4.2 Matching index (MI)

Matching index (MI) is defined as the ratio of the intersection of ITV A ($ITV_{10phases}$) with ITV B ($ITV_{3phases}$ or ITV_{MIP}) to the union of ITV A and ITV B. The formula is as follow,

$$MI(A,B) = \frac{ITV\,A \cap ITV\,B}{ITV\,A \cup ITV\,B}$$

The maximum value of MI is 1 if two volumes are identical and the minimum value is 0 if values are completely non-overlapping.

5. Helical tomotherapy treatment planning

For each patient, treatment plans of $PTV_{10phases}$, $PTV_{3phases}$ and PTV_{MIP} were designed on 3DCT data set. All plans were optimized using the Tomotherapy Hi-Art TPS, version 5.1.0.4 using the same optimization parameters with 2.5 cm field width (FW), 0.287 pitch factor (PF) and 3.5 modulation factor (MF). Dose distribution for each beamlet was calculated using a convolution/superposition algorithm. Dose prescription was 60 Gy for 2 Gy per fraction delivered to the PTVs.

6. Dosimetric parameters evaluation

Planning target volumes (PTVs) obtained using three different ITV definitions were evaluated and compared. For this study, $PTV_{10phases}$ was set as a reference volume. D50 was normalized to 60 Gy in all cases and all types of PTV following ICRU 83[9]. For each plan, dosimetric parameters of PTV were evaluated including V95 and V107, while organs at risk (OARs) were evaluated in according to radiation therapy oncology group (RTOG) 0617[10] report that include the following parameters: percentage volume of Ipsilateral lung receiving 20 Gy and 30 Gy (V20, V30); percentage volume of contralateral lung receiving 20 Gy (V20); Dmax of Spinal cord; Dmean of Esophagus and D33 of Heart.

7. Statistical analysis

Statistical analysis was performed using the SPSS 19.0 for window. Volume of ITV, ratios of ITV, matching index (MI) and dosimetric parameters were compared using pair t- test and $p<0.05$ was considered to be statistically significant difference.

Results

Volume of Internal target volume (ITV)

Volume of ITVs of each patient is shown in Table 4. Mean volume of ITVs were 64.09±63.05 cc, 60.40±60.09 cc and 59.85±60.23 cc for $ITV_{10phases}$, $ITV_{3phases}$ and ITV_{MIP}, respectively. The $ITV_{10phases}$ was the largest volume for all patients. $ITV_{3phases}$ and ITV_{MIP} were significantly smaller than $ITV_{10phases}$ ($p<0.05$). Extreme large absolute volume differences were observed for case number 3, 4 and 5 with the difference in range of 5.46 to 8.34 cc. For case 7 with early stage patient, the volume of $ITV_{3phases}$ and ITV_{MIP} are very closed to $ITV_{10phases}$ with the volume differences of 0.07 and 0.11 cc for $ITV_{3phases}$ and ITV_{MIP}, respectively.

Table 4 Volume of internal target volume (ITV) for $ITV_{10phases}$, $ITV_{3phases}$ and ITV_{MIP}.

Patient No.	Volume of ITVs (cc.)		
	$ITV_{10phases}$	$ITV_{3phases}$	ITV_{MIP}
1	32.66	31.89	31.11
2	16.00	13.18	13.34
3	186.67	181.03	178.33
4	88.60	80.78	82.41
5	86.37	79.98	78.54
6	33.18	30.86	30.16
7	5.15	5.08	5.04
Mean±SD	64.09±63.05	60.40±60.99	59.85±60.23

Ratio of Internal target volume (ITV)

Table 5 shows the ratios of internal target volume (ITV) for $ITV_{3phases}$ and ITV_{MIP} relative to the reference $ITV_{10phases}$. If consider in the percent volume change, case number 2 was the maximum difference with the changed around 20% volume. All of the ratio values were less than 1 that represented to the smaller of $ITV_{3phases}$ and ITV_{MIP} compared with $ITV_{10phases}$. Mean ratios between $ITV_{3phases}$ and $ITV_{10phases}$ and between ITV_{MIP} and $ITV_{10phases}$ are 0.93±0.06 and 0.92±0.05, respectively. There was no statistic significant differences supported by *p* value between mean ratios of $ITV_{3phases}$ to $ITV_{10phases}$ and between ITV_{MIP} to $ITV_{10phases}$ (*p*=0.182)

Table 5 Ratio of internal target volumes (ITVs) for $ITV_{3phases}$ and ITVMIP relative to the reference $ITV_{10phases}$.

Patient No.	Ratio of ITVs	
	$ITV_{3\ phases}$ / $ITV_{10phases}$	ITV_{MIP}/ $ITV_{10phases}$
1	0.98	0.95
2	0.82	0.83
3	0.97	0.96
4	0.91	0.92
5	0.92	0.91
6	0.92	0.90
7	0.99	0.98
Mean±SD	0.93±0.06	0.92±0.05
	p=0.182	

Matching index (MI)

Table 6 shows Matching index (MI) for $ITV_{3phases}$ and ITV_{MIP} relative to the reference $ITV_{10phases}$. MI index presented good agreement with ratio of ITV results that case number 2 was the worst case for matching and vice versa in case number 7. From the data as shown in Table 6, the mean MI of $ITV_{3phases}$ and ITV_{MIP} compared with $ITV_{10phases}$ were 0.90±0.05 and 0.87±0.07, respectively. There were no significant differences of the mean MI between $ITV_{3phases}$ and ITV_{MIP} related to $ITV_{10phases}$ (*p*=0.38).

Table 6 Matching index (MI) for $ITV_{3phases}$ and ITV_{MIP} relative to the reference $ITV_{10phases}$.

Patient No.	Matching Index (MI)	
	$ITV_{3phases}$ vs. $ITV_{10phases}$	ITV_{MIP} vs. $ITV_{10phases}$
1	0.87	0.85
2	0.80	0.74
3	0.94	0.90
4	0.91	0.92
5	0.92	0.87
6	0.90	0.82
7	0.95	0.96
Mean±SD	0.90±0.05	0.87±0.07
	p=0.38	

Dosimetric parameters of PTV and OARs

Dosimetric parameters are presented in Table 7. PTV coverage was very closed for three ITV definitions. Average D50 of $PTV_{10phases}$, $PTV_{3phases}$ and PTV_{MIP} were 60 Gy. The average V95 of $PTV_{10phases}$, $PTV_{3phases}$ and PTV_{MIP} were 99.51%, 99.65% and 99.68%, respectively. Average V107 of $PTV_{10phases}$, $PTV_{3phases}$ and PTV_{MIP} were 0.24%, 0.22% and 0.23%, respectively. For dosimetric parameters of OARs, only statistically significant difference was found in the Ipsilateral lung dose (V20 and V30) of PTV_{MIP} compared to $PTV_{10phases}$ as shown in Table 8.

Table 7 Dosimetric parameters result of PTVs.

Dosimetric parameter	$PTV_{10phases}$ (mean±SD)	$PTV_{3phases}$ (mean±SD)	PTV_{MIP} (mean±SD)
V95 (%)	99.51±0.75	99.65±0.65	99.68±0.62
V107 (%)	0.24±0.40	0.22±0.40	0.23±0.39

Table 8 Dosimetric parameters result of OARs.

OARs	Parameters	$PTV_{3phases}$ (±SD)	$PTV_{10phases}$ (±SD)	*p* value	PTV_{MIP} (±SD)	$PTV_{10phases}$ (±SD)	*p* value
Ipsilateral lung	V_{20} (%)	37.46±8.55	38.07±8.75	0.055	37.47±8.68	38.07±8.75	0.032
	V_{30} (%)	27.81±8.10	28.24±8.17	0.053	27.53±8.05	28.24±8.17	0.008
Contralateral lung	V_{20} (%)	8.88±9.44	8.98±9.47	0.087	8.83±9.21	8.98±9.47	0.569
Heart	D_{33} (Gy)	4.88±6.50	4.93±6.42	0.280	4.59±5.98	4.93±6.42	0.121
Esophagus	D_{mean} (Gy)	3.97±3.76	4.85±4.10	0.174	3.85±3.86	4.85±4.10	0.206
Spinal cord	D_{max} (Gy)	26.76±10.50	26.80±10.72	0.923	26.36±10.65	26.80±10.72	0.418

Discussion

In lung cancer, respiration is the major cause of tumor motion during treatment. Four-dimensional computed tomography (4DCT) images were used to generate Internal target volume (ITV), but the drawback is the time required to delineate all sets of CT scans, the post processing tool of Maximum intensity projection (MIP) and selected phases of 4DCT datasets were used to delineate the ITV to solve the drawback of time consuming. This study purpose to compare volume of ITV and dosimetric parameters of different target volume that were created by MIP images and selected phases (3 phases) images compared with 10 phases images (standard method) in Non small cell lung cancer (NSCLC).

This study found, that the ratios of ITV and MI value from $ITV_{3phases}$ and ITVMIP are similar to the value from $ITV_{10phases}$. The best case of smallest difference in volume change that presented the ITV ratio and MI values near ideal value was patient no.7. It was because of early stage NSCLC with tumor locate at peripheral lung that relatived to the study of Underberg RWM[2] and Muirhead R.[6] The explanation about these ratios depend on position of the tumor, if tumor locates in peripheral lung, it is liable to distinguish the tumor from nearby organ. For locally advance stage NSCLC (Case 1-6), ratios of ITV and MI values from ITV_{MIP} are not similar to the value from $ITV_{10phases}$ because tumor locate adjacent to tissue of equal density that resemble of CT number value such as mediastinum and chest wall. Thus, on MIP image, boundaries between tumor and nearby organ may not be clearly seen by observer. This study can conclude that MIP method may not suitable for creating an ITV in locally advance stage NSCLC patients compared to the study of Ezhil et al.[8] Ezhil reported the value of MI decrease in patients who have locally advance stage NSCLC that tumor involve to nearby organ such as chest wall, diaphragm or mediastinum. About 3 phases method, volume of ITV, ratios of ITV and matching (MI) value are similar to the value of $ITV_{10phases}$ in both early stage and locally advance stage NSCLC. Results represent that movement of tumor in all patients in this study are moving in straightforward superoinferior (SI) direction and tumor deformation during breathing are minimal.

For PTV coverage, no significant differences were observed for PTVs that generating from three different ITV definitions because of using the same dose constraints.

Limitation of this study was small sample size due to short timing of study and small number of early stage NSCLC patient. Future study should increase the sample size to confirm the accuracy of study.

Conclusion

MIP images are reliable and fast tool for creating ITVs from 4DCT images of early stage NSCLC patients. However, it should be considered in case of tumor near mediastinum or chest wall. The 3 phases images are reliable for generating ITVs for all stage of NSCLC which tumor moves straightforward superoinferior (SI) direction and that tumor deformation during breathing are minimal. For dosimetric parameters, there is no significant differences observed for 3 PTVs that generating from three different ITV definitions.

Acknowledgements

I would like to thank the Division of Therapeutic Radiology and Oncology, Department of Radiology, Faculty of Medicine, Chiang Mai University. Many thanks for Lecturer Pitchayaponne Klunklin, M.D and Asst.Prof. Somsak Wanwilairat for suggestions and supports in this research work.

References

[1] Keall PJ, Mageras GS, Balter JM, Emery RS, Forster KM, Juang SB, et al. The management of respiratory motion in radiation oncology report of AAPM Task Group76. Med Phys 2006; 33: 3874-900.

[2] Underberg RWM, Lagerwaard FJ, Slotman BJ, Cuijpers JP, Senan S. Use of maximum intensity projections (MIP) for target volume generation in 4DCT scans for lung cancer. Int Radiat Oncol Biol Phys2005;63:253-60.

[3] Khan F, Bell G, Antony J, Palmer M, Balter P, Bucci K, et al. The use of 4dct to reduce lung dose: a dosimetric analysis. Med Dosim 2009; 34: 273-8.

[4] Bai T, Zhu J, Yin Y, Lu J, Shu H, Wang L, et al. How does four-dimensional computed tomography spare normal tissue in non-small cell lung cancer radiotherapy by defining internal target volume. Thoracic Cancer2014; 5: 537-42.

[5] Wang L, Hayes S, Paskalev K, Jin L, Buyyounouski MK, Ma CM, et al. Dosimetric comparison of stereotactic body radiotherapy using 4D CT and multiphase CT images for treatment planning of lung cancer: evaluation of the impact on daily dose coverage. Radiother Oncol 2009; 91: 314-24.

[6] Muirhead R, Stuart G, Featherstone C, Moore K, Muscat S. Use of maximum intensity projections (MIPs) for target outlining in 4DCT radiotherapy planning. Journal of Thorac Oncol 2008; 3: 1433–8.

[7] Rietzel E, Liu AK, Doppke KP, Wolfgang JA, Chen AB, Chen GT, et al. Design of 4D treatment planning target volumes. Int Radiat Oncol Biol Phys2006; 66: 287-95.

[8] Ezhil M, Vedam S, Balter P, Choi B, Mirkovic D, Starkschall G, et al. Determination of patient-specific internal gross tumor volumes for lung cancer using four-dimensional computed tomography. Radiat Oncol 2009; 4: 1-4.

[9] Menzel HG, Wambersie A, Jones DTL, et al. The ICRU report 83, Prescribing, Recording, and Reporting Photon-Beam Intensity-Modulated Radiation Therapy (IMRT). Journal of the ICRU 2010 april;10.

[10] Bradley J, Schild S, Bogart J, Dobelbower M, Choy H, Adjei A, et al. A randomized phase III comparison of standard- dose (60 Gy) versus high- dose (74 Gy) conformal radiotherapy with concurrent and consolidation carboplatin/paclitaxel +/- cetuximab (ind #103444) in patients with stage IIIA/IIIB non-small cell lung cancer [Internet]. 2016 [cited 2017 Jul 20]. Available from: https://www.rtog.org/ClinicalTrials/ProtocolTable/StudyDetails.aspx?study=0617

[11] Zhou YQ, Xie CY, Yi JL,Han C, Zheng XM, Jin XC. Volumetric and Dosimetric Influences of Internal Target Delineation Based on 4D CT Measured Tumor Motion in the Treatment of Lung Cancer with Stereotactic Body Radiotherapy. Austin J Radiat Oncol & Cancer 2015; 1(1): 1005

Instructions for Authors

Instructions for Authors

Original article/thesis can be submitted through the on-line system via website https://www.tci-thaijo.org/index.php/bulletinAMS/

General Principles

Journal of Associated Medical Sciences is a scientific journal of the Faculty of Associated Medical Sciences, Chiang Mai University. The articles submitted to the journal that are relevant to any of all aspects of Medical Technology, Physical Therapy, Occupational Therapy, Radiologic Technology, Communication Disorders, and other aspects related to the health sciences are welcome. Before publication, the articles will go through a system of assessment and acceptance by at least three experts who are specialized in the relevant discipline. All manuscripts submitted to Journal of Associated Medical Sciences should not have been previously published or under consideration for publication elsewhere. All publications are protected by the Journal of Associated Medical Sciences' copyright.

Manuscript categories

1. **Review articles** must not exceed 20 journal pages (not more than 5,000 words), including 6 tables/figures, and references (maximum 75, recent and relevant).
2. **Original articles** must not exceed 15 journal pages (not more than 3,500 words), including 6 tables/figures, and 40 reference (maximum 40, recent and relevant).
3. **Short communications** including technical reports, notes, and letter to editor must not exceed 5 journal pages (not more than 1,500 words), including 2 tables/figures, and references (maximum 10, recent and relevant).

Manuscript files

To submit your manuscript, you will need the following files:

1. A Title page file with the names of all authors and corresponding authors*
2. Main document file with abstract, keywords, main text and references
3. Figure files
4. Table files
5. Any extra files such as Supplemental files or Author Biographical notes

Manuscript Format

1. **Language**: English, Caribri 10 for text and 7 for all symbols. PLEASE be informed that the Journal only accept the submission of English manuscript.
2. **Format**: One-side printing, double spacing. Use standard program and fonts and, add page and line number for all pages.
3. **A Title page**: Include article title, names of all authors and co-authors, name of the corresponding author and acknowledgements. Prepare according to following contents;
   - *Title of the article*: Concise and informative. Titles are often used in information-retrieval systems. Avoid abbreviations and formulate where possible.
   - *Author names and affiliation*: Where the family name may be ambiguous (e.g. a double name), please indicate this clearly. Present the authors' affiliation addresses (where the actual work was done) below the names. Indicate all affiliations with superscript number immediately after author's name and in front of appropriate address. Provide the full postal address of each affiliation, including the province, country and, if available, the e-mail address of each author.
   - *Corresponding author*: Clearly indicate who will handle correspondence at all stages of refereeing and publication, also post-publication, ensure that telephone and fax numbers (with postal area code) are provided in addition to the e-mail address and the complete postal address. Contact details must be kept up to date by the corresponding author.
   - *Acknowledgements*: Acknowledgements will be collated in a separate section at the end of the article before the references in the stage of copyediting. Please, therefore, include them on the title page, List here those individuals who provided help during the research (e.g. providing language help, writing assistance or proof reading the article, etc.)
4. **Main article structure**: The manuscripts should be arranged in the following headings: Title, Abstract, Introduction, Materials and Methods, Results, Discussion and Conclusion, and Reference. Prepare according to following contents;
   - *Abstract*: Not exceeding 400 words, abstract must be structured with below headings in separated paragraph:
     - Background,
     - Objectives,
     - Materials and methods,
     - Results,
     - Conclusion, and
     - Keywords (3-5 keywords should be included)
   - *Introduction*: State the objectives of work and provide an adequate background, avoiding a detailed literature survey or a summary of the results.
   - *Materials and Methods*: Provide sufficient detail to allow the work to be reproduced. Methods already published should be indicated by a reference, only relevant modifications should be described. Ensure that each table, graph, or figure is referred in the text. According to the policy of ethical approval, authors must state the ethical approval code and conduct informed consent for human subject research (If any) and for animal research, authors must include a statement or text describing the experimental procedures that affirms all appropriate measures (if any) in this section.
   - *Results*: Results should be clear and concise. Present the new results of the study such as tables and figures mentioned in the main body of the article and numbered in the order in which they appear in the text or discussion.
   - *Discussion*: This should explore the significance of the results of the work, not repeat them. A combined Results and Discussion

section is often appropriate. Avoid extensive citations and discussion of published literature.
- *Conclusion*: The main conclusions of the study may be presented in a short Conclusions section, which may stand alone or form a subsection of a "Discussion" or "Results and Discussion".
- *Conflict of interes*t: All authors must declare any financial and personal relationship with other people or organization that could inappropriately influence (bias) their work. If there is no interest to declare, then please state this: "The authors declare no conflict of interest".
- *Ethic approval*: Ethic clearance for research involving human and animal subjects.
- *References*: Vancouver's style.

5. **Artwork Requirements**
   - Each table, graph and figure should be self-explanatory and should present new information rather than duplicating what is in the text. Prepare one page per each and submit separately as supplementary file(s).
   - Save the figures as high resolution JPEC or TIFF files.

Note: Permission to reprint table(s) and/or figure(s) from other sources must be obtained from the original publishers and authors and submitted with the typescript.

Ensuring a blind peer review

To ensure the integrity of the double-blinded peer-review for submission to this journal, every effort should be made to prevent the identities of the authors and reviewers from being known to each other. The authors of the document have deleted their names from the main text, with "Author" and year used in the references and footnotes, instead of the authors' name, article title, etc. After the journal was accepted, the name of authors and affiliation and the name of the corresponding author must be included into the document and re-submitted in the copyediting stage.

Proof correction

The Proofs of final paper approved for publication are to be returned by email to the researcher before publication.

Page charge

No page charge.

References Format

1. References using the Vancouver referencing style (see example below).
2. In-text citation: Indicate references by number(s) in the order of appearance in the text with superscript format. Reference numbers are to be placed immediately after the punctuation (with no spacing). The actual authors can be referred to, but the reference number(s) must always be given. When multiple references are cited at a given place in the text, use a hyphen to join the first and last numbers that are inclusive. Use commas (with no spacing) to separate non-inclusive numbers in a multiple citation e.g. (2-5,7,10). Do not use a hyphen if there are no citation numbers in between inclusive statement e.g. (1-2). Use instead (1,2).
3. References list: number the references (numbers in square brackets) in the list must be in the order in which they are mentioned in the text. In case of references source from non-English language, translate the title to English and retain "in Thai" in the parentheses.
4. Please note that if references are not cited in order the manuscript may be returned for amendment before it is passed on to the Editor for review.

Examples of References list

Multiple Authors: List up to the first 6 authors/editors, and use "et al." for any additional authors.

Journal Articles (print): In case of reference source contains DOI, retain doi: at the end of reference. Vancouver Style does not use the full journal name, only the commonly-used abbreviation: "Physical Therapy" is cited as "Phys Ther". As an option, if a journal carries continuous pagination throughout a volume (as many medical journals do) the month and/or issue number may be omitted. Allow one space after semi-colon and colon and end each reference with full stop after page number.

- Pachori P, Gothalwal R, Gandhi P. Emergence of antibiotic resistance Pseudomonas aeruginosa in intensive care unit; a critical review. Genes Dis. 2019; 6(2): 109-19. doi: 10.1016/j.gendis.2019.04.001.
- Hung Kn G, Fong KN. Effects of telerehabilitation in occupational therapy practice: A systematic review. Hong Kong J Occup Ther. 2019; 32(1): 3-21. doi: 10.1177/1569186119849119.
- Wijesooriya K, Liyanage NK, Kaluarachchi M, Sawkey D. Part II: Verification of the TrueBeam head shielding model in Varian VirtuaLinac via out-of-field doses. Med Phys. 2019; 46(2): 877-884. doi: 10.1002/mp.13263.
- Velayati F, Ayatollahi H, Hemmat M. A systematic review of the effectiveness of telerehabilitation interventions for therapeutic purposes in the elderly. Methods Inf Med. 2020; 59(2-03): 104-109. doi: 10.1055/s-0040-1713398.
- Junmee C, Siriwachirachai P, Chompoonimit A, Chanavirut R, Thaweewannakij T, Nualnetr N. Health status of patients with stroke in Ubolratana District, Khon Kaen Province: International Classification of Functioning, Disability and Health-based assessments. Thai J Phys Ther. 2021; 43(1): 45-63 (in Thai).

Book / Chapter in an Edited Book References

PLEASE be informed that references of books and chapter in edited book should not be include in the research article, but others manuscript categories.

- Grove SK, Cipher DJ. Statistics for Nursing Research: A Workbook for Evidence-Based Practice. 3rd Ed. St. Louis, Missouri: Elsevier; 2019.
- Perrin DH. The evaluation process in rehabilitation. In: Prentice WE, editor. Rehabilitation techniques in sports medicine. 2nd Ed. St Louis, Mo: Mosby Year Book; 1994: 253–276.

E-book

- Dehkharghani S, editor. Stroke [Internet]. Brisbane (AU): Exon Publications; 2021 [cited 2021 Jul 31]. Available from: https://www.ncbi.nlm.nih.gov/books/NBK572004/ doi: 10.36255/exonpublications.stroke.2021.
- Tran K, Mierzwinski-Urban M. Serial X-Ray Radiography for the Diagnosis of Osteomyelitis: A Review of Diagnostic Accuracy, Clinical Utility, Cost-Effectiveness, and Guidelines [Internet]. Ottawa (ON): Canadian Agency for Drugs and Technologies in Health; 2020 [cited 2021 Jul 31]. Available from: https://www.ncbi.nlm.nih.gov/books/NBK562943/

Dissertation/Thesis

- Borkowski MM. Infant sleep and feeding: a telephone survey of Hispanic Americans [Dissertation]. Mount Pleasant (MI): Central Michigan University; 2002.
- On-Takrai J. Production of monoclonal antibody specific to recombinant gp41 of HIV-1 subtype E [Term paper]. Faculty of Associated Medical Sciences: Chiang Mai University; 2001 [in Thai].

Conference Proceedings

- Lake M, Isherwood J, Clansey. Determining initial knee joint loading during a single limb drop landing: reducing soft tissue errors. Proceedings of 34th International Conference of Biomechanics in Sport; 2016 Jul 18-22; Tsukuba, Japan, 2016. Available from: https://ojs.ub.uni-konstanz.de/cpa/article/view/7126.
- Ellis MD, Carmona C, Drogos J, Traxel S, Dewald JP. Progressive abduction loading therapy targeting flexion synergy to regain reaching function in chronic stroke: preliminary results from an RCT. Proceedings of the 38th Annual International Conference of the IEEE Engineering in Medicine and Biology Society; 2016: 5837-40. doi: 10.1109/EMBC.2016.7592055.

Government Organization Document

- Australian Government, Department of Health. Physical activity and exercise guidelines for all Australian. 2021 [updated 2021 May 7; cited 15 Jul 2021]. Available from: https://www.health.gov.au/health-topics/physical-activity-and-exercise/physical-activity-and-exercise-guidelines-for-all-australians.
- Department of Health. Situation survey on policy and implementation of physical activity promotion in schools for first year 2005. (in Thai). Nonthaburi: Ministry of Public Health; 2005.
- Department of Local Administration, Ministry of Interior Affairs. Standard of Sports Promotion. (in Thai). Bangkok. 2015:7–9.
- World Health Organization. WHO guidelines on physical activity and sedentary behaviour. Geneva: World Health Organization; 2020. Licence: CC BY-NC-SA 3.0 IGO.

Journal History

Established in 1968

- 1968-2016 As the Bulletin of Chiang Mai Associated Medical Sciences
  - Vol1, No1 - Vol.49, No3
- 2017, the Journal of Associated Medical Sciences
  - Vol.50, No1 and forward.

Journal Sponsorship Publisher

Faculty of Associated Medical Sciences, Chiang Mai University

Sponsors

Faculty of Associated Medical Sciences, Chiang Mai University

Sources of support

Faculty of Associated Medical Sciences, Chiang Mai University